

PALEOCENE DEPOSITION OF THE HOBACK  
FORMATION ON THE LA BARGE  
PLATFORM OF THE  
GREEN RIVER  
BASIN

BY

DAVID EDWARD SCHMUDE

Bachelor of Science

Oklahoma State University

Stillwater, Oklahoma

1989

Submitted to the Faculty of the  
Graduate College of the  
Oklahoma State University  
in partial fulfillment of  
the requirements for  
the Degree of  
MASTER OF SCIENCE  
December, 1991

Thesis  
1991  
S356p

PALEOCENE DEPOSITION OF THE HOBACK  
FORMATION ON THE LA BARGE  
PLATFORM OF THE  
GREEN RIVER  
BASIN

Thesis Approved:

*Arthur W. Cleaves, II*

Thesis Adviser

*Gary J. Stewart*

*E. L. Bell*

*Thomas C. Collins*

Dean of the Graduate College

## ACKNOWLEDGMENTS

I would like to thank Dr. Cleaves for his help throughout my graduate program and Dr. Al-Shaieb for his input on the diagenetic aspects of the Hoback Formation. I would also like to thank Dr. Stewart, Ed Burritt, and Dwaine Edington for their help in reviewing the text, and Special thanks to Jim Kreutzfeld, who suggested the topic.

Most importantly I would like to thank Texaco for their complete financial support. Without their involvement the study would not have been possible. I would also like to extend special thanks to Shelly Stone for drafting all of my maps.

I extend my deepest appreciation to my father, who typed and reviewed the manuscript for me, and to both of my parents, for their support and encouragement throughout my educational career.



## TABLE OF CONTENTS

Chapter	Page
I. INTRODUCTION.....	1
Location of Study Area .....	1
Purpose and Scope of the Study.....	1
Methods of Investigation.....	6
Subsurface studies.....	6
Field Studies.....	10
Previous Investigations.....	10
Stratigraphy .....	10
Paleocene Production .....	12
Structural Geology.....	13
II. STRUCTURAL FEATURES.....	14
Tectonic Setting .....	14
Gros Ventre Mountains.....	14
Wind River Mountains.....	16
Rock Springs Uplift.....	16
Uinta Mountains.....	17
Overthrust Belt .....	17
Influential Structural Elements .....	20
Moxa Arch (La Barge Platform).....	20
Darby (Hogsback) Thrust.....	21
Hilliard (La Barge) Thrust.....	23
Other Faulting.....	26
Timing of Important Structural Events.....	28
III. STRATIGRAPHY.....	32
Background.....	32
Late Cretaceous.....	33
Frontier Formation .....	34
Hilliard Formation .....	39
Mesaverde formation .....	41
Tertiary.....	44
Stratigraphic Nomenclature.....	44
Hoback Formation .....	49
Wasatch Formation.....	51
Lookout Mountain Conglomerate Member	

Chapter	Page
of the Wasatch Formation.....	52
Chappo Member of the Wasatch Formation.....	54
IV. CORE AND FIELD STUDIES.....	55
Core Descriptions.....	55
Palynology of the Hoback Formation.....	56
Field Investigations.....	56
V. SUBSURFACE GEOLOGY BASED ON ELECTRIC LOG STUDIES..	64
Introduction .....	64
Cross-Sections.....	64
Stratigraphic .....	64
Structural.....	65
Structure Maps.....	65
Base Of Hoback Sand .....	65
Top of TH-3 Interval ("X" Marker) Map .....	66
Hilliard Fault Plane Map.....	66
Net Sand Isolith Maps.....	66
TH-1 Interval Net Sand Map.....	67
TH-2 Interval Net Sand Map.....	67
TH-3 Interval Net Sand Map.....	67
TH-4 Interval Net Sand Map.....	68
TH-5 Interval Net Sand Map.....	68
Interval Isopach Maps.....	69
TH-2 Interval Isopach Map.....	69
TH-3 Interval Isopach Map.....	69
TH-4 Interval Isopach Map.....	69
VI. DEPOSITIONAL ENVIRONMENT OF THE HOBACK FORMATION....	71
Environmental Interpretation .....	71
Bedforms of Sand Dominated Braided Rivers .....	76
Bars .....	80
Longitudinal Bars.....	81
Lingoidal (Transverse) Bars .....	82
Compound Bars.....	83
Sand Waves .....	83
Dunes.....	84
Classification of the Hoback Braided River Deposits.....	85
Source Area.....	86
Paleocene Paleoenvironment.....	89
VII. PETROLEUM GEOLOGY .....	94
Introduction .....	94

Chapter	Page
Possible Source And Migration Path.....	96
Source .....	96
Migration Path .....	99
Trapping Mechanisms .....	100
Structural Traps.....	100
Stratigraphic Traps.....	101
Cumulative Production Map .....	101
Possible Reservoir Communication Problems.....	102
 VIII. SUMMARY AND CONCLUSIONS.....	 104
REFERENCES CITED .....	106
APPENDICES .....	113
APPENDIX A - CORE DISCRIPTIONS.....	114
WELL M327 .....	116
WELL TI-4.....	122
WELL K634W .....	128
WELL J503Y.....	134
APPENDIX B - WELL LOG DATA.....	141

## LIST OF TABLES

Table		Page
I.	Stratigraphic Names Assigned to the Paleocene Producing Sands of La Barge .....	46
II.	Lithofacies and Sedimentary Structures of Modern and Ancient Braided River Deposits .....	77
III.	Facies Assemblages and Environments of the Six Principal Braided Stream Models .....	79
IV.	Hoback Reservoir Characteristics in the La Barge Field.....	95
V.	Identification and API Gravity of Oil Samples.....	96

## LIST OF FIGURES

Figure	Page
1. Geographical Location of the Study Area.....	2
2. Major Structural Elements of the Green River Basin .....	3
3. Type Log of Hoback Formation.....	5
4. Electric Log Shape Codes for Net Sand Isoliths.....	8
5. Base Map Showing Cross-Section and Core Locations.....	9
6. Generalized Tectonic Map of the Green River Basin Showing Major Tectonic Elements.....	15
7. Trend of Cordilleran Fold and Thrust Belt .....	18
8. Index Map of Idaho-Wyoming-Utah Salient of the Overthrust Belt .....	19
9. Cross-Section Through the Study Area Showing Major Structural Features.....	22
10. Geologic Map of the Hogsback Ridge, La Barge Area.....	24
11. Late Albian Paleogeography of the Southern Terminus of the Mowry Sea at Its Greatest Extent.....	34
12. Type Log of Late Cretaceous Formations of the La Barge Area .....	36-38
13. Paleobathymetric Curve of the Hilliard Formation .....	40
14. Approximate Shoreline Limits of Mesaverde or Equivalent Regression.....	43
15. Correlation of Upper Cretaceous and Lower Tertiary Units of Western Wyoming.....	47
16. Tertiary Stratigraphic Relationships of the La Barge Field Area .....	52
17. Outcrop Locations of the Evanston and Almy Formations at Their Type Locations.....	57

Figure	Page
18. Outcrop of the Almy Formation at Its Type Location.....	58
19. Type Location of the Evanston Formation .....	59
20. Type Location of the Chappo Member of the Wasatch Formation Along Chappo Gulch.....	61
21. Outcrop of the Chappo Member Within the La Barge Field.....	63
22. Geomorphic and Sedimentary Characteristics of Various Channel Types and Their Deposits.....	73
23. Thin Section of Hoback Formation Showing Clay Drapes Associated with Cross-Bedding .....	75
24. General Stratigraphic Models for Sand Dominated Braided Streams .....	78
25. Block Diagram Summarizing the Major Morphological Elements and Their Associated Bedforms and Stratifications. ....	80
26. Morphology, Pattern of Growth, and Water Flow Over and Near Bars Commonly Found in Braided Channels.....	81
27. Tabular Cross-bedding Formed by Migrating Sand Waves.....	83
28. Trough Cross-Bedding Formed by Migrating Dunes.....	85
29. Late Middle Paleocene Paleogeographic Cartoon .....	88
30. Early to Middle Paleocene Paleoenvironment .....	90
31. Middle Paleocene Paleoenvironment .....	90
32. Late Middle Paleocene Paleoenvironment (TH-1 Deposition).....	91
33. Late Middle Paleocene Paleoenvironment (TH-2 Deposition).....	91
34. Early Late Paleocene Paleoenvironment (TH-3 Deposition).....	92
35. Early Late Paleocene Paleoenvironment (TH-4 Deposition).....	93
36. Early Late Paleocene Paleoenvironment (TH-5 Deposition).....	93
37. Group Analysis of the Seven Samples Listed in Table V.....	97-98
38. Hydrocarbon Migration Paths of Hoback Oil.....	100

## CHAPTER I

### INTRODUCTION

#### Location of Study Area

The La Barge field is located along the western flank of the Green River Basin of southwestern Wyoming in sections 2, 3, 4, 9 and 10, T.26N., R.113W., and sections 22, 27, 28, 33, 34 and 35, T.27N., R.113W, Lincoln and Sublette counties (Figure 1). The Green River Basin is one of the largest Tertiary intermountane topographic basins, with a maximal east-west dimension of 90 miles and a north-south dimension of approximately 180 miles (Krueger,1960). The basin is bounded to the north and northeast by the Gros Ventre and Wind River Mountains, to the east by the Rock Springs uplift, to the south by the Unita Mountains, and to the west by the overthrust belt (figure 2). The field is located on an intrabasin structural high known as the La Barge platform (Moxa arch) (Figure 2). This structurally positive feature was present during Hoback deposition and therefore played a role in governing the distribution and extent of the Hoback sands.

#### Purpose and Scope of the Study

The purpose of studying the Paleocene Hoback Formation of the La Barge field, was to define the geometry, depositional environments and trends of the individual producing sandstones will be more precisely defined. Success of the effort would aid in future development of the field, as well as providing possible

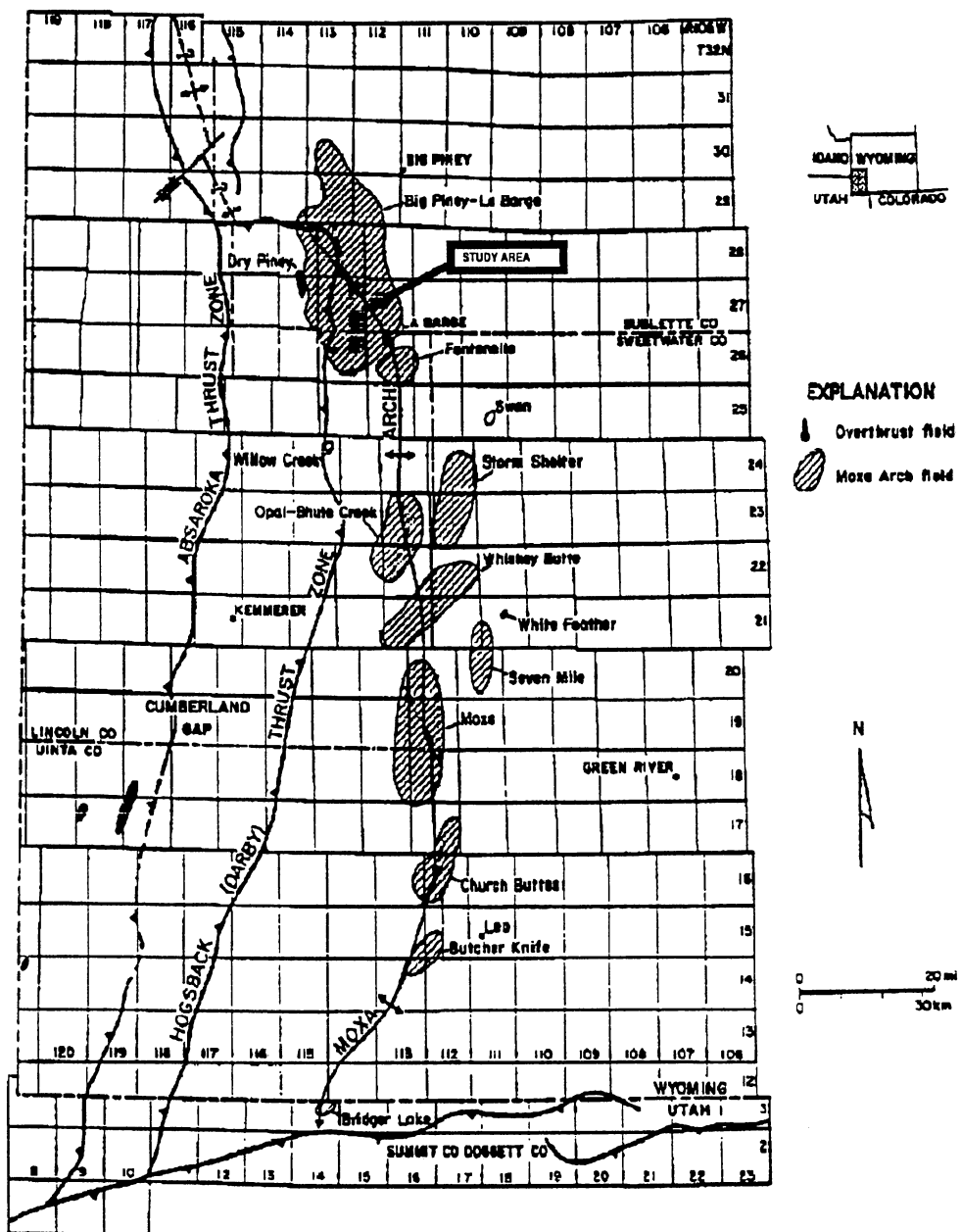


Figure 1. Geographical location of the study area showing the location of various Moxa arch and overthrust fields (from Hamlin, 1991)



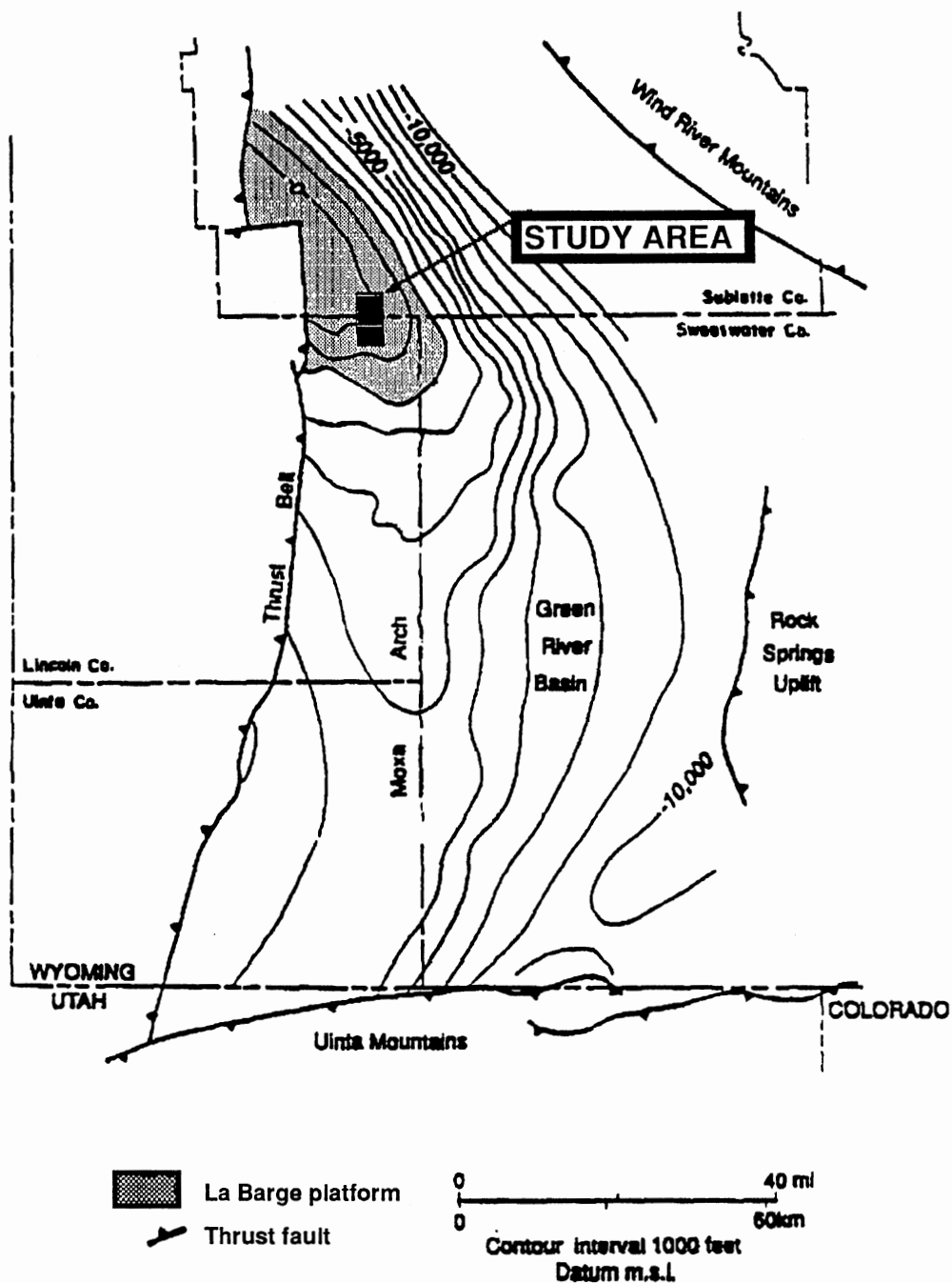


Figure 2. Major structural elements of the Green River Basin with contour map on the top of the Second Frontier, showing the Moxa arch and the La Barge platform (from Hamlin, 1991)

explanations for the unsatisfactory results of enhanced oil recovery (EOR) programs.

Active oil and gas production from sandstones of the Paleocene Hoback Formation (previously referred to as the Almy, Evanston or Fort Union Formation) along the eastern edge of the overthrust belt of western Wyoming, has been taking place since the 1920's. However, little work has been conducted dealing with these producing sands at the La Barge field because of the poor quality and limited availability of data, and complexity of structural influences in this area. For the purpose of this study, producing sands at La Barge were divided into five intervals separated by prominent shale markers (Figure 3). The intervals have been named TH-1 through TH-5, with TH meaning "Tertiary Hoback". In the course of this study, stratigraphic nomenclature, depositional environment, and geometries of producing sands were clarified through use of well logs, seismic data, cores, and production records. Results of this study will provide information for a better understanding of the continuity of the individual reservoir sand bodies within the field as well as providing insight on the tectonic influence on fluvial deposition.

Specific objectives were: 1) To determine depositional environments, age, stratigraphic nomenclature and reservoir characteristics of the individual producing sands. Field descriptions, cores, and palynologic data provided the basis for this.

2) To determine the nature of fault and fracture patterns in the field by mapping micro and macro-structural features, aided by aerial photo data. Minor faults or fracture patterns may be visible in the field, but they are difficult, if not impossible, to distinguish on well logs. Fault segmentation of the reservoir has been interpreted as the reason for poor EOR response (Hefta and Larson, 1978).

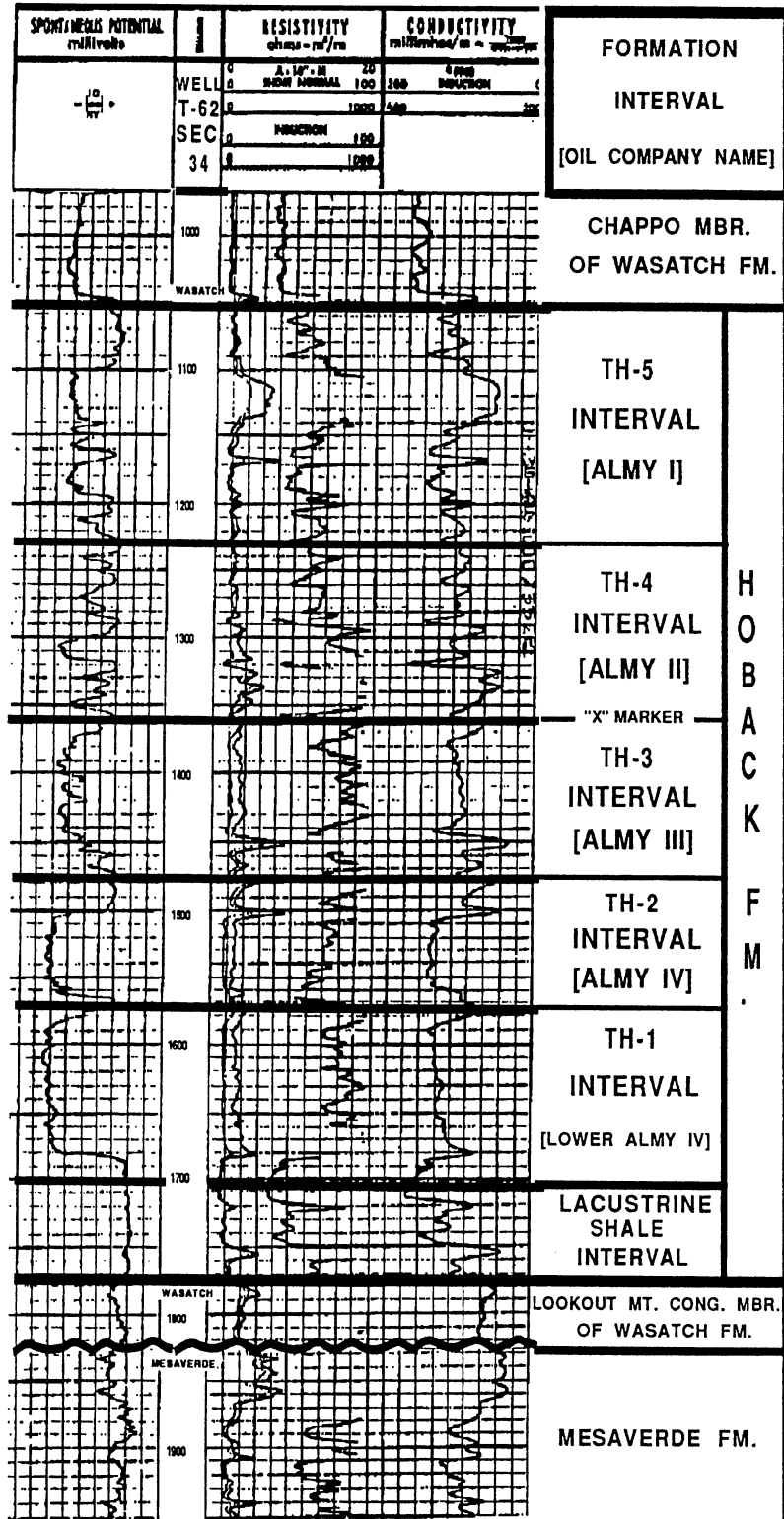


Figure 3. Type Log of Hoback Formation (well T-62, T27N., 113W., Sec. 34)

3) To study the subsurface stratigraphy of the Hoback Formation by constructing cross-sections, structure maps, net sand isolith maps, and interval isopach maps. Data for these maps came from well logs.

4) To understand the depositional environments of the producing units. This included a study of electric log shape distributions, sediment texture and composition variations, sand body geometry, and sandstone distribution throughout the field. Generalized paleoenvironment maps were made to determine source areas and trends of the various Hoback intervals. Data were derived from core descriptions as well as from well log data.

5) To outline the production history of the field, which included a cumulative production map as well as a discussion of the trap types. This also included an overview of the possible hydrocarbon migration paths into the field, as well as possible factors governing reservoir communication problems.

## Methods of Investigation

### Subsurface Studies

More than 600 wells within the study area were examined for possible inclusion into the data base. Problems with approximately two-thirds of these left only 229 wells for the study. Unreliable logging suites resulted in the drastic decrease in data points. Most wells drilled before 1950 had only a gamma ray run, whereas some wells were not logged at all. Gamma ray logs alone could not be relied upon for correlation due to the radioactive nature of the Hoback sands. Reliable data could only be obtained if a neutron, density or induction log was run with the gamma ray log. Since most of the logs used only partially penetrated the basal Hoback sand, it was not possible to prepare maps of the Tertiary-Cretaceous unconformity or the basal lacustrine shale interval (Figure

3). Since this study was concerned with the producing intervals of the Hoback Formation, exclusion of the lacustrine shale interval did not present a problem.

From the 229 data points used, subsurface maps were prepared to show: 1) structure of the La Barge field, 2) distribution and thickness of the various Hoback sands across the field and, 3) distribution of production. These maps include a structural contour map on the base of the lowest Hoback sand interval (Plate II), a structure map on the "X" marker (top of TH-3) (Plate III), a structure map on the Hilliard thrust plane (Plate IV), a net sand isolith map of each of the five identified Hoback intervals (Plates V, VI, VII, VIII, IX), an interval isopach map of intervals TH-2, TH-3 and TH-4 (Plates X, XI, XII), and a cumulative production map (Plate XVIII). A 50 percent clean sand cutoff was used in construction of the net sand isolith maps. To aid in depositional environment interpretation, the number of sand bodies, and the log shapes of sand bodies greater than 10 feet thick, were posted along with net sand values. Where more than one shape code was indicated, sand body shapes were posted from left to right in order of decreasing thickness. The various shape codes used are shown in Figure 4.

A total of five cross-sections were made (Figure 5): three west-east stratigraphic cross-sections; A-A' (Plate XIII), B-B' (Plate XIV), and C-C' (Plate XV); one north-south stratigraphic cross-section, E-E' (Plate XVI), and one structural dip cross-section across the producing structure, D-D' (Plate XVII).

Four cores were described. The descriptions included sediment composition, source, grain size and shape, as well as the types and sequence of sedimentary structures and bedding characteristics. This aided in determining the depositional environment of the Hoback Formation. Age determination was based on palynological evaluations of one of the cored wells.

## shape codes

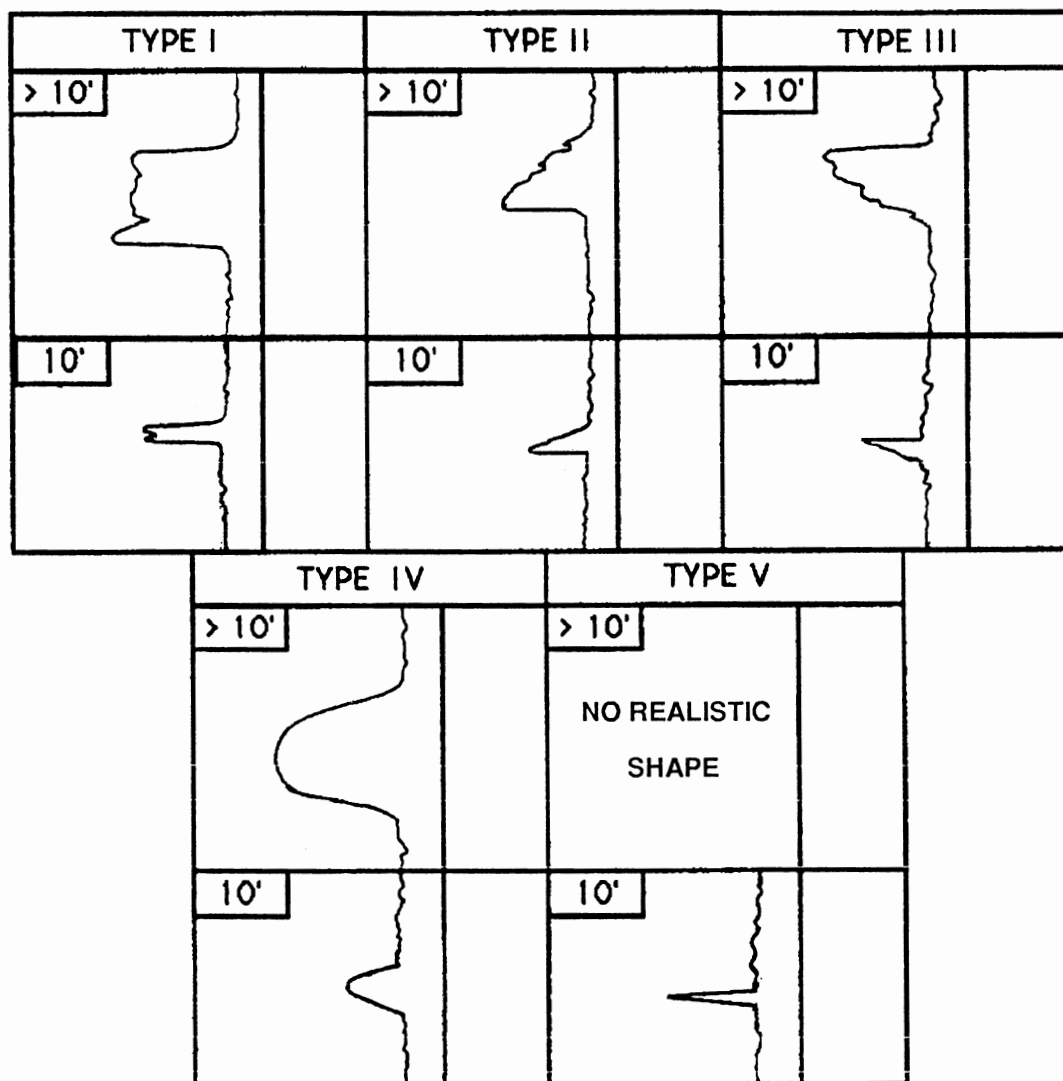


Figure 4. Electric log shape codes for net sand isoliths

Seismic data were available, but were not used because: (1) quality of data was poor, (2) the seismic grid was not sufficiently dense to conduct seismic stratigraphy, and (3) only one synthetic log was available near a seismic line and all other synthetic logs were one half mile or further away from the seismic

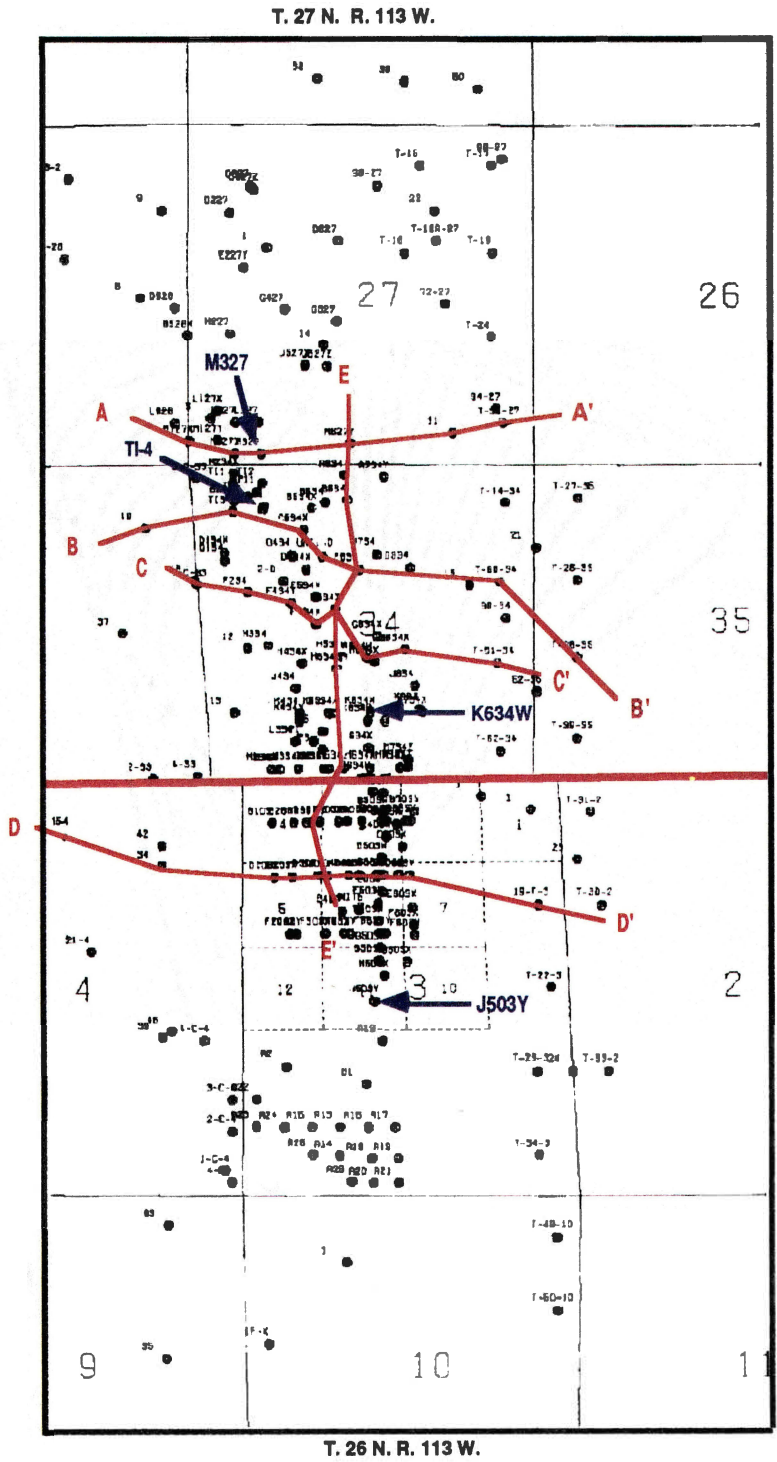


Figure 5. Base map showing cross-section locations in red and slabs core locations in blue

grid. Even with the dense well control, correlation of the Hoback sands was difficult. For these reasons seismic interpretation was omitted from the study.

### Field Studies

Methods of field investigation included examination of aerial photographs for possible structural features within the field area. Observed anomalies were examined. Other field investigations included outcrop examination of beds described as equivalent to the producing Hoback Formation and comparison of these outcrops to cores collected within the study area.

### Previous Investigations

#### Stratigraphy

The earliest recorded geologic investigation within the study area was done by Cope in 1873. He conducted an expedition up the Green River from the town of Green River, Wyoming to the mouth of La Barge Creek and continued up Fontenelle Creek nearly to its source. Cope's report contained very generalized geologic descriptions of the stratigraphy. Schultz did a very detailed study of the area in his 1914 report. Detailed descriptions of the stratigraphy and major structural features were given. He also gave a brief description of the occurrence of oil in the La Barge area, including an analysis of oil collected from one of the oil springs within the study area. Bertagnolli (1941), included a geologic map of the south part of the La Barge field, as well as outcrop descriptions within this mapped area. The most comprehensive and detailed surficial study of the local stratigraphy was carried out by Oriel in 1969 in a region just south of the study area.



It was not until 1969 that the producing Paleocene sands at the La Barge field would first be referred to as the Hoback Formation. Previous to this, authors and oil company workers called the producing sands the Almy formation (Schultz, 1914; Bertagnolli, 1941; Christensen and Marshall, 1950; Krueger, 1955, 1960; Michael, 1960). This interpretation was based on similarity in appearance of outcropping conglomerates within the study area to those of the type locality described by Veatch at Almy, Wyoming (Veatch, 1907). Mammalian paleontology conducted by Oriel, Gazin and Tracy in 1962 revealed an early Eocene age for the Almy at its type locality, while the surface "Almy" at La Barge was dated as Paleocene. Oriel's paper in 1962, confronted the Almy misnomer at La Barge Wyoming. Oriel renamed the surface "Almy Formation" in the La Barge area, calling it the Chappo Member of the Wasatch Formation and the subsurface producing unit, which does not outcrop here, the Hoback(?) Formation. In Oriel's work on the Fort Hill quadrangle (1969), which included the southern part of the La Barge field, he interpreted the upper part of the Hoback Formation as a facies change of the Chappo Member of the Wasatch. In 1980, Dorr and Gingerich presented more support for a Middle Paleocene, possibly even older, age for the Chappo Member in the La Barge area based on additional paleontologic evidence. They also suggested that most of the Hoback(?) Formation was older than the Chappo Member and claimed that only the uppermost Hoback(?) Formation interfingered with the Chappo Formation, based on their understanding of the Hoback Formation and its relationship with the Chappo in its type section to the north. In their cross-section across the La Barge field they show the Paleocene producing unit of La Barge as the Hoback Formation.

## Paleocene Production

Several authors have written papers specifically on the Paleocene producing sands of the La Barge platform and the surrounding area. Robbins (1940), conducted a study of the Tertiary producing sands of the north end of the La Barge field. In 1945, Lindsey wrote a Texaco in-house report concerning the Paleocene reservoir at La Barge which included several sample-log cross-sections and isopach maps of the north half of the field. Christensen and Marshall (1950), discussed the stratigraphy and structure of the La Barge field based on cross-sections and a structure map constructed from sample logs. Krueger (1955), provided brief descriptions of the individual producing Paleocene sands in the Big Piney field just north of the La Barge field. Krueger briefly mentioned the La Barge field and included a cross-section across the field in his 1960 paper that described the occurrence of natural gas in the western part of the Green River Basin. Also in 1960, Michael described the productive Paleocene in an area surrounding the La Barge field. Asquith (1966) conducted a study of the Late Cretaceous and Paleocene production in the Birch Creek unit, located on the east side of the study area. He also included depositional environment interpretations for the individual producing sands. In 1969, Dunnewald published a very brief report on the Tertiary oil and gas of the Big Piney and La Barge fields. Finally, in 1973 McDonald published several maps and descriptions of the Paleocene oil and gas production at La Barge.

Several Texaco in-house reports deal with EOR proposals and program results for the Hoback reservoir over the past 25 years. Important studies include those by Moreland (1968), Spelman (1976), Ulrich (1976), O'Hare and Ulrich (1976), Baker (1977), and Wendte (1989).

## Structural Geology

The Idaho-Wyoming-Utah thrust belt is one of the most studied thrust belt in the world and ample amounts of literature are available. A brief list of some of the important works pertinent to this study include: Eardley (1960), Armstrong and Oriel (1965), Mountjoy (1966), Oriel and Armstrong (1966), Lowell (1977), Ver Ploeg (1979), Jordan (1981), Wiltschko and Dorr (1983), Webel (1987), Fahy (1987), Gibson (1987), Beck and others (1988), and Craddock and others (1988).

The Moxa or Curches Butte arch, a structural feature forming the La Barge platform, was an important influence on the structural and sedimentological development of this region (Figures 1 and 2). Informative data concerning the formation, timing and influences of this feature are described by Thomadis (1973), Wach (1977), Wiltschko and Eastman (1983) and (1988), Kraig and others (1987) and (1988), and Woodward (1988).

Several papers dealing with structural geology of the La Barge area include: Blackstone's 1979 work on the geometry of the Prospect-Darby and Hilliard faults at their junction with the La Barge platform, Murray's 1960 article on interpretation of the Hilliard thrust fault, Kraig's and Wiltschko's 1988 paper which analyzed calcite fabric of the Madison Formation for stress orientations prior to the Darby thrusting to quantify the strain effects of uplift of the Moxa arch on Darby thrust orientation, and Hefta's and Larson's 1978 report on fault interpretation of the southern half of the La Barge field.

## CHAPTER II

### STRUCTURAL FEATURES

#### Tectonic Setting

The Green River Basin of western Wyoming can be classified as a continental multicycle craton margin (Klemme, 1980), an intracratonic, yoked basin (Krumbein and Sloss, 1963), and a perisutural basin on a rigid lithosphere associated with a compressional megasuture (type 222) (Bally and Snelson, 1980). The principle synclinal axis of the structural basin trends approximately N 30° E, with a minor axis developed to the north in the Pinedale area trending N 30° W (Fidlar, 1950). The Green River Basin is bounded to the north by the Gros Ventre Mountains, to the northeast by the Wind River Mountains, to the east by the Rock Springs uplift, to the south by the Unita Mountains, and to the west by the overthrust belt (Figure 6).

#### Gros Ventre Mountains

The southwest flank of the Gros Ventre Mountains confines the Green River Basin to the north (Figure 6). Although this range is less than one third the size of the Wind River Mountains, the two are similar in age and structural style (Horberg, 1949). The Gros Ventre Mountains are a small granitic cored symmetric anticline which trends northwest-southeast with a gently dipping northeast flank and a steep southwest face. It is separated from the Wind River anticline by a shallow syncline and is the product of southward thrusting along

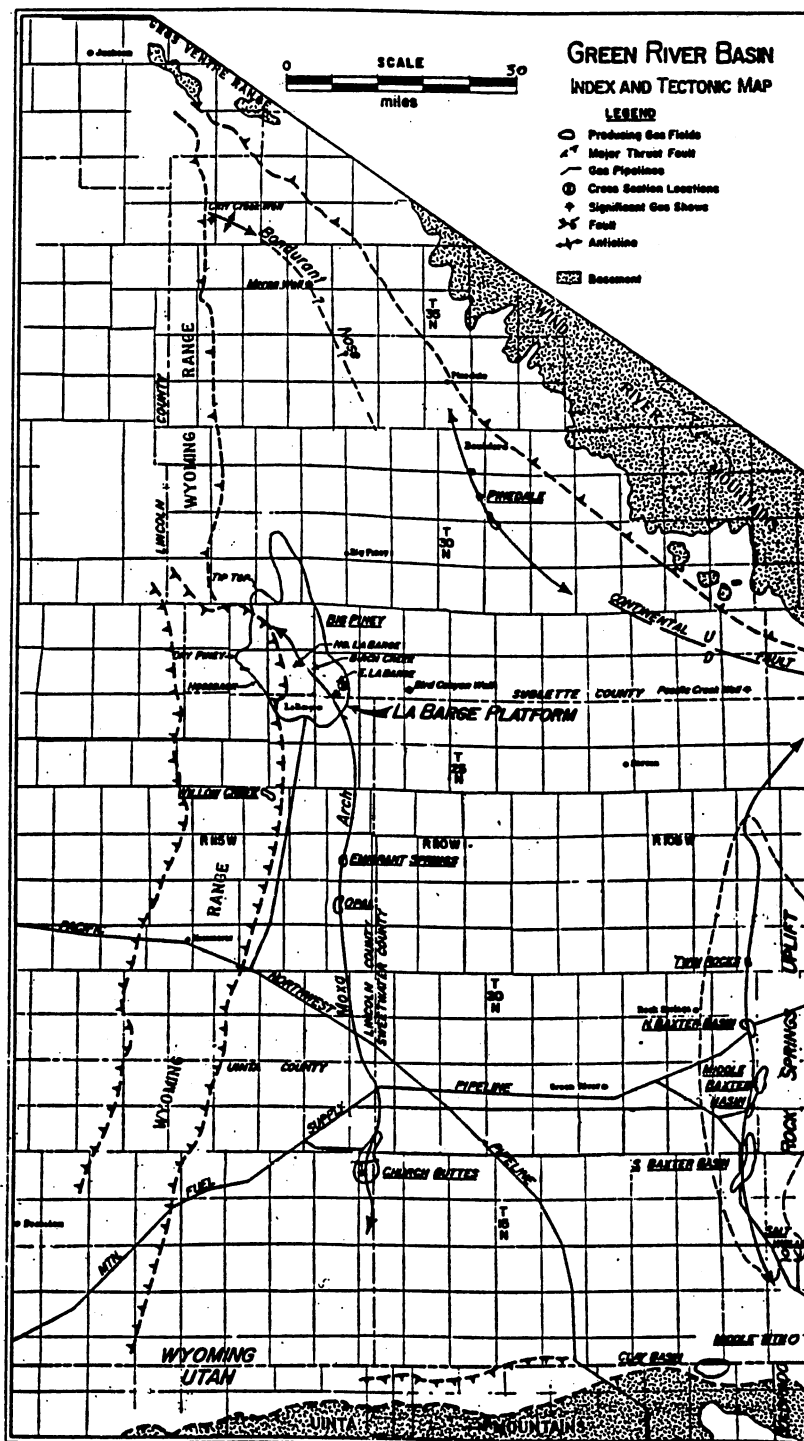


Figure 6. Generalized tectonic map of the Green River Basin showing major tectonic elements (modified from Krueger, 1960)

the Cache thrust. The feature is divided into three large blocks by north-south transverse faults. Orogenic movements of the Gros Ventre Mountains occurred from the Late Cretaceous to Late Tertiary (Spearing, 1969).

### Wind River Mountains

The Wind River range is a northwest trending asymmetric anticline (Figure 6). This feature represents asymmetric folding along an arcuate trend involving extreme deformation of the Precambrian, followed by overturning and thrusting (Berg, 1962). The asymmetric anticline has low dips on the northeast flank and very steep to overturned dips on the thrust-bounded southwest flank. Tertiary and younger strata overlap the southwest flank and conceal the extensive Continental thrust. The Precambrian crystalline core is exposed in an area 125 miles long and 25 miles wide (Berg, 1961). Orogeny was more or less continuous from Late Cretaceous until the end of the Paleocene (Berg, 1961). Material shed from the Precambrian core provided sediment for the Hoback Formation at La Barge.

### Rock Springs Uplift

Bounding the Green River Basin to the east is a large north-south trending anticlinal flexure known as the Rock Springs uplift (Figure 6). This feature is over 60 miles long and 35 miles wide and is somewhat asymmetrical with a steep western flank. The core is eroded only to the Baxter Shale (Hilliard Shale). Faulting at the north end and near the southeastern corner of the uplift indicates that folding occurred during the Late Eocene (Krueger, 1960).

## Uinta Mountains

The southern limit of the Green River Basin is defined by the Uinta Mountains (Figure 6). This range is tectonically anomalous because of its east-west trend, which is contrary to the general trend of the Rocky Mountain folding and faulting. The Uinta range is approximately 150 miles long and 30 to 40 miles wide, making it the largest east-west trending mountain range in the United States (Knight, 1950). The core of the range is composed of quartzite and massive silica-cemented sandstone of Precambrian age. This large anticlinal feature exhibits an imbricate northward thrust along its north flank, the trace of which is covered in part by Eocene lacustrine beds (Krueger, 1960). Evidence suggests that faulting continued along this thrust zone well into the Eocene, for these reasons the Uinta uplift is considered to be Laramide to post Laramide in age (Krueger, 1960).

## Overthrust Belt

The western limit of the Green River Basin is confined by the eastern edge of the Idaho-Wyoming-Utah salient of the overthrust belt. This zone of compression is part of the Cordilleran fold-and-thrust belt that extends from Alaska to Guatemala (Figure 7). The overthrust belt of Wyoming is characterized by low-angle, west-dipping thrust faults that have transported material eastward for up to 45 miles. The major thrusts of the Idaho, Wyoming and Utah salient of the overthrust belt from west to east are: Paris, Meade, Crawford, Tunp, Absaroka, Darby and Prospect (Figure 8). The Darby thrust is the only major thrust that affects the study area directly. A minor thrust called the Hilliard thrust by oil company geologists and the La Barge thrust by others will be discussed in detail. The Hilliard thrust is one of the youngest and

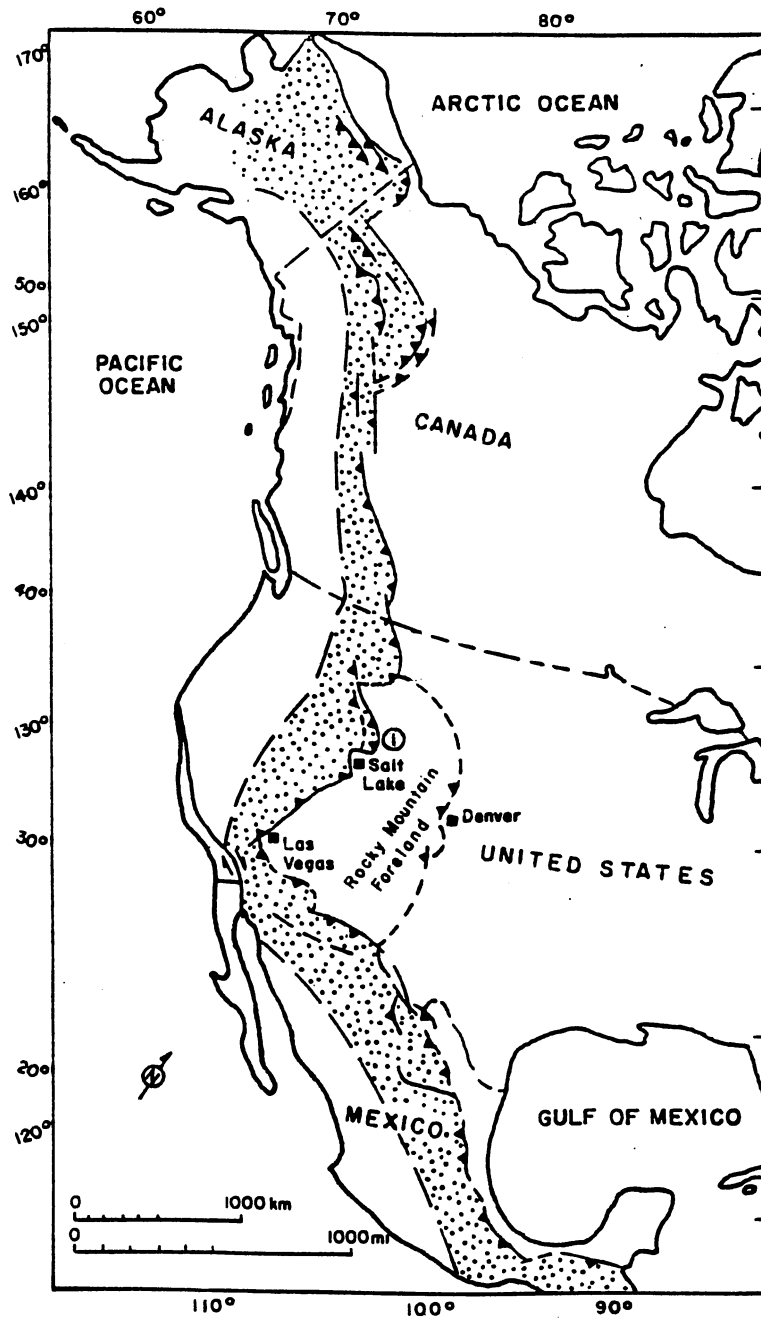


Figure 7. Trend of Cordilleran fold and thrust belt. The Idaho-Wyoming-Utah salient is shown by the number 1. Stippled area is outline of Cordilleran orogenic belt (from Ver Ploeg and De Bruin, 1982)



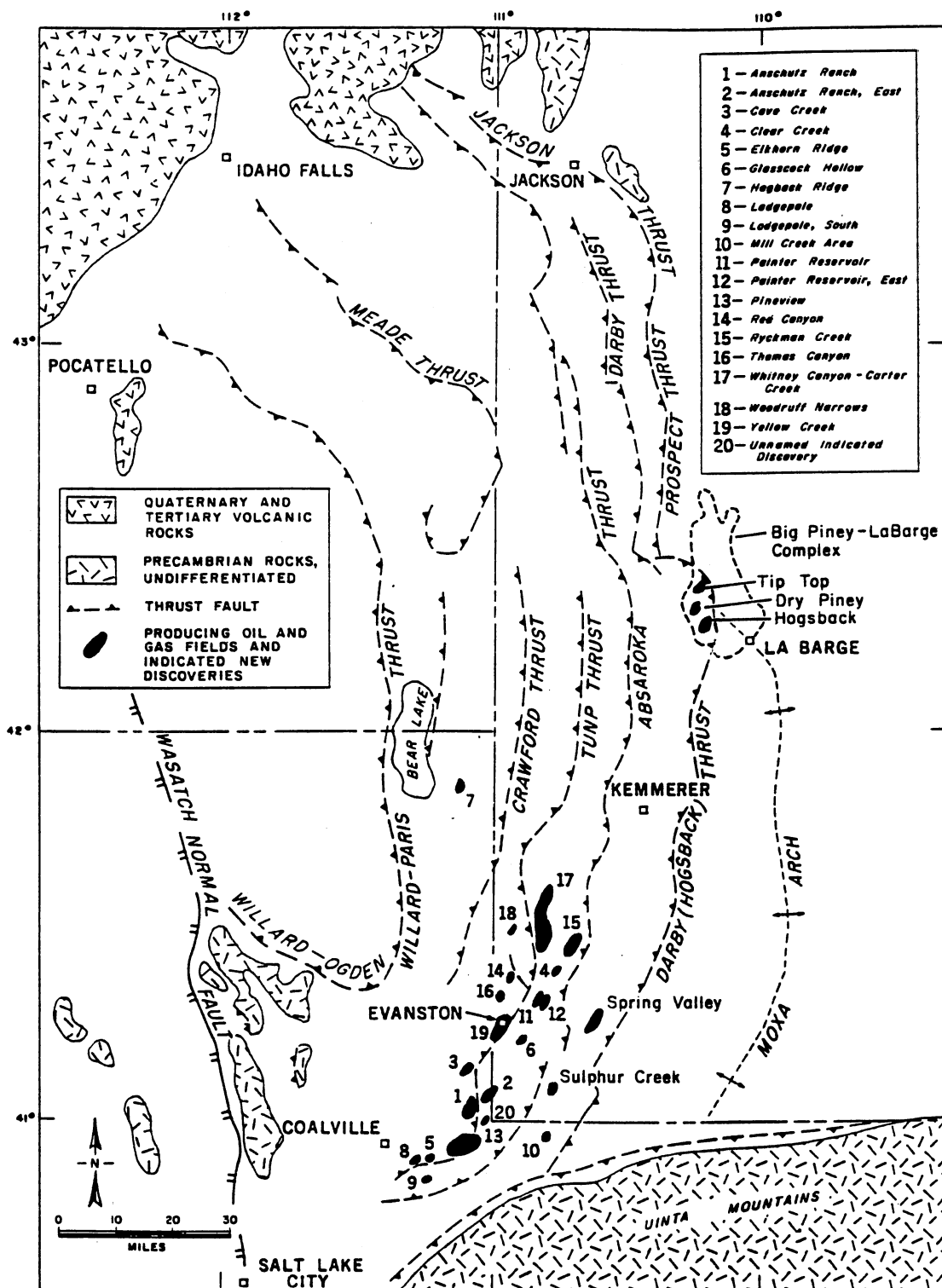


Figure 8. Index map of Idaho-Wyoming-Utah salient the overthrust belt showing overthrust oil and gas fields (from Ver Ploeg and De Bruin, 1982)

easternmost faults of the Overthrust Belt. This fault defines the western limit of the study area and is of extreme importance to the producing Hoback sands. Initial movement in the overthrust belt occurred in Late Jurassic (Portlandian) and continued until Early Eocene (Lost Cabin) (Wiltschko, Dorr, 1983).

### Influential Structural Elements

Several structural features affected deposition, distribution, composition and production of the Hoback Formation in the La Barge field. These features include: the Moxa arch (La Barge platform), the Darby thrust, the Hilliard (La Barge) thrust and several minor faults. Brief descriptions of the formation and orientation of these influential structures are given below. Timing of these features will be discussed at the end of this chapter.

#### Moxa Arch (La Barge Platform)

The Moxa arch is a broad, north-trending, gently folded, basement uplift extending north from the Uinta Mountain front for approximately 90 miles, where it bends northwestward for approximately 31 miles and is termed the La Barge platform (Figure 2). North of La Barge (T. 28 N.), the Moxa arch continues in a northwesterly direction where it is either scalped or overridden by the Prospect and Darby thrust sheets (Figure 6) (Kraig, Wiltschko and Spang, 1987). Seismic data revealed an east-dipping basement thrust (Moxa thrust) below the arch in this area. The arch is an asymmetric anticline with a steep eastern limb, except in the northern region where the structure is faulted and the west flank is steeper (Kraig, Wiltschko and Spang, 1987).

The northern portion of the Moxa arch, or La Barge platform is the region of concern. In this area the southwest limb has greater than 2,600 feet of structural

relief; hence the term platform (Kraig, Wiltschko and Spang, 1987). Subsurface studies suggest this feature was present during Hoback deposition and was later responsible for providing a locus for Hoback hydrocarbon migration and accumulation.

Thomaidis (1973) observed that the arch parallels the Absaroka thrust. Based on this he postulated that the arch formed in response to eastward compression along the Absaroka thrust, where a future thrust would have propagated given adequate compressional forces. Evidence from Late Paleozoic carbonate buildups associated with the southern end of the Moxa arch suggests that this feature formed here first and continued to uplift northward with time (Wach, 1977).

Webel (1987) explained the La Barge platform as having formed in response to backthrusting on the Moxa arch, resulting from compression on the arch from the Darby thrust sheet. She postulated that when the Darby thrust began to lose its compressional force it began to propagate to the surface, as a result of increased resistance to eastward propagation from the Moxa arch (Webel, 1987). Further compression on the Darby thrust sheet caused deformation of the opposing flank of the Moxa arch (east limb), which resulted in a low-angle backthrust (to the west) known as the Calpet thrust (Figure 9). Thrusting of the Moxa arch along the Calpet fault and other related backthrusts accentuated the lateral extent of this basement uplift through formation of drag folds on the east flank of the arch (Figure 9), resulting in formation of the La Barge platform.

#### Darby (Hogsback) Thrust

The Darby thrust is a north-south trending feature. A 13 mile east-west offset in its trend occurs just north of the study area, in the Snider Basin (Figure 8).

## LA BARGE PLATFORM

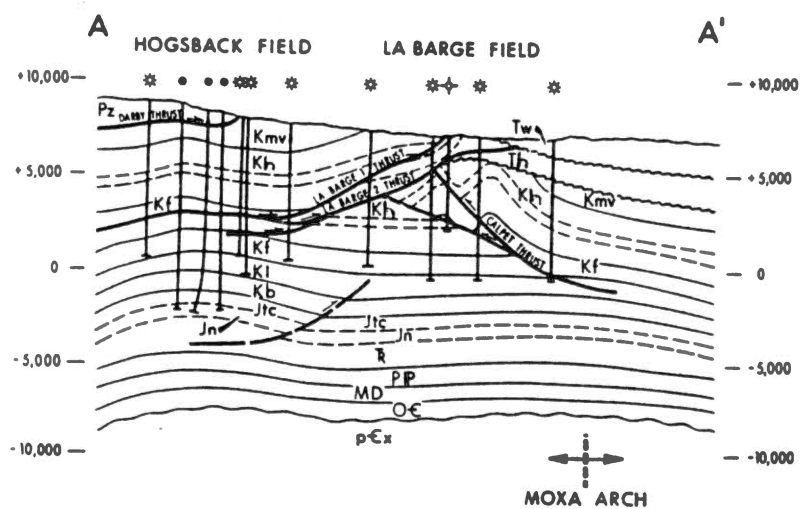
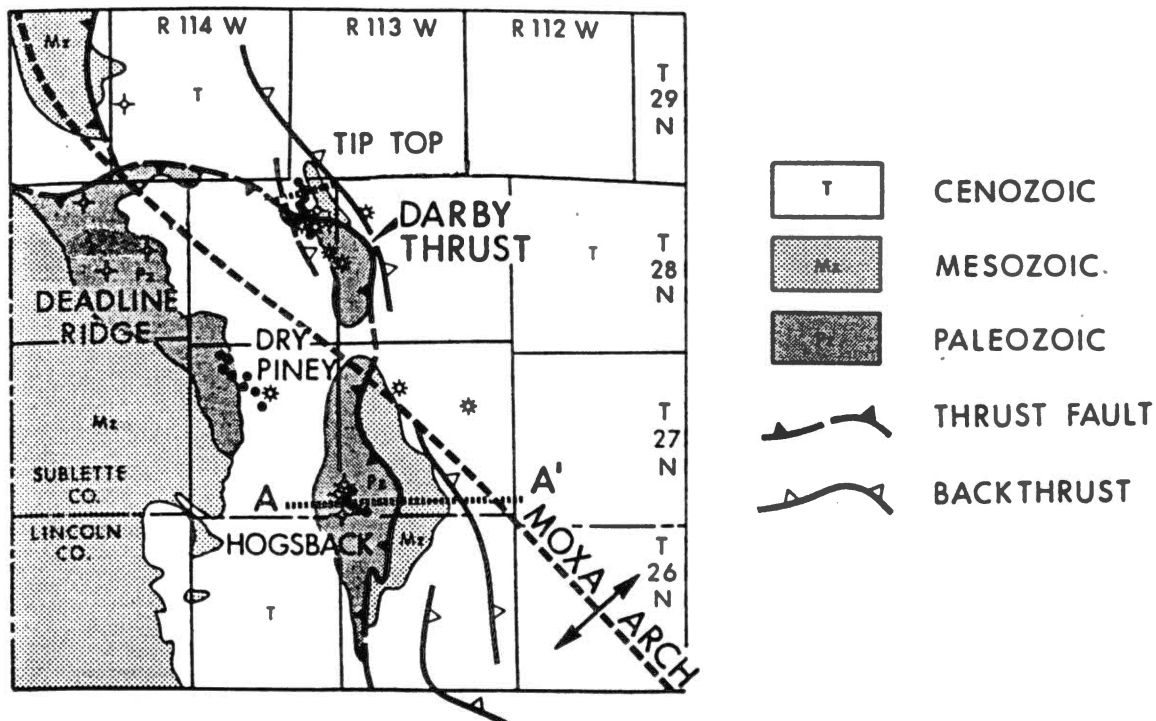


Figure 9. Cross-section through the study area showing major structural features. Interaction of Darby thrust, La Barge or Hilliard thrust, Calpet thrust and Moxa arch are shown. Horizontal and vertical scales are equal. (Tw=Wasatch, Th=Hoback, Kmv=Mesaverde, Kh=Hilliard and Kf=Frontier) Modified from Webel, 1987

Because of this offset in its trend, Armstrong and Oriel (1965) thought that the southern half of the Darby fault, which crops out along the Hogsback Ridge (Figure 10), was a different fault and therefore named it the Hogsback thrust. Early workers such as Schultz (1914) and Bertagnolli (1941) speculated that the Darby thrust continued south of the Snider Basin along Hogsback Ridge, but insufficient data at that time prevented acceptance of this idea. Blackstone (1979) presented six lines of evidence supporting the connection of these two fault segments. Based on this evidence he suggested abandonment of the term Hogsback thrust.

Although the Darby thrust is not located in the study area, it has had an important influence on the area. As mentioned, the Darby thrust was responsible for forming the La Barge platform which controlled the distribution of the onlapping Hoback sands. In addition, the Darby thrust provided sediment for the Lookout Mountain Conglomerate Member of the Wasatch Formation.

#### Hilliard (La Barge) Thrust

The Hilliard thrust (Figure 10) originates in sec. 3, T. 27 N., R 114 W., where it can be traced southward in the subsurface for 12 miles through the La Barge field to the Fort Hill quadrangle; here it is lost due to lack of data (Blackstone, 1979). The fault has no surface exposure, therefore descriptions come from subsurface data. The Hilliard thrust strikes approximately north-south with a dip of 30° west near the surface, to a nearly horizontal dip at depth. Maximum horizontal separation is at least 15,000 feet (Blackstone, 1979). This fault has been called the Tip Top, Hilliard and La Barge thrust.

Schultz (1914) did not map any faults east of the Darby thrust, although he suggested the possible existence of a thrust fault in the La Barge area along

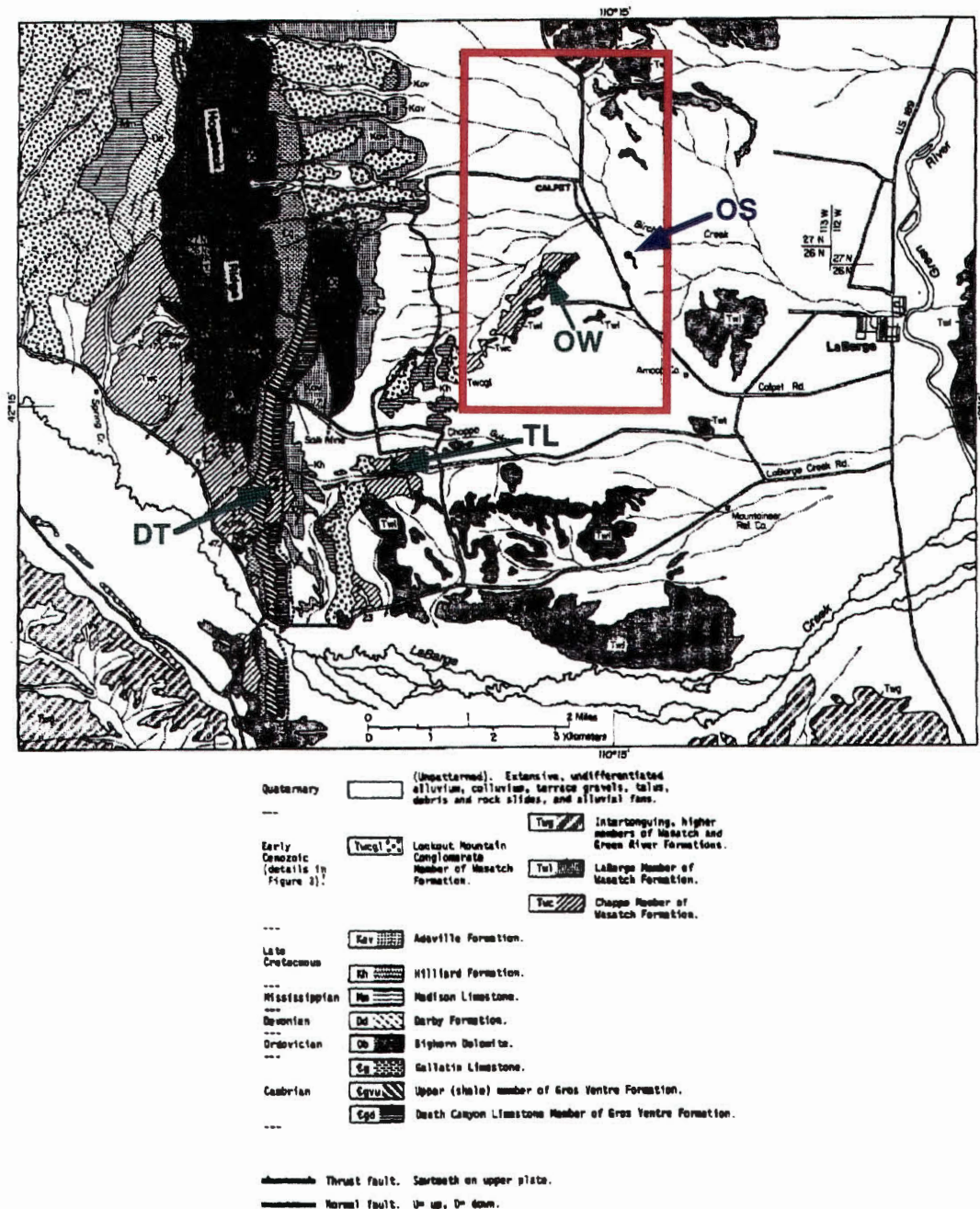


Figure 10. Geologic map of Hogsback Ridge, La Barge area, northern Lincoln and southern Sublette Counties, Wyoming. Study area is outlined in red. Outcrop locations of Chappo Member are shown by green arrows (OW=oil well locality, TL=type Chappo location and DT=Darby thrust locality). Location of oil spring is shown by blue arrow (OS=oil spring). Modified from Dorr and Gingerich (1980)

which oil could have migrated to the surface, forming the oil springs he examined there. Bartram and Hupp (1929) were the first to describe the Hilliard fault in the La Barge field. Believing that the fault was responsible for forming the La Barge anticline (La Barge platform), they named this fault the La Barge thrust. Christensen and Marshall (1950) were the first authors to call the thrust the Hilliard. Based on subsurface data from the La Barge field, they noticed that the La Barge anticline (La Barge platform) was formed prior to this thrust; therefore they argued for abandoning the name La Barge thrust. In Murray's (1960) descriptions of the Hilliard thrust he described it as terminating to the north in an east-west tear fault in the Tip Top Field. He explained the Hilliard thrust south of the study area as terminating in a fold near the edge of the La Barge platform where the Moxa arch begins to move east of the thrust belt. Blackstone (1979), disagreed with the interpretation of an east-west tear fault at the northern limit of the Hilliard thrust trace as described by Murray (1960) and Shipp and Dunnewald (1962). His reasoning was that no fault can terminate a low-angle thrust situation of which it is a part, since the tear fault must be limited to the hanging wall and terminate against the sole fault (Blackstone, 1979). He explained that based upon subsurface data, the Hilliard thrust terminates in sec 3, T. 27 N., R 114 W., where it is intersected by a younger unrelated east-west trending fault.

The study area for this project is bounded to the west by the Hilliard thrust, where the Cretaceous Hilliard Formation is thrust over the Paleocene Hoback Formation and Chappo Member of the Wasatch Formation. Well logs within the study area provided data sufficient to construct a fault-plane map on the Hilliard thrust (Plate IV). This map was used to delineate the position of its Hilliard trace on the other structural contour maps (Plates II, III). Three oblique tear faults have been interpreted within the Hilliard thrust plane, in areas of curvature of



the fault plane (Plate IV). Well data show the presence of the Hilliard thrust in the shallow subsurface below the La Barge field, but no outcrop exists due to concealment by the undeformed La Barge Member of the Wasatch Formation. The only evidence of this fault's existence at the surface within the field is in SW 1/4, NW 1/4 sec. 3. T26N., R. 113 W. of Lincoln County. At this location, approximately 148 feet west of well E 303 (Figure 10 and 21) along the north side of a gully, the Chappo was observed striking north and dipping vertically, as a result of deformation within the Hilliard thrust sheet. Other than this very limited exposure (20-30 feet), no other surficial expression of the Hilliard thrust was observed within the field

Although the Hilliard thrust was not responsible for formation of the La Barge platform, movement along the fault accentuated the size of the platform and its structural closure. It is also believed that loading caused by movement along the Hilliard thrust generated temperatures sufficient for oil maturation in the late Cretaceous shales, and provided a conduit for migration to the porous Hoback sands along the thrust and to fractures in the axial trace of the reactivated La Barge platform. This topic will be discussed further in Chapter VII.

### Other Faulting

Several other faults were observed in the study area, all of which were minor. Due to the absence of sufficient data to support the existence of these faults they were not included on any maps.

Hefta and Larson (1978) describe nine east-west trending faults in the southern half of the field. The exact nature of these faults is unclear, since they were referred to as both strike-slip faults and minor thrust faults. Some were drawn solely on minor elevation differences of nearby wells. Subsurface



correlations did not support these faults. The confusion in describing these faults, as well as the lack of supportive data, brings their existence into question.

Two wells in section 10 showed a minor thrust fault within the TH-2 interval (wells 1F-X and Unit 20). Due to the lack of other well control in section 10 it was difficult to determine if these two wells exhibited a single low angle thrust or two separate thrust faults. Well 1F-X showed 140 feet of repetitive TH-2 interval, while Unit 20 showed 110 feet of repeat section in the same interval. This may indicate a minor low angle splay of the Hilliard thrust. However, without further data it is difficult to even determine the trend of this fault across section 10.

Two wells along the eastern border of the study area cross minor normal faults. Well T-23-3 shows 20 feet of missing section in the TH-5 interval, and well T-33-2 shows 90 feet of missing section in the TH-3 interval. Based upon the position of the missing sections in these wells, it is unlikely that they represent stratigraphic thinning. It could not be determined if these two wells document the same or separate faults. Connection of the two faults is unlikely due to the distance between the two wells and the lack of supporting evidence from intervening wells. Again, lack of control points prevented mapping of these faults.

Although it does not deform the Tertiary units of the La Barge field, the Calpet thrust does exist below the Tertiary unconformity. The Calpet thrust is a north-south trending feature which bends to the northwest with the Moxa arch north of the study area. The thrust plane has a dip of 30° to 40° east and a horizontal separation of at least 3,000 feet is evident (Blackstone, 1979). Because the Tertiary strata conceal all expression of the Calpet thrust, it was not until the late 1960's that it was first described by workers of the Calpet Corporation. As mentioned earlier, Webel (1987) described this fault as a backthrust formed in

response to stress on the Moxa arch from Darby thrusting. This resulted in the formation of the La Barge anticline or La Barge platform (Figure 9).

### Timing of Important Structural Events

The timing of structural events is largely based upon the general geologic principle of cross-cutting relationships and subsequent dating of deformed versus undeformed units. For this reason the dates of these events are subject to an inherent degree of variance.

As expected in large compressional thrust belts, faulting within the overthrust belt exhibits progressively younger thrusts forming in the direction of tectonic transport (eastward) with time. All older thrust plates moved eastward as new fault planes developed at the front of the salient, and motion was transferred to new sole faults at the toe of the mass (Blackstone, 1979). Tear faults, folds and imbricate back limb thrusts provided releases for differential movement within individual thrust plates.

Thrusting within the overthrust belt began in the Late Jurassic with initial movements of the Paris thrust and continued through the Eocene with movement of the Hilliard (La Barge) thrust (Wiltschko and Dorr, 1983). Further discussion of timing will be limited only to thrusting directly affecting the study area. Diagrammatic representation of most of these structural events can be seen in chapter VI, where a series of figures depict the changing paleoenvironment of the study area.

Initial uplift along the Moxa arch in the La Barge area began during the Turonian or early Late Cretaceous. Indications that major uplift of the Moxa arch occurred at this time would include thinning of the Upper Cretaceous Frontier Formation, deposition of a Hilliard bar sand along the trend of the arch

and the presence of an angular unconformity at the base of the Paleocene-Upper Cretaceous boundary (Kraig, Wiltschko and Spang, 1988; Dunnewald, 1969).

Initial folding and minor faulting of the Wind River and Gros Ventre Mountains occurred approximately 72 million years ago, during the Campanian or Late Cretaceous (Wiltschko, Dorr, 1983). Berg (1961) supports evidence of this from ages of flanking basin deposits, as well as from cross-cutting relationships of minor faults along the southwestern limb of the range.

Final major movement of the Absaroka thrust occurred during the Latest Cretaceous (Late Campanian or Early Maestrichtian), as evidenced by dating of the Hams Fork Conglomerate Member of the Evanston Formation which was shed from the thrust plate during thrust movement (Wiltschko, Dorr, 1983). It is possible that minor deformation of the Darby thrust sheet began at this time in response to the final stress buildup on the Absaroka thrust.

Movement of the Darby and Calpet thrusts occurred during the Early to Middle Paleocene. Judging from the amount and aerial extent of the conglomerate shed from Darby thrust movement, it is evident that movement on the northern segment of the Darby thrust (Hoback Basin area) was much greater than that of the southern segment near the study area. This can be explained by partial stress release of the Darby thrust sheet in the La Barge area along the Calpet backthrust, as described by Webel (1987). Westward movement along the Calpet thrust formed a drag fold on the east limb of the Moxa arch which in turn formed the La Barge anticline (Figure 9). Evidence of this comes from the fact that the Calpet thrust is truncated by the younger Hilliard thrust (cross-cutting relationship) and its trace is unconformably overlain by the Lookout Mountain Conglomerate Member of the Wasatch Formation.

The presence of the Lookout Mountain Conglomerate Member of the Wasatch Formation which blankets the Tertiary-Cretaceous unconformity at La Barge, is interpreted as evidence of initial Darby thrusting within the study area (Wiltschko and Dorr, 1983). Age dating from the base of the overlying lacustrine shale interval of the Hoback Formation (Asquith, 1966) indicates a possible latest Early Paleocene to early Middle Paleocene age for the basal tongue of the Lookout Mountain Conglomerate. As explained by Oriel (1969), this basal Tertiary unit can be traced to the south for approximately 100 miles along the eastern margins of the thrust. Much thicker equivalent conglomerate north in the Hoback Basin (Hoback Conglomerate) have been dated as Early to early Middle Paleocene (Guennel, Spearing and Dorr, 1973). All of these Early to Middle Paleocene conglomerates are interpreted to tie together in the subsurface and collectively represent synorogenic conglomerates shed from the first major movements of the Darby thrust (Wiltschko, Dorr, 1983).

Major movement along the southern extension of the Darby thrust is believed to have occurred in the Late Paleocene (Middle to Late Tiffanian). This is evidenced by mammalian age dating of a lacustrine unit of the Chappo Member of the Wasatch Formation (Dorr and Gingerich, 1980). This unit unconformably overlies the trace of the Darby thrust on top of Hogsback Ridge and is of Clarkforkian age (Figure 10). The age of movement is further evidenced by the much thicker Late Paleocene wedge of the Lookout Mountain Conglomerate Member, which thins eastward of the thrust and interfingers with the Chappo Member (Dorr and Gingerich, 1980).

According to Royse, Warner and Reese (1975), Prospect thrust movement to the north in the Hoback Basin was linked to the southern extension of the Darby plate in the Hoback Ridge area. They suggested that the Darby thrust south of the Snider Basin was reactivated during the Late Paleocene to compensate for

the movement of the Prospect thrust. This agrees with the relationship seen at La Barge which suggests major movement of the Darby thrust during this time.

The Hilliard thrust is the easternmost and youngest thrust of the overthrust belt (Wiltschko and Dorr, 1983). Movement along this thrust is well dated in the La Barge area, where the undeformed La Barge Member of the Wasatch unconformably overlies the deformed Chappo Member. Mammalian fossils date the Chappo Member as Early Eocene (Graybullian to Lysite), and the La Barge Member as late Early Eocene (Lost Cabinian) (Dorr, Gingerich, 1980). Based upon this evidence the Hilliard thrust moved eastward during the Middle to Early Eocene time. This movement deformed the La Barge platform (anticline) further, resulting in its present structural relief. Migration of the hydrocarbons which charged the Paleocene Hoback Formation at La Barge occurred during Hilliard thrusting.

The final episode of deformation in the La Barge area included a normal faulting event. A couple of minor normal faults were observed within the subsurface along the eastern edge of the field. Although no normal faults were observed at the surface within the study area, several were described southward by Oriel (1969). Oriel states that these faults formed prior to and after the late Early Eocene.

## CHAPTER III

### STRATIGRAPHY

#### Background

A rather complete sedimentary sequence has been identified along the western margin of the Green River Basin. According to Schultz (1914), the stratigraphic column of Wyoming attains its greatest thickness in the western part of the state, representing a sequence from middle Cambrian to the end of the Eocene. Recognizable unconformities occur throughout this interval. The Cretaceous-Tertiary unconformity is the most important to this study. Exposures of pre-Tertiary rocks surrounding the study area are scarce except for limited exposures within fault blocks of the overthrust belt. Because these exposures exhibit extreme structural complexity, the stratigraphy has been under continuous reinterpretation over time. Another complicating factor is the adoption of a unique nomenclature for equivalent units within the overthrust belt and the Green River Basin. Furthermore, a large portion of the stratigraphy for the western margin of the Green River Basin is based on subsurface data alone and is therefore fairly recent. All these factors combined have led to a composite stratigraphic column for the western Green River Basin which has been compiled from data spanning over ninety years of work (Plate I). Since this study is concerned with the early Tertiary, in particular the Paleocene, descriptions of the Late Cretaceous to Eocene will be discussed in order to set

the stage for Paleocene deposition. For descriptions of older Mesozoic as well as Paleozoic units in this region, refer to Schultz (1914) and Oriel (1969).

### Late Cretaceous

During the Cretaceous, several marine transgressive and regressive episodes flooded and drained the Western Interior foreland basin of North America. At the earliest Albian (latest Early Cretaceous) the Mowry sea reached its greatest extent (Figure 11), only to begin its long regressive episode during the Late Cretaceous. During this regressive episode the Frontier, Hilliard and Mesaverde Formations were deposited. Important transgressive episodes are evident throughout this time along the western margin of the Green River Basin, but the dominant trend was a major marine regression. For this reason the Late Cretaceous units show a general trend of marine, to marginal marine, to continental deposits as the Cretaceous period came to a close.

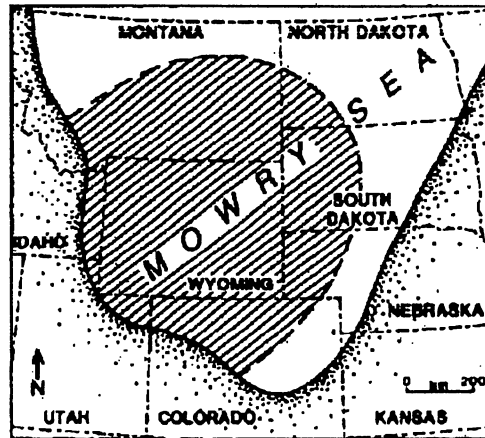


Figure 11. Late Albian paleogeography of the southern terminus of the Mowry sea at its greatest extent. Region of Mowry Shale and Aspen Shale deposition is shown by diagonal pattern. (from Davis, Byers, and Pratt, 1989)

### Frontier Formation

The Frontier Formation of the western margin of the Green River Basin, represents an early Late Cretaceous marginal marine unit. It was first described by Knight in 1902, as a coal-bearing formation containing a prominent sandstone layer (Schultz, 1914). Cobban and Reeside (1952), described approximately 2000 feet of exposure at its type location at Frontier, Wyoming. However, these descriptions indicate a rock unit strikingly different in composition and thickness from the Frontier described from core below the Darby thrust. These differences are so great that stratigraphic names for rocks found near the Rock Springs uplift of south central Wyoming are sometimes used for rocks below the thrust (Krueger, 1960), rather than the nomenclature of westernmost Wyoming. Comparative descriptions of Cretaceous rocks above and below the thrust are beyond the scope of this study, but brief descriptions of the sub-thrust Frontier at La Barge Field are given.



Approximately 2,200 feet of the Frontier Formation is present beneath the Darby thrust within the study area, as shown by well log data ( Figure 12). As evident from Figure 12, the Frontier Formation consists mainly of mudstone with three prominent, hydrocarbon productive sandstone units that are informally referred to in descending order as, the first, second, and third Frontier sands. Petroleum geologists have designated the top of the first sand and the base of the third sand as the formation's contacts, except in areas where the upper sandstone is not well developed or evident. In these cases electric-log properties are used to define the top (Figure 12).

As mentioned earlier, the Frontier generally represents a marginal marine depositional environment. On the La Barge platform the Frontier varies from predominantly marine to nonmarine deposits. The basal sand (third sand) is a nonmarine distributary deposit as evidenced by core and well log data. Deposition of the second sand marked the beginning of the most widespread transgressive episode within the Late Cretaceous in this area. The second sand is interpreted as a wave dominated delta with associated delta-flank strandplains (Hamlin,1991), which prograded eastward given an increase in sediment and accommodation space due to thrusting from the west. The third sand is a deeper water off-shore bar that seems to be localized in a linear fashion consistent with the trend of the Moxa arch within the La Barge field. Elsewhere this interval is occupied by near shore mudstones and shales. The orientation of this off-shore bar is possibly related to the early stages of uplift of the Moxa arch. Major movement of the Moxa arch occurred during the latest Late Cretaceous to Earliest Tertiary (Wach,1977).



Figure 12. (1 of 3)

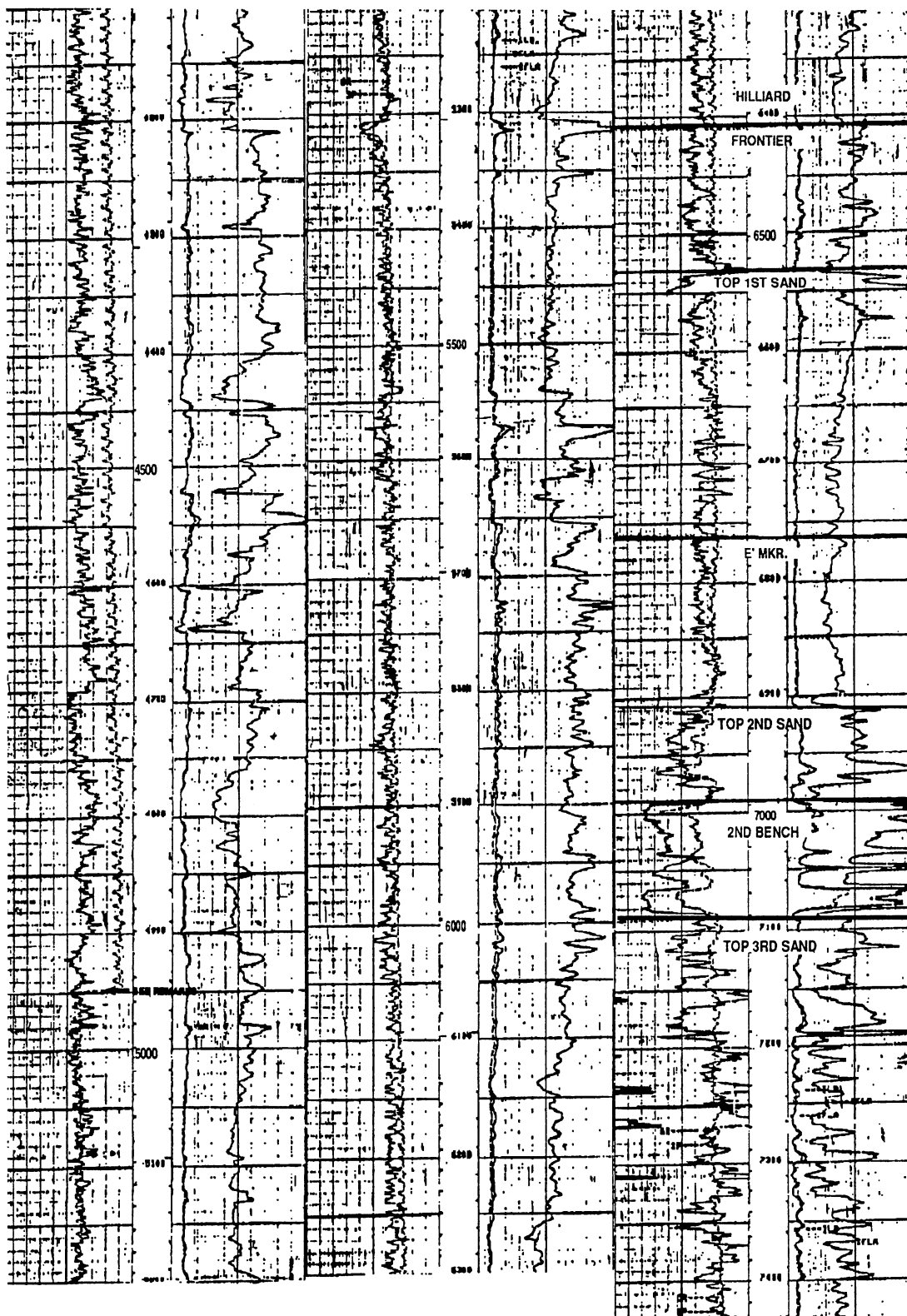


Figure 12. (2 of 3)

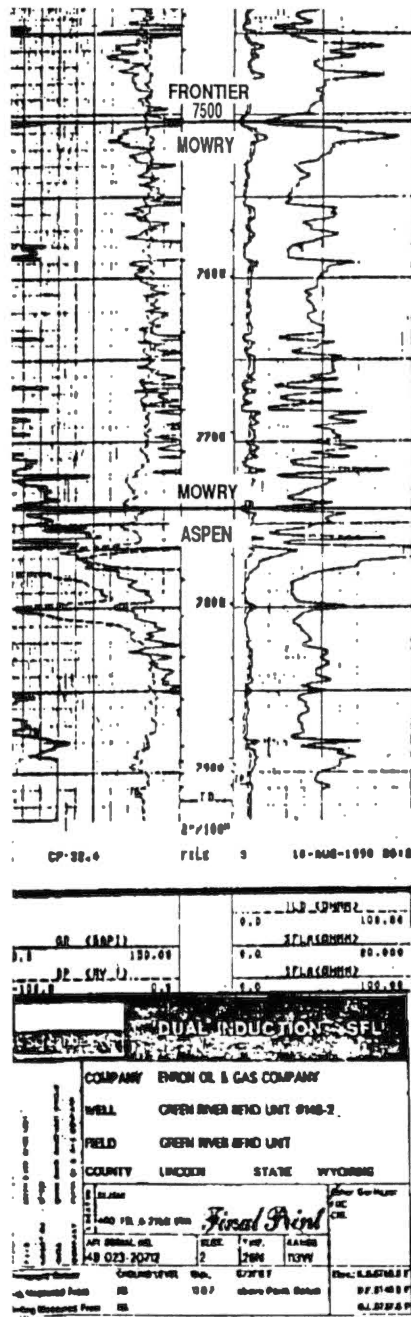


Figure 12. (3 of 3) Type Log of Late Cretaceous formations of the La Barge area. Log was taken from the Green River Bend unit to the east in order to show a complete, unfaulted section

## Hilliard Formation

The Hilliard Formation overlies the Frontier. Totalling approximately 3,600 feet thick, the Hilliard consists of dark-gray marine mudstone with interbedded siltstone and sandstone. Exposures of the upper portions of the unit are located just west of the study area, north of Chappo Gulch (figure 10). The mudstone here is dark gray, weathering light gray and contains mica and interbedded bentonites. The very fine grained sandstones and siltstones are angular grained, laminated, calcareous and light gray in outcrop. This sequence has been called the Hilliard Formation by Schultz (1914), Christensen and Marshall (1950) and Murray (1960), while Krueger (1960) and others referred to it as the Baxter Formation. Petroleum geologists in the region have referred to this middle Late Cretaceous unit by both the names, but the Hilliard is more commonly accepted. Reasons for this include the proximity to the type location of the Hilliard (southwestern Wyoming), as well as a younger (Montana) age for the Baxter in its type locality in the Rock Springs area.

The formation generally consists of three units: a lower black shale, a middle sandstone, and a thick upper unit of interbedded sandstone, shale and coal (Frerichs and Steidtmann, 1971). Outcrop studies conducted by Frerichs and Steidtmann northeast of the study area resulted in the development of a sea-level curve for the Hilliard based on Foraminifera and microplankton assemblages. The data demonstrate an overall regression with minor transgressive pulses (Figure 13), which agrees with the observations made earlier.

Depositional environments of the Hilliard can be supported by both lithologic and paleontologic evidence. The lower shale is undoubtedly of marine origin. The lack of coarse clastic sediment and abundant marine microfauna provide

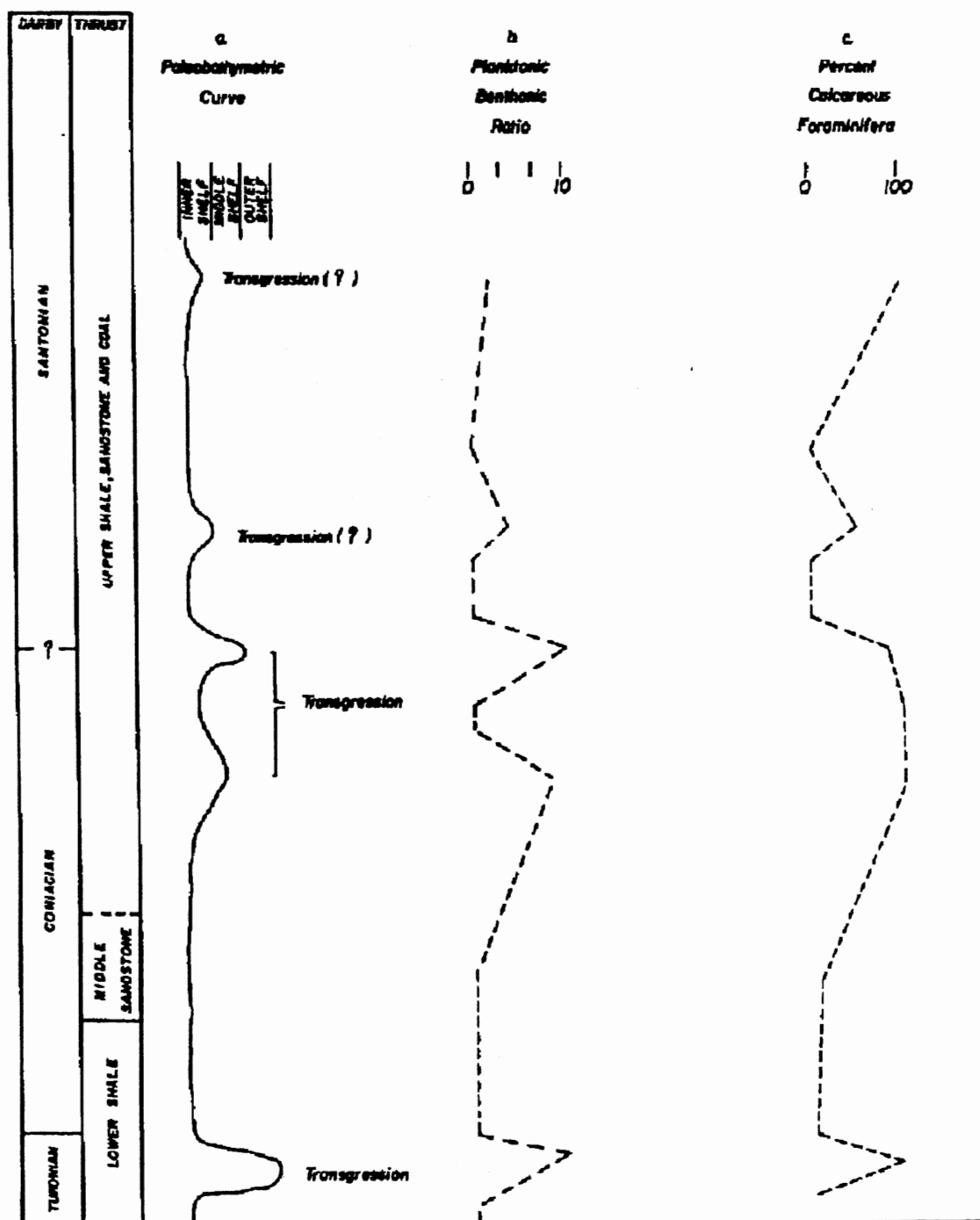


Figure 13. (a) Paleobathymetric curve of the Hilliard Formation showing the stratigraphic position of marine transgressions from measured sections surrounding the La Barge area. Note scale showing general location on shelf. (b) Plot of planktonic-benthonic Foraminiferal ratios, note the increase of planktonics associated with each transgression. (c) Plot of percent calcareous Foraminifera, note increases correspond to transgressions (from Frerichs, and Steidtmann, 1971).

overwhelming evidence to support this conclusion (Frerichs and Steidtmann, 1971). The fairly well developed, low-dipping trough cross-stratification and abundance of *Inoceramus* found in the middle sandstone unit suggest a beach deposit for this middle unit (Toots, 1961). The upper sandstone, shale and coal sequence is most likely representative of a paludal or mixed marine-nonmarine environment (Frerichs and Stiedtmann, 1971). Evidence comes from the lack of internal lateral continuity, abundant plant debris and coal units, a general lack of marine microfauna and microplankton, and low velocity, unidirectional current, micro-cross-stratification. The overall depositional nature of the Hilliard Formation is that of marine regressive depositional environments with minor transgressive pulses, as indicated by microfossil ratios as well as lithological variations. This represents the typical regressive sequence common in the Late Cretaceous of the Rocky Mountain region.

The Tertiary usually rests with angular unconformity above the Hilliard in the La Barge area except in the eastern portion of the field, where the Mesaverde Formation occupies this position (Figure 9).

### Mesaverde Formation

The latest Cretaceous Mesaverde Formation or Adaville Formation represents the close of the Mesozoic Era at La Barge. Outcrops of the Adaville Formation occur all along the Hogsback (La Barge) Ridge just west of the study area and were first described by Schultz in 1914. The abundance of coal within this unit in the La Barge area has been known for some time and as a result, it has been extensively strip mined. Usage of Mesaverde or Adaville is based upon personal convention or preference, as adequate data supports either usage based on stratigraphic age. The term Adaville Formation has been used

by some workers in the La Barge area because of the proximity of the type location to the study area. Problems arise with this reasoning, since the exposures east of La Barge Ridge cannot be traced westward into the belt containing the type Adaville (described by Veatch, 1907) above the Darby thrust, because of fault interrupted structure (Oriol, 1969). Due to the problems of correlating outcrop above and below the thrust, as well as the convention of other workers in this area who use Mesaverde for units within the basin block of the Green River Basin, the term Mesaverde Formation is used in this study.

The thickness of the Mesaverde on the La Barge platform varies widely due to the angular unconformity present at the Cretaceous-Tertiary boundary. In the subsurface, the thickest portions of the Mesaverde occur along the eastern flank of the study area, where it is approximately 800 feet (Figure 12). Throughout the majority of the field, the Mesaverde is only a few hundred feet thick to completely absent due to erosional truncation on the La Barge platform.

The lithology of the Mesaverde from base to top, ranges from a dark marine shale with siltstones and thin silty sandstones to a littoral, nearshore and marine sandstone of a barrier island or strandplain origin, to an upper lagoonal carbonaceous shale siltstone, thin sandstone, coal and lignite unit. This shallowing upward sequence of the Mesaverde Group has been interpreted by Asquith (1966) and others as a minor transgressive pulse followed by low-order cyclic progradation of the epeiric seaway shoreline in response to a major sea level regression. The transgressive and regressive limits of the Latest Cretaceous (Campanian) Western Interior sea is shown in Figure 14.



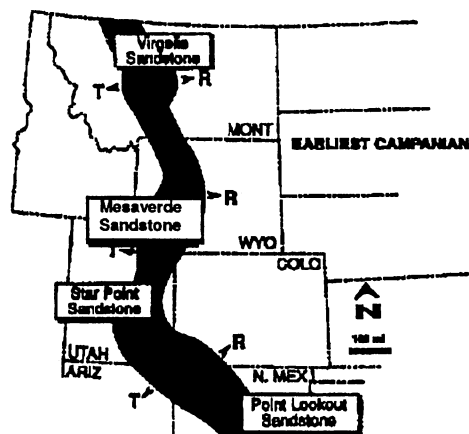


Figure 14. Approximate shoreline limits of Mesaverde or equivalent regression. Maximum landward limit of transgressive seas (T) prior to progradation is shown on the west. Maximum seaward limit of regression (R) is shown on the east (modified from Devine, 1991)

Devine (1991), proposes a different depositional model for the San Juan Basin equivalent deposits, which is also applicable for the La Barge platform. He suggests that costal swamps or lagoonal deposits of the back barrier environment are best explained as the product of episodic transgressions that interrupted the progradational history of the regional regressive sequence. Devine's explanation seems the most plausible, especially for the La Barge platform. Several transgressive-regressive couplets within a major regression seem more likely than a uniform gradual regression, especially when considering the tectonic influences in this area. During this time tectonic influences were actively controlling the early developmental stages of the La Barge platform.

## Tertiary

The Cretaceous-Tertiary boundary in the study area is represented by an angular unconformity, where the synorogenic Lookout Mountain Conglomerate Member of the Wasatch Formation overlies the Hilliard and Mesaverde Formations. The timing of this unconformity coincides with the final retreat of the sea in Wyoming. All later deposits are of continental origin, consisting of mainly fluvial or lacustrine beds. The hiatus represented here ranges from the end of the Late Cretaceous Maestrichtian to the end of the Early Paleocene Puercan, during which Darby thrusting and faulting of the Moxa arch by the Calpet backthrust occurred.

The Tertiary at La Barge is composed, in ascending order, of the Hoback, Wasatch, Green River and Bridger Formations. The Hoback and lower members of the Wasatch Formation (Chappo, Lookout Mountain Conglomerate and La Barge Members) will be reviewed in this study. These Tertiary units are composed of fluvial braided and meandering streams, lacustrine and arid area alluvial fan deposits. For information on the New Fork and Upper Tongues of the Wasatch Formation, as well as the Green River and Bridger Formations, refer to Oriel (1969) and Donovan (1950).

### Stratigraphic Nomenclature

Some of the problems in establishing a consistent nomenclature for the Tertiary in the study area were discussed in Chapter I under Previous Investigations. A confusing stratigraphic nomenclature resulted from early assumptions that the hydrocarbon producing unit outcropped within the field area. Based on this reasoning, descriptions of the producing formation came from outcrops of Wasatch units. These complications were partly the result of

the similarities in appearance and age of the Hoback and Wasatch Formations in the La Barge area but, as indicated in Chapter IV, several notable differences are observable. A final complicating factor was insufficient subsurface data prior to the 1960's. Before 1960, subsurface data consisted primarily of sample logs and cuttings which were of little help in distinguishing these subtle differences.

Due to these complications, the drab colored Paleocene producing sandstones of the La Barge field have been called the Almy Formation, the Almy Member of the Wasatch Formation, the Evanston Formation, the Fort Union Formation, and the Hoback Formation (Table I).

Use of the name Almy Formation and the Almy Member of the Wasatch Formations are incorrect due to discrepancies of age with the type Almy, which was discussed in Chapter I under Previous Investigations. Other factors include major compositional differences between the two. The Almy at its type location is composed primarily of a cobble to boulder size conglomerate with clasts of sedimentary origin, whereas the Hoback in the subsurface at La Barge consists mainly of medium to coarse grained sandstone beds of igneous and metamorphic provenance.

<b>ASSIGNED NAME</b>	<b>REFERENCE</b>
1) ALMY FORMATION	SCHULTZ (1914) TEXACO DOCUMENTS BERTAGNOLLI (1941) CHRISTENSEN AND MARSHALL (1950) KRUGER (1955, 1960)
2) ALMY MEMBER OF THE WASATCH FORMATION	MICHAEL (1960)
3) EVANSTON FORMATION	MURRAY (1960)
4) FORT UNION FORMATION	BERG (1961) ASQUITH (1966) DUNNEWALD (1969) CURRY III (1973) McDONALD (1973)
5) HOBACK FORMATION	ORIEL (1969) DORR AND GINGERICH (19800)

Table I. Stratigraphic names assigned to the Paleocene producing sands of the La Barge area

Reasons for abandoning the term Evanston Formation were developed during field investigations and are discussed under that topic in Chapter IV. The usage of Fort Union seems reasonable in regards to relative age and general composition, but this term has been applied to such a wide variety of sequences in many basins that it has unfortunately become a synonym for Paleocene (Oriel, 1969).

It was not until 1969 that the name Hoback Formation was first suggested. Oriel adapted this term from observed similarities in age and composition between the subsurface unit at the La Barge field with the type section in the Hoback Basin further to the north. The Hoback Formation named by Eardly and others (1944) and defined by Dorr (1952), is 15,000 feet thick in its type locality at T. 38N., R. 114 W., along the Hoback River, Sublette County, Wyoming (Oriel, 1969). It outcrops along the northwestern margins of the greater Green River

Basin (Hoback Basin area) and probably connects in the subsurface with the strata in the La Barge field (Figure 15).

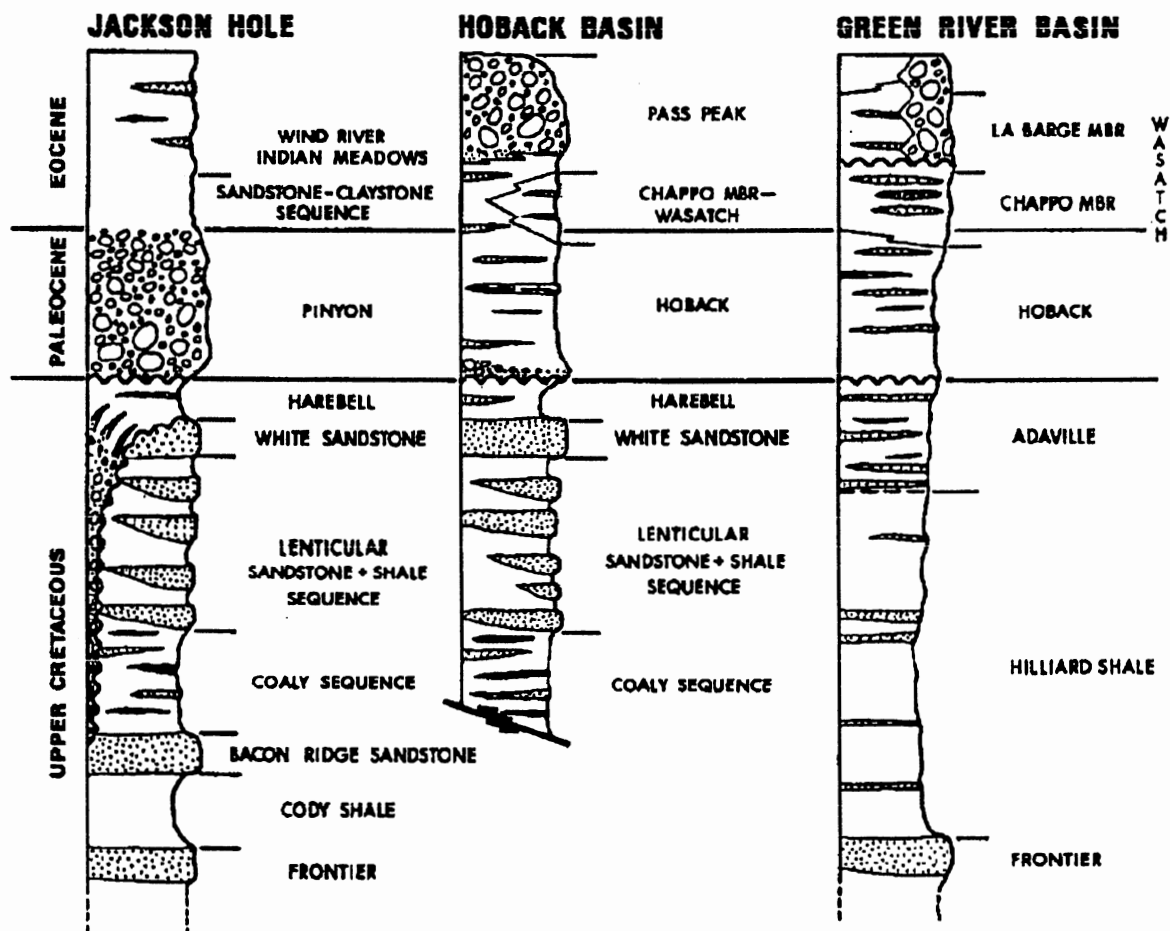


Figure 15. Correlation of upper Cretaceous and lower Tertiary units of western Wyoming (from Dorr, Spearing, and Steidtmann, 1977)

The only problem in equating the Hoback in its type area with the Hoback at La Barge is compositional differences. The majority of the Hoback sandstone units described in the type location are composed of rounded grains of

sedimentary origin, which according to paleocurrent analysis reveal a westerly source (Spearing, 1969; Dorr, Spearing, and Steidtmann, 1977). The Hoback at La Barge is composed mainly of igneous and metamorphic grains believed to be sourced from the Wind River Mountains to the northeast. An exception to a westerly sedimentary source for the Hoback in its type area is indicated by Dorr (1952), where he describes some of the lower Hoback sands as angular, quartz-rich, arkoses of igneous origin. He postulates the source being the Gros Ventre-Wind River uplift which was the only active basement-exposed uplift in this area during Hoback deposition. Spearing (1969), also mentions some problems with assuming a western source for all of the Hoback Formation in the Hoback Basin. He explains that some intertonguing of the Hoback sands in the south central part of the Hoback Basin exhibit a different composition and, therefore suggest a dominance of an additional source in this area.

These compositional differences can be explained by tectonic interaction prior to and during Hoback deposition. As mentioned in Chapter II, movement of the Darby thrust was believed to be much greater along the northern segment of this thrust in the Hoback Basin. This would explain the dominance of westerly-sourced sediment in the type area well into the time of Hoback deposition. The length of time this westerly sourced sediment would influence the study area was much less than that to the north, since movement along the Darby thrust near La Barge was only minor. Reasons for this were given in Chapter I. This fault movement is represented by the diamictite bed of the Lookout Mountain Conglomerate Member found on the unconformity surface (Figure 3). Because of these conditions, Hoback sands from the northeast were able to onlap on the La Barge platform as they prograded west toward the basin axis.

The lower Hoback sands described by Dorr in the Hoback Basin probably represent deposits from the east prior to overwhelming influence of sedimentary material shed from Darby thrust. The anomalous sands described by Spearing in the south central part of the Hoback Basin most likely represent the commingling of streams sourced from the eastern igneous and metamorphic terrain and the western sedimentary terrain. Due to distance from the western source and the presence of a basin of deposition in the central portions of the present day Hoback Basin where the majority of Hoback sediments collected, these deposits were dominated by material from the eastern source. This would explain the presence of minor amounts of sedimentary clasts, mainly chert, which are seen in the Hoback sands of La Barge. Further descriptions of Hoback depositional environments and varied source areas are discussed in Chapter VI. Because of this interconnection of the Hoback Formation of the Hoback Basin with strata at La Barge, the name Hoback Formation best describes deposits within the study area.

### Hoback Formation

The gray noncalcareous diamictite unit above the Tertiary-Cretaceous unconformity in the study area, is interpreted as the basal tongue of the synorogenic Lookout Mountain Conglomerate Member of the Wasatch Formation (Figure 3). This unit represents alluvial fan material shed by the Darby thrust sheet. Reasons for assigning this unit to the Wasatch Formation are based on similarities in composition of clasts and age of equivalent synorogenic units north and south of the study area. Further descriptions of this unit are given with the Wasatch Formation.

Based on this interpretation, the base of the Hoback Formation in the study area is the top of the lacustrine shale unit above the diamictite bed (Figure 3). Evidence from the few wells that logged this lacustrine interval and core from well TI-4 suggests that this lacustrine deposit was confined to the eastern flank of the La Barge platform. Core from well TI-4 shows the diamictite facies of the Lookout Mountain Conglomerate Member directly below interval TH-2. Confronted with this, and the fact that less than five percent of the logs studied actually penetrated the lacustrine shale interval or the unconformity, this lowermost interval of the Hoback was omitted from the study.

Five distinct productive intervals within the Hoback Formation were identified from well log data in the La Barge field as shown in the type log (Figure 3). These intervals were named in ascending order as TH-1 (Tertiary Hoback 1) through TH-5. Due to the onlapping nature of these sands onto the La Barge platform, TH-1 is only found on the eastern half of the field. Where TH-1 is missing, TH-2 is considered the basal sand unit. As stated by Curry (1973) and others, the top of the Hoback Formation is difficult to pick on well logs due to the similarities of the overlying Wasatch Formation. The top used here for the Hoback Formation is based on observable changes in sand distribution and overall electrical log variations above and below this point. Whether or not this is the actual top of the Hoback Formation is unknown, but the top picked includes all of the oil productive sands at La Barge, which is the major concern of this study.

The composition of the Hoback sandstone beds are very similar to each other. They are composed of moderately sorted, angular, medium to coarse grained, igneous, metamorphic and to a lesser degree, sedimentary grains, which are poorly cemented and have a salt and pepper texture resulting from black chert grains. The source of this sediment is from the Wind River uplift to



the northeast, with minor input from material sourced from the west. Reasons for this interpretation are discussed later in Chapter VI. Minor amounts of very fine grained to silty beds are also present, but they are relatively thin and few in number. Thin coal beds and stringers are also present, but they are not laterally extensive. For this reason the thin calcareous black to gray shales distributed throughout the formation were the only correlation markers available.

Well log and core data of the Hoback Formation suggest a transition from a sand-rich perennial braided stream deposit to an ephemeral braided stream deposit by TH-5 time. Reasons for this interpretation are given in Chapter VI. Thickness of the Hoback at La Barge varies, but the average thickness, including the basal lacustrine shale interval, is 670 feet.

The Hoback Formation at La Barge has been assigned a late Middle Paleocene (Torrejonian) to early Late Paleocene (Tiffanian) age. Palynological dating of the lacustrine shale interval in a well in the Birch Creek unit east of the study area (Asquith, 1966) supports the basal age limit. The age of the top of the Hoback is given as latest Early Tiffanian based on a maximum age of the overlying Chappo Member of the Wasatch Formation which outcrops within the field area (Dorr and Gingerich, 1980).

### Wasatch Formation

Within the study area the Wasatch Formation is composed of five members: (1) the Lookout Mountain Conglomerate Member, (2) the Chappo Member, (3) the La Barge Member, (4) a middle tongue named the New Fork Tongue, and (5) an Upper Tongue. A minor unconformity is present between the folded Chappo Member (previously referred to as Fort Union or Almy) and the undeformed La Barge member (Oriol, 1962). This Wasatch shows an interesting

intertonguing relationship with the Green River Formation which adds to the complexity of the interrelationships of all of these laterally changing members. A diagram showing this intertonguing relationship is shown in Figure 16. This study deals only with the Wasatch members in direct contact with the Hoback Formation. These include the Lookout Mountain Conglomerate Member and the Chappo Member. For description of the remaining Wasatch members as well as the Green River Formation and their interfingering relationship refer to Donovan (1950) and Oriel (1962).

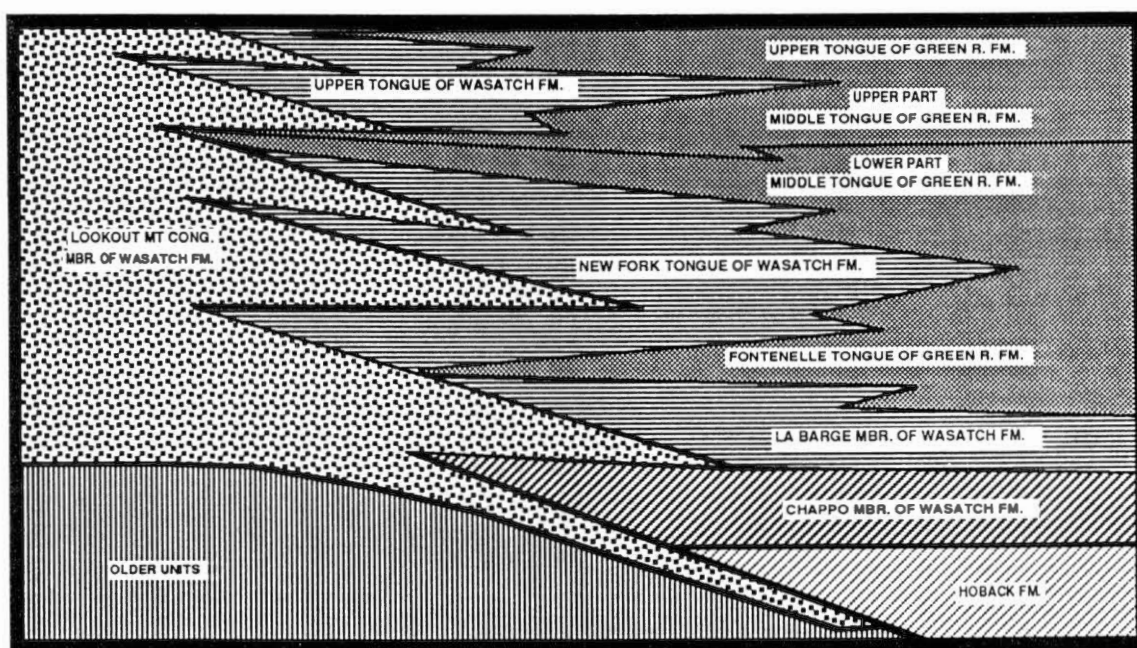


Figure 16. Tertiary stratigraphic relationships of the La Barge field area

Lookout Mountain Conglomerate Member of the Wasatch Formation. This unit represents a synorogenic alluvial fan deposit of the Darby thrust sheet.

Evidence of this comes from the composition, age, and distribution of this unit. The Lookout Mountain Conglomerate Member is dominated by conglomerate, but also includes gray to brick red interbedded diamictite, sandstone and mudstone beds (Oriol, 1962). This conglomerate member includes most of the strata assigned by Schultz (1914) to the Almy Formation along the eastern flank of the Wyoming thrust belt (Oriol, 1962).

A variety of pebbles are found within the Lookout Mountain Conglomerate, some of which include sandstone and quartzite from the Nugget sandstone, Ankareh and Wells Formations, and carbonate rocks from the Twin Creek and Thaynes Limestones, Phosphoria Formation and Madison Limestone (Oriol, 1962). The main constituents are quartzite and chert pebbles. Pebbles observed in well TI-4 consisted entirely of quartzite and chert. The diamictite bed at the unconformity surface mentioned earlier is the only facies of this unit seen in the subsurface within the field (Figure 3). This diamictite bed thickens toward its westerly source in the subsurface, except in areas where it is evident that interval TH-2 down cut and reworked this bed. Evidence for reworking of the diamictite bed was seen in core from well TI-4. Although this diamictite bed does not produce in the La Barge field, it does produce to the east in the Birch Creek field, where oil from the Mesaverde has seeped through the unconformity and has charged this conglomerate.

Due to poor exposure, the thickness of this unit at La Barge is not known, but further north an incomplete section of 1,000 feet is exposed, suggesting a possible thickness of several thousand feet. Only a few fossils have been found in this unit which suggest the upper parts as Lost Cabin age. In other parts of the Green River Basin (Hoback Sub-Basin) this peripheral conglomerate has been assigned a Paleocene to Middle Eocene age, which agrees with the age of active movement of the Darby thrust. Pollen dating of the lacustrine shale

dominance of fine grained overbank material.

interval given by Asquith (1966), indicates a possible latest Early Paleocene (late Puercan) to early Middle Paleocene (early Torrejonian) age for this basal bed.

Chappo Member of the Wasatch Formation. Conformably overlying the Hoback Formation is the Chappo Member of the Wasatch. The limited exposures of the Chappo within the study area reflect the anticlinal structure of the La Barge platform or Moxa arch. For this reason it was assumed by most early workers in this region that the oil producing sands of the La Barge field were from the Chappo Member of the Wasatch. As discussed in the section on field investigations, compositional and chronological differences between outcrop and core disprove this assumption. Composition, age and thickness of this unit are discussed under field investigations.

The implied depositional environments of the Chappo are lacustrine and meandering stream deposits with minor shallow oxbow lakes. The compositional nature of this unit suggests that it originated from a sedimentary source to the west in the overthrust belt. In addition to a change in source area from that of the Hoback, the Chappo Member may represent more arid conditions, as evidenced by the lack of coal beds in the Chappo, despite its dominance of fine grained overbank material.

## CHAPTER IV

### CORE AND FIELD STUDIES

#### Core Descriptions

Four slabbed cores were described to determine sedimentary structure trends and sediment composition, size and shape. Depositional environment interpretations were made based upon these observations and Maill's facies code classification system. Reasoning for interpreted depositional environment based on core and well log data is given in Chapter VI.

The locations of the four wells; M327, TI-4, K634W, and J503Y are shown in Figure 5. Cored intervals vary, but most include all or portions of intervals TH-2, TH-3, and TH-4. Interval TH-1 was not cored because none of the wells were far enough east to include this interval. None of the wells cored included interval TH-5 because this interval was not known to be productive at the time of coring. Only well TI-4 included the Lookout Conglomerate Member and the Tertiary-Cretaceous unconformity, therefore it was used for the palynology study.

Core descriptions with a correlated gamma ray log are included for each well and are found in Appendix A. Most siltstones and mudstones were found to be calcareous in nature, except for the black to dark gray fossiliferous and carbonaceous mudstones. Sandstones showed only very minor calcite and dolomitic cement and for the most part were poorly silica cemented and highly friable.

## Palynology of the Hoback Formation

Four core samples from well TI-4 were prepared for palynological analysis and sent to the Shuler Museum of Paleontology at Southern Methodist University. These samples were taken from the the diamictite bed of the Lookout Mountain Conglomerate Member and from several intervals of the Hoback Formation. The top, middle and base of the Hoback were sampled (Appendix A). Analysis of these samples revealed significant quantities of organic material but no intact pollen or spores. Although this analysis proved to be inconclusive, palynology data presented by Asquith (1966) provided a Middle Paleocene age for the basal part of the lacustrine shale interval. These data provide a minimum age for the Hoback Formation on the La Barge platform as well as a fairly good time constraint for initial movement on the southern segment of the Darby thrust.

## Field Investigations

Field investigations were conducted for three reasons: to examine the type locations of the Almy and Evanston Formations, to determine if outcrop in the field area is equivalent to the producing unit, and to examine regional and local structural features for their effect on Hoback sedimentation. Type locations for the Almy and Evanston Formations are conveniently located within a few miles of each other, outside of the town of Evanston Wyoming (Figure 17). The other outcrop areas were located in an around the La Barge area and are shown in Figure 10.

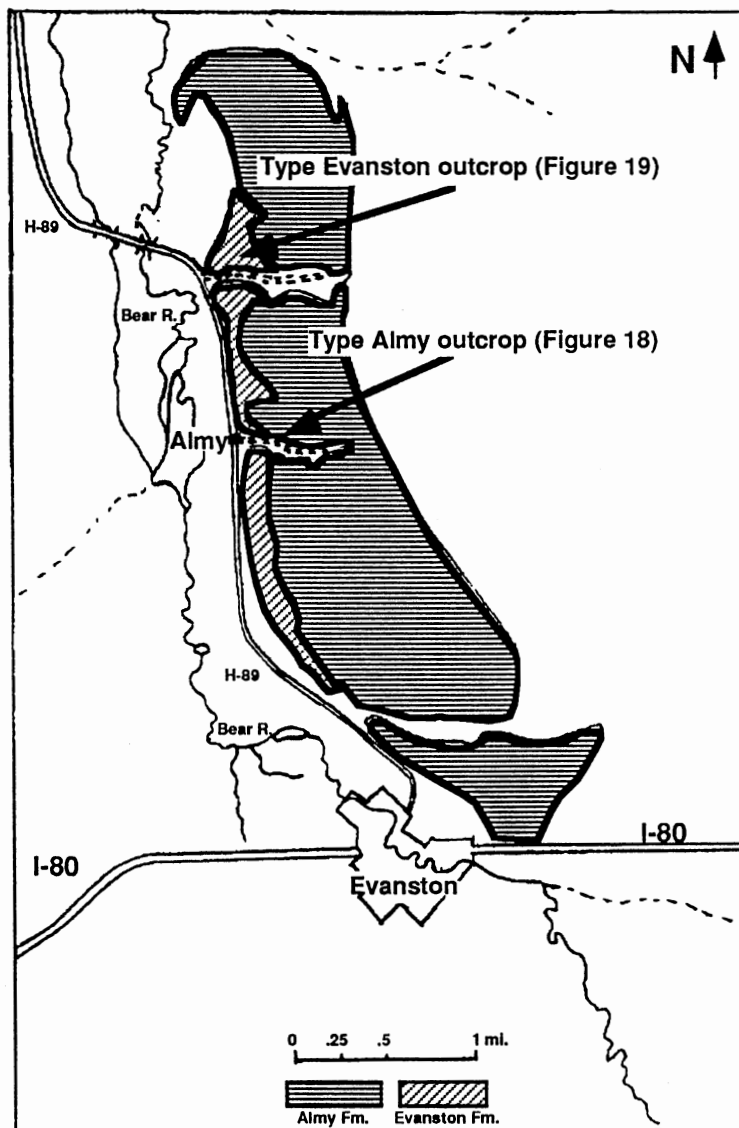


Figure 17. Outcrop locations of the Evanston and Almy Formations at their type locations

As mentioned earlier, the usage of the term Almy Formation at La Barge field has been abandoned in light of lithologic and age discrepancies with the type location at Almy, Wyoming. The purpose then, in examining Almy outcrop at its type location was purely historic. Figure 18 shows the large scale cross-

bedded conglomerates and coarse to cobbly sandstones observed at the type location.

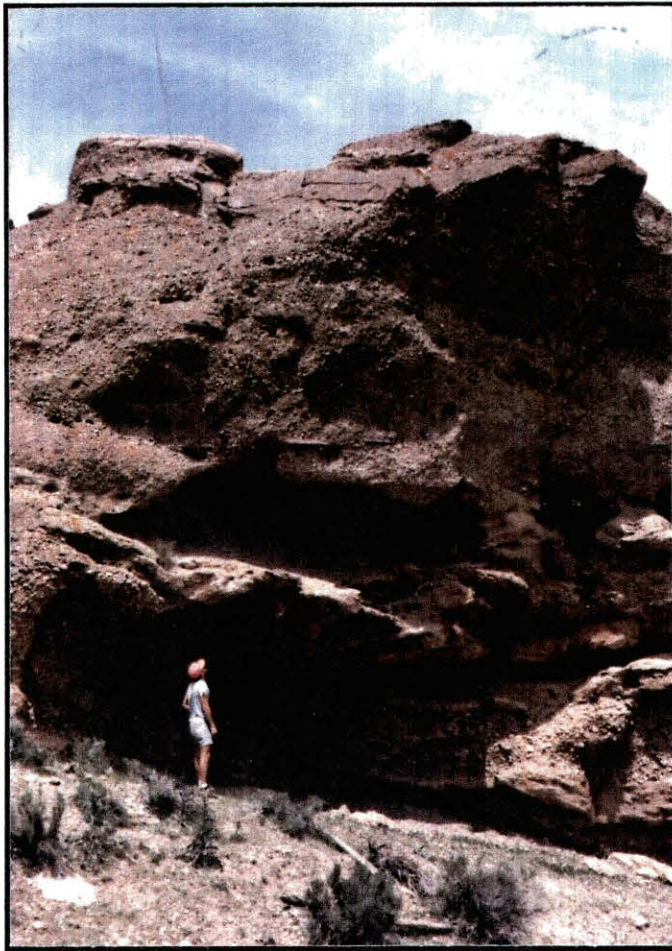


Figure 18. Outcrop of the Almy Formation at its type locality (see Figure 17)

The Evanston Formation had more importance in that it is time equivalent with the producing unit (Middle to earliest Late Paleocene) (Rubey, Oriel and Tracy, 1961). Examination of outcrop of the Evanston Formation at its type



locality revealed a larger percentage of shale and coal than that seen with the producing Hoback Formation of La Barge (Figure 19). The sandstones, when present in the Evanston Formation, lacked the arkosic, igneous and metamorphic rich grains of the Hoback at La Barge. The Evanston Formation is also believed to be an isolated deposit confined to the limits of the Fossil Basin. Therefore, due to the provincial and observed sedimentological differences of the Evanston Formation with those of the producing unit, the use of the term Evanston Formation, at La Barge, is not recommended.

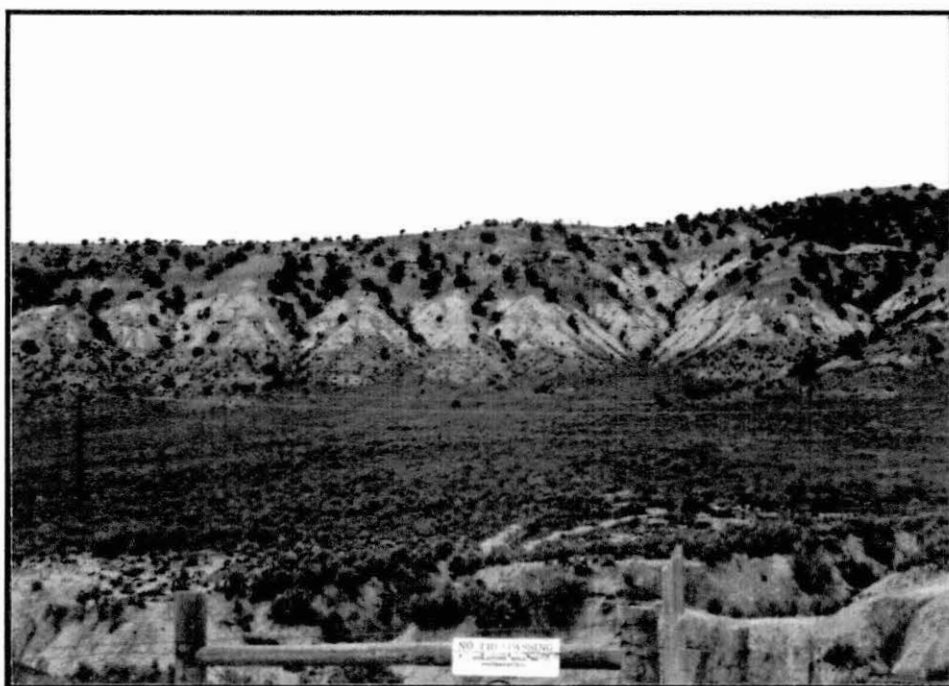


Figure 19. Type location of the Evanston Formation (see Figure 17)

Some authors (Christensen and Marshall, 1950; Asquith, 1966 and Dunnewald, 1969) suggested that the producing formation outcropped within

the La Barge field in an area described by Oriel (1969) as the lower most Wasatch or the Chappo Member of the Wasatch Formation. Several other outcrops of the Chappo Member in the La Barge area were described by Oriel (1962) and by Dorr and Gingerich (1980). During field work these outcrops were reexamined to determine their possible inclusion within the producing sand of La Barge (Figure 10). Findings were consistent with Oriel, Dorr and Gingerich in that these deposits differed from those observed in the core and are in fact part of the Wasatch Formation (Chappo Member).

Where exposed, the Chappo showed large amounts of mudstones and limestone in addition to the siltstones and sandstones. Core examined from the field showed only minor amounts of mudstones and no well developed limestone beds as seen in the Chappo on outcrop, although a fair amount of calcareous mudstone was observed in the core (Appendix A). The distinctive pisolite beds of the Chappo Member were not observed in the core. In outcrop, these pisolite beds ranged in thickness from 4 to 10 or more feet and were seen in most exposures. The coal beds and stringers found throughout the core were not observed in the Chappo outcrop. Most importantly, the composition and amount of sandstones beds differed. The core revealed more angular fragments with considerable amounts of mica and feldspar grains and a much higher sandstone to mudstone ratio, while the Chappo outcrop demonstrated more rounded grains with no observed mica, and a much lower sandstone to mudstone ratio. In addition, the Chappo sands were not as clean and contained grains of a sedimentary origin.

Age dating from core and outcrop also suggested the Chappo Member and the Hoback Formation are two distinct units. Age determination for the Chappo, as derived from mammalian fossil assemblages collected by Dorr, Gingerich, Gazin and others, revealed a Late Paleocene (middle Tiffanian) age for the

stratigraphically lowest outcrop portions of the Chappo Member. Although none of the outcrop locations described in the La Barge area contain the basal contact, it is believed that most of the formation is exposed at the type locality at Chappo Gulch, where measured sections by Dorr and Gingerich totaled 538.35 feet (Figure 20). A Middle Paleocene age (Asquith, 1966) suggests that the Hoback Formation is older than the Chappo Member. For detailed measured section descriptions of the Chappo in the La Barge area refer to Dorr and Gingerich (1980). In light of field observations discussed here and other factors described in Chapter III, the term Hoback Formation was chosen for the Tertiary producing sands of the La Barge field.

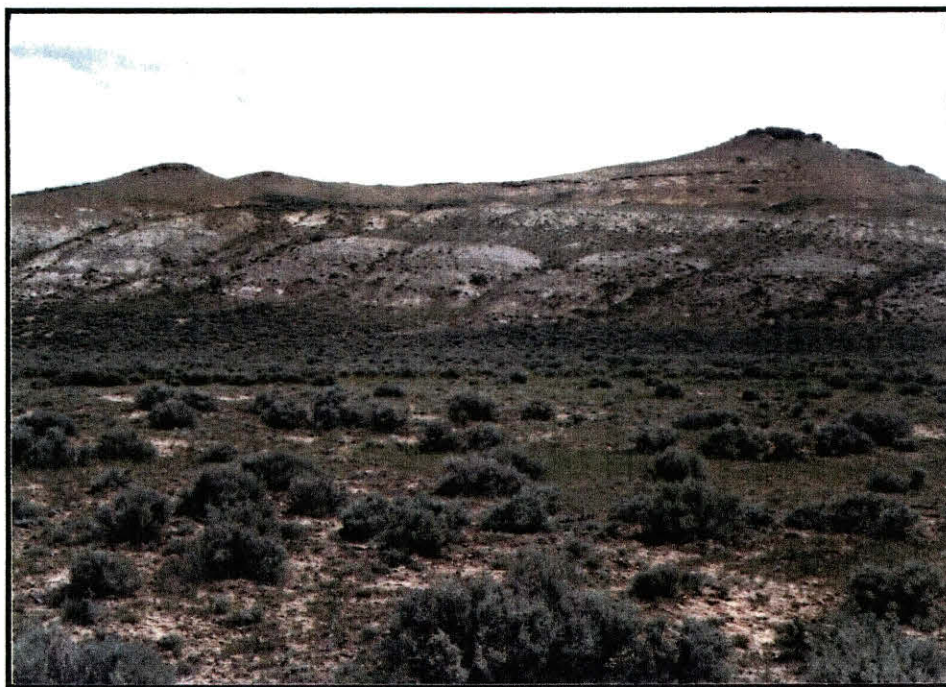


Figure 20. Type location of the Chappo Member of the Wasatch Formation along Chappo Gulch. See Figure 10 for location (TL=type locality)

The final field objective was to examine the study area for any surface structural features. Rather thorough observations revealed only one area of surface-expressed faulting. This occurred in the Rainbow Camp area near well E 303 in the SW1/4, NW1/4 sec. 3 T. 26N., R 113W., Lincoln County, Wyoming (Figure 21). At this location Chappo beds strike north and dip vertically, due to deformation within the La Barge thrust sheet. Extrapolations of these vertical beds along strike were not possible due to concealment by the undeformed La Barge Member of the Wasatch Formation. Previous work within the study area shows an extensive amount of faulting trending east-west throughout the field (Hefta and Larson, 1978). This faulting has been used to explain segmentation of the reservoir within the field. Aerial photos, subsurface studies and field investigations do not support this assumption. It is therefore believed that one or several other factors govern the segmentation of the reservoir.



Figure 21. Outcrop of the Chappo Member within the La Barge field. Arrow shows the location of the vertical Chappo beds. See Figure 10 for location (OW=oil well locality)

CHAPTER V  
SUBSURFACE GEOLOGY BASED ON ELECTRIC  
LOG STUDIES

Introduction

In order to decipher the nature of the Hoback Formation at La Barge, a number of subsurface cross-sections and maps were made. These data provided insight on the depositional environments, distribution, thickness, structural influences and trends of the Hoback sands. Since the Hoback Formation does not outcrop here, this information and four well cores provided the data upon which Chapter VI was based. All maps and cross-sections with the exception of the cumulative production map (Plate XVIII) will be discussed in this Chapter. Explanation of the cumulative production map is given in Chapter VII.

Cross-Sections

Stratigraphic

Four stratigraphic cross-sections were made; three west-east (A-A', B-B', and C-C'), and one north-south (E-E') as shown in Plates XIII, XIV, XV and XVI. The "X" marker bed shown in Figure 3, was used as the stratigraphic datum on all stratigraphic cross-sections except in B-B'. Cross-section B-B' was hung on the top of interval TH-2 because the "X" marker was faulted out on the



westernmost well by the Hilliard Thrust. The overlapping nature of interval TH-1 along the eastern portion of the field can be seen in all cross-sections except E-E'. The other four intervals show a relatively consistent thickness across the field, but a high variance in number, size, and character of sand bodies per interval is evident.

### Structural

One structural cross-section was made to show the structural characteristics of the La Barge field (D-D', Plate XVII). The overall size of the anticlinal structure as well as the up-dip pinch out of TH-1, the lacustrine shale interval, and the lower TH-2 sand can be seen. The cross-section was hung on a datum 6,000 feet above sea level.

### Structure Maps

Three structural maps were made, two structure maps on stratigraphic horizons and one on the Hilliard thrust plane. A contour interval of 50 feet was used on the basal Hoback sand structure map (Plate II). The top of interval TH-3 ("X" marker) structure map (Plate III) and the Hilliard fault plane map (Plate IV) were constructed on a 100 foot contour interval.

### Base Of Hoback Sand Map

This map (Plate II) shows the north-south trend of the La Barge platform (La Barge anticline). The western curvature of the northern part of the structure is a product of the change in trend of the Moxa arch and its related backthrust, the Calpet thrust. Three structural closures are present within the study area along the anticline. The position of the Hilliard thrust on this map is based on the

Hilliard fault plane map. All wells within the study area appear on this map to show the overall number of wells and the distribution of usable data points.

#### Top of TH-3 Interval ("X" Marker) Map

A second structure map was made on the top of the TH-3 interval (Plate III) to show how Hoback deposition was affected by the underlying structure. This map revealed the same general trend as the previous structure map. The position of the Hilliard thrust is based on the thrust plane structure map.

#### Hilliard Fault Plane Map

Based on data from wells that intersected the Hilliard thrust, a map was constructed on the Hilliard fault plane. The map (Plate IV) shows a rather sinuous north-south fault trend with three tear faults along which differential movement of the thrust plane occurred. The data from this map were used to determine the position of this fault trace on the other structure maps.

#### Net Sand Isolith Maps

A sand isolith map was made for each of the five intervals. To avoid problems with different drilling fluids and logging types employed throughout the field, net sand values were obtained from a 50 percent clean sand line rather than using absolute gamma-ray or SP scale cutoffs. The number of sand bodies in each interval was posted for all data points. In addition, a shape code was posted for all the sand bodies ten feet or greater in thickness. When more than one shape code was present, codes were posted from thickest to thinnest. These data, along with shading areas containing forty feet or less net sand, provided a generalized paleoenvironment map for each of the intervals. Since



these intervals contain several individual fluvial sand bodies in a rapidly changing fluvial system, only an average or dominant channel position for each interval could be established. All net sand maps were made with a 20 foot contour interval except the map for TH-5 which was mapped on a 40 foot contour interval because of the high degree of variance in net sand values.

#### TH-1 Interval Net Sand Map

This interval is better represented to the east in the Birch Creek unit, but the westernmost channel of this fluvial system is seen overlapping the eastern flank of the structure (Plate V). The updip termination of this interval nearly duplicates the +5,650 foot contour line on the basal Hoback sand structure map (Plate II). The western termination of TH-1 reflects the northwestern curvature of the La Barge platform in the north part of the field (T. 27 N., R. 113 W., Sec. 26).

#### TH-2 Interval Net Sand Map

Interval TH-2 shows an eastern dominance of sand, but also reflects channel deposition on the western flank of the structure (Plate VI). It appears that the large basal sand of interval TH-2 terminates a little further west than the TH-1 sand body. The upper sand of TH-2 was the first sand body to exhibit substantial deposition on the west limb of the structure. This relationship of the upper versus lower sand body of TH-2 can be seen in structural cross-section D-D' (Plate XVII).

#### TH-3 Interval Net Sand Map

Interval TH-3 shows an even distribution on both flanks of the structure (Plate VII). The noticeable difference between TH-2 and TH-3 is the shift of thicks to

the west in TH-3, where the thins of interval TH-2 were located. The converse is also true in that major thicks of TH-2, especially on the eastern flank, are occupied by thins of TH-3. The end of TH-3 deposition represented approximately equal deposition of the Hoback sand on both flanks of the structure due to channel shifting accommodating depositional lows.

#### TH-4 Interval Net Sand Map

TH-4 deposition dominated the central part of the map area, or the structural high of the La Barge platform. Thins are located on the east and west flanks, while thicks occupy both flanks of the three structural highs noted on the basal Hoback sand structure map (Plate VIII). Some of the prominent thicks located in the central part of the map area during TH-3 deposition became thins during TH-4 deposition. An example of this would include the southwest 1/4 of section 3, T. 26 N., R. 113 W.

#### TH-5 Interval Net Sand Map

Interval TH-5 (Plate IX) is unique in several regards. It is the first interval net sand map which suggests an absence of channels to the east of the study area. This map is also the first to suggest major input from the northwest, as opposed to the dominant northeasterly trend seen in the previous intervals. Finally, and most unique, is the higher degree of variance of net sand values, which merited a change in the contour interval. TH-5 is also the first interval to have zero net sand values for some data points. The thicks of this interval are located near the western flanks of the structural highs of the field, except in the southern half of the field, where the thicks occupy both flanks of the structure. Thin areas in

the central portion of the study area duplicate those of TH-4 and occupy the apex areas of the La Barge platform.

### Interval Isopach Maps

Interval isopach maps were made for TH-2, TH-3 and TH-4. Isopach maps for intervals TH-1 and TH-5 were not constructed for different reasons. Interval TH-1 had a average sand value of 92 percent (Appendix B), therefore an isopach map of this interval would not show anything different than the net sand map. Interval TH-5 had such a variable interval thickness that contouring it would have required a contour interval so large that the map would have been uninformative. The three isopach maps made were contoured on a 20 foot contour interval.

#### TH-2 Interval Isopach Map

TH-2 interval isopach map (Plate X) closely replicates the TH-2 net sand map. Its main value then, is exhibiting the proportion of sand versus the overall thickness of the interval when comparing the two maps.

#### TH-3 Interval Isopach Map

As with TH-2, interval TH-3 (Plate XI) closely imitates the net sand map. Its main value is the same as that given for TH-2.

#### TH-4 Interval Isopach Map

This map (Plate XII) shows fewer similarities to its net sand map than the previous two maps. Areas noted as thins on the net sand map reflect thicks on the isopach map. The most interesting of these areas being the north central

portion of section 34 T. 26 N., R. 113 W. on one of the structural highs defined by the structure maps. The difference observed in the trends seen in TH-4 versus those of the lower sands reflects a change in the depositional nature of the upper Hoback Formation, which will be discussed in Chapter VI.

CHAPTER VI  
DEPOSITIONAL ENVIRONMENT OF THE  
HOBACK FORMATION

Environmental Interpretation

The Hoback Formation of La Barge represents fluvial deposition on a broad alluvial plain. Spelman (1976) described this formation as a meandering stream deposit based on electric log shapes and a fining upward sequence seen in core taken from the field. Electric log cross-sections, subsurface maps and core suggest these deposits represents a sand dominated braided stream deposit.

Braided rivers consists of a series of broad, shallow channels and bars with elongated areas active only during floods, and dry islands (Miall, 1977). At low and moderate flows, individual channels are wide and shallow and generally floored by dunes and bars (Busch and Link, 1985). Bars are composed of three main types; longitudinal bars, comprising crudely bedded gravel or coarse sand sheets; transverse to linguoid bars, consisting of downstream avalanche-face progradation of sand or gravel, and point or side bars formed by bedform coalescence and chute and swale development in areas of low energy (Miall, 1977).

Sand dominated braided stream and meandering stream deposits are similar in many regards, and for this reason are difficult to distinguish in the

geologic past. Notable distinguishing characteristics of braided streams and examples from the Hoback Formation are given below.

Braided river deposits have channels with high width to depth ratios. The sheet like Hoback channel sands are composed of several shallow, wide channel deposits. Evidence of this is seen in net sand maps of individual Hoback sand intervals. Individual channel sequences are relatively thin (less than 40 feet thick) but up to or greater than a mile in width.

A second characteristic of braided stream deposits is a high sand to mud ratio. Sand to mud/silt ratios in the lower Hoback sands (TH-1, TH-2 and TH-3) are 50 percent or greater, while TH-4 and TH-5 reflect higher mud and silt ratios (Appendix B). The reason for this change is discussed later.

Flashy discharge indicative of braided rivers is exemplified by the cyclic deposits (fining upward) of the Hoback Formation. These upward fining sequences seen in the core show interruption by scour trough cross-bedding which dominate or interrupt this cyclic deposition. The dominance of these deposits throughout the section indicates flashy discharge.

Another characteristic of braided rivers is unconfined flow, which in the Hoback Formation is suggested by the lack of a single prominent channel and the absence of laterally extensive overbank deposits. Another indicator of unconfined flow of the Hoback Formation is the large lateral extent of these sheet sands. Most of these sand units are seen throughout the entire study area.

Braided stream deposits have a characteristic multilateral geometry (Figure 22). The multilateral nature of the Hoback sands can be seen from the well log cross-sections. These multilateral channel fills volumetrically exceed overbank deposits, resulting in this characteristic bed load channel geometry. Differences

between braided bed load geometries and meandering mixed load geometries are shown in Figure 22

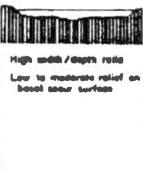



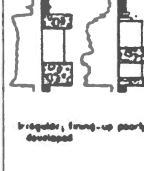
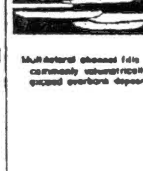
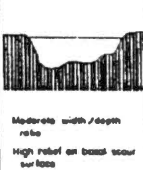

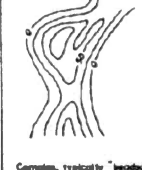

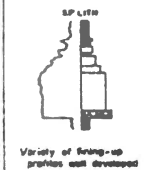
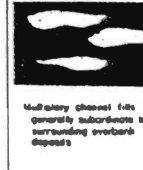
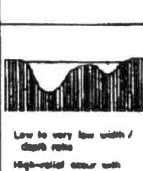
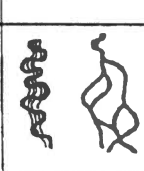

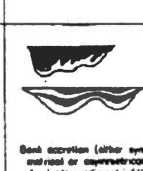
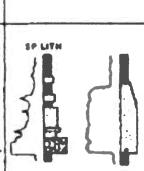
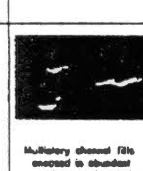
CHANNEL TYPE	COMPOSITION OF CHANNEL FILL	CHANNEL GEOMETRY			INTERNAL STRUCTURE		LATERAL RELATIONS
		CROSS SECTION	MAP VIEW	SAND ISOLITH	SEDIMENTARY FABRIC	VERTICAL SEQUENCE	
BEDLOAD CHANNEL	Dominantly sand	 High width / depth ratio Low to moderate relief on basal scour surface	 Straight to slightly sinuous	 Broad continuous bed	 Bed accretion dominated by subparallel silt	 Irregular, fining-up poorly developed	 Multistage channel fills commonly superimposed on overbank deposits
MIXED LOAD CHANNEL	Mixed sand, silt, and mud	 Moderate width / depth ratio High relief on basal scour surface	 Sinuous	 Complex, typically "beaded" bed	 Bank and bed accretion both preserved in sequential silt	 Variety of fining-up profiles well developed	 Multistage channel fills generally subordinate to surrounding overbank deposits
SUSPENDED LOAD CHANNEL	Dominantly silt and mud	 Low to very low width / depth ratio High-relief scour with steep banks, some oxbow-like with multiple thalwegs	 Highly sinuous to anastomosing	 Shoestring or pad	 Bed accretion (either symmetrical or asymmetrical) dominated by subparallel silt	 Sequences dominated by fine material, thus vertical trends may be obscure	 Multistage channel fills enclosed in abundant overbank mud and silt

Figure 22. Geomorphic and sedimentary characteristics of various channel types and their deposits (from Galloway and Hobday, 1983)

A high variability of sedimentation units is another characteristic of braided river deposits. This is due to mainly to the flashy nature of flow in this depositional environment. The degree of variance in electric log shapes of time equivalent sands in nearby wells suggests a variability in sedimentation units within individual Hoback sands. Core data supports the assumption that individual sheet sands are not homogenous, but in fact are composed of a

variety of sub-facies, which exhibit characteristic bedforms. Descriptions of these sub-facies included within the braided environment will be given later. This lack of homogeneity is the cause of reservoir segmentation, which will be discussed in Chapter VII.

Braided rivers are composed of multiple channels, where as meandering and distributary channel systems have only one prominent channel. The Hoback Formation shows a multichannel configuration on the net sand maps generated. This constantly changing multiple channel configuration makes mapping of individual channel sands difficult and in turn, results in complicated segmentation of individual sheet sands.

The final characteristic of braided alluvial deposition is low bank stability. The Hoback Formation exhibits this with the lack of laterally extensive overbank deposits. This would suggest a low preservation potential of this material due to the unconfined nature of the channel system. Considerable amounts of overbank and low flow regime bedforms are redeposited as rip-up clast within channel scours during periodic flooding conditions, when the entire alluvial plain is flooded. Under these conditions bank stability is rarely achieved.

Other less diagnostic features of braided deposition would include high gradient, low sinuosity and dominance of angular to subangular sand and gravel deposits. Structural complexities in the La Barge region make calculations of Paleocene stream gradient difficult to determine. For this reason the gradient during deposition is unknown. Sinuosity of the overall belt of Hoback deposition is low, but within this belt the diagnostic braided channel pattern is evident and in many cases is highly sinuous. Grain size of the Hoback formation ranges from fine to coarse sand with a dominance of medium grained sand. Grain shape ranges from subangular to angular with a dominance of angular grains (Figure 23).



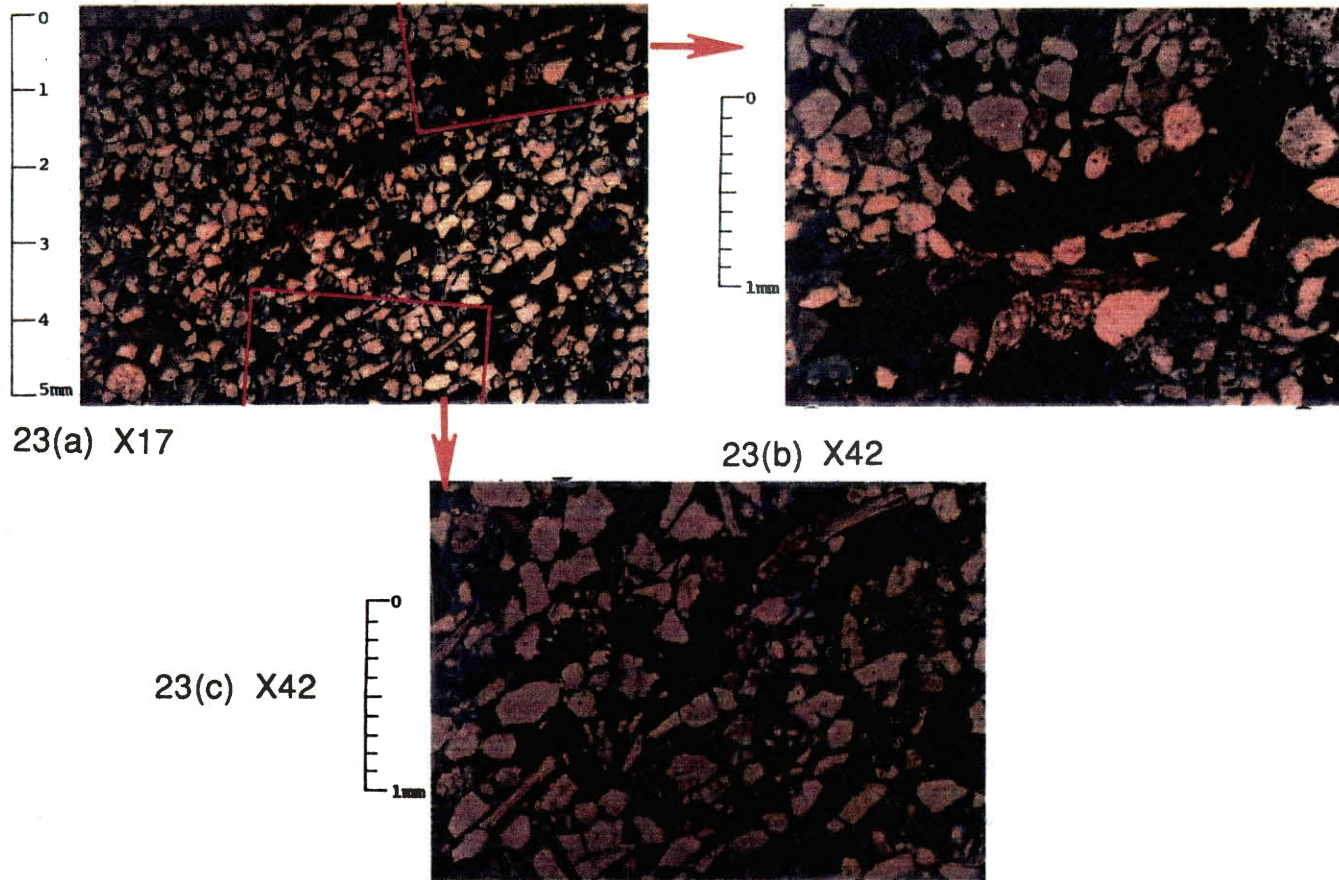


Figure 23. Thin section of the Hoback Formation showing clay drapes associated with cross-bedding. Red squares indicate magnified areas shown in 23 (b) and (c). Clay drapes are intermixed with pyrite mica and silt. These clay drapes would probably hinder horizontal fluid movement. Note the angularity of the grains as well as the dominance of quartz (from Spelman, 1976)

It is evident that the Hoback formation meets almost all the criteria indicative of a braided fluvial environment and therefore should be classified as such. Miall (1985b) believes that this classification of braided streams is too broad and should be further subdivided. He states that some of these diagnostic characteristics can be present in other fluvial regimes and therefore, fluvial classification should be based on overall geometry and frequency of specific facies types. A list of his different facies types, their assigned facies code, characteristic sedimentary structures and depositional interpretations are given in Table II. Based on these criteria, Miall proposed six main classes for interpretation of ancient braided river deposits in the surface and subsurface. Half of these models are gravel-dominated, whereas the other half are sand dominated systems. The three sand dominated models are shown in Figure 24. Dominant and minor facies code associations for each of these models are given in Table III.

#### Bedforms of Sand Dominated Braided Rivers

As mentioned earlier, the main bedforms of sand dominated braided rivers are bars (several varieties), sand waves and dunes. Vegetated islands are of minor importance and form on pre-existing bars or emergent dunes during waning flow. The position and internal composition of the major bedforms within the braided environment are shown in Figure 25. This block diagram reflects depositional conditions present during Hoback deposition. Brief descriptions of these various bedforms and their internal structure are given below.

<b>Facies Code</b>	<b>Lithofacies</b>	<b>Sedimentary structures</b>	<b>Interpretation</b>
<i>Gms</i>	massive, matrix supported gravel	none	debris flow deposits
<i>Gm</i>	massive or crudely bedded gravel	horizontal bedding, imbrication	longitudinal bars, lag deposits, sieve deposits
<i>Gt</i>	gravel, stratified	trough crossbeds	minor channel fills
<i>Gp</i>	gravel, stratified	planar crossbeds	linguoid bars or deltaic growths from older bar remnants
<i>St</i>	sand, medium to v. coarse, may be pebbly	solitary (theta) or grouped (pi) trough crossbeds	dunes (lower flow regime)
<i>Sp</i>	sand, medium to v. coarse, may be pebbly	solitary (alpha) or grouped (omikron) planar crossbeds	linguoid, transverse bars, sand waves (lower flow regime)
<i>Sr</i>	sand, very fine to coarse	ripple marks of all types	ripples (lower flow regime)
<i>Sh</i>	sand, very fine to very coarse, may be pebbly	horizontal lamination parting or streaming lineation	planar bed flow (l. and u. flow regime)
<i>Sl</i>	sand, fine	low angle (<10°) crossbeds	scour fills, crevasse splays, antidunes
<i>Se</i>	erosional scours with intraclasts	crude crossbedding	scour fills
<i>Ss</i>	sand, fine to coarse, may be pebbly	broad, shallow scours including eta cross-stratification	scour fills
<i>Sse, She, Spe</i>	sand	analogous to <i>Ss, Sh, Sp</i>	eolian deposits
<i>Fl</i>	sand, silt, mud	fine lamination, very small ripples	overbank or waning flood deposits
<i>Fsc</i>	silt, mud	laminated to massive	backswamp deposits
<i>Fcf</i>	mud	massive, with freshwater molluscs	backswamp pond deposits
<i>Fm</i>	mud, silt	massive, desiccation cracks	overbank or drape deposits
<i>Fr</i>	silt, mud	rootlets	seatearth
<i>C</i>	coal, carbonaceous mud	plants, mud films	swamp deposits
<i>P</i>	carbonate	pedogenic features	soil

Table II. Lithofacies and sedimentary structures of modern and ancient braided river deposits (from Miall, 1978)

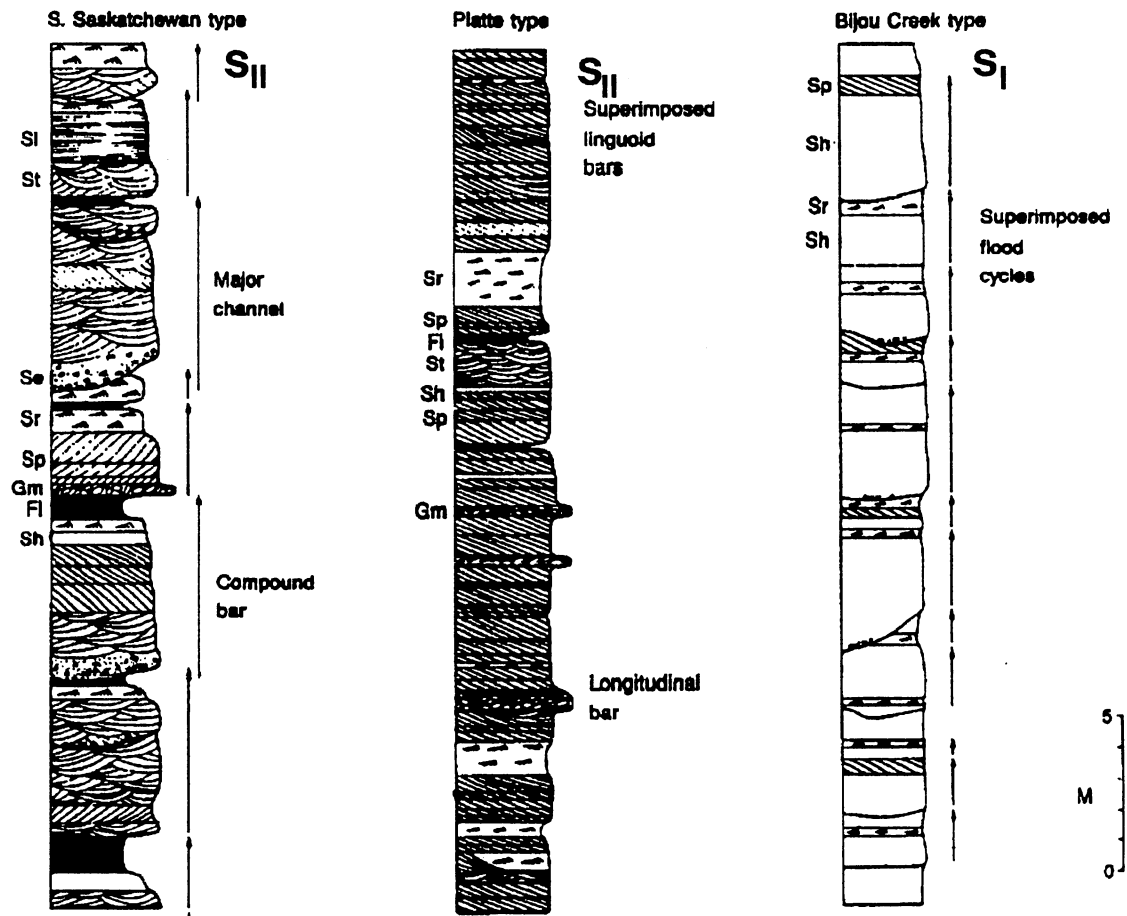


Figure 24. General stratigraphic models for sand dominated braided streams. Descriptions of individual facies are given in Table II (from Miall, 1978)

<b>Name</b>	<b>Environmental setting</b>	<b>Main facies</b>	<b>Minor facies</b>
Trollheim type (G <sub>i</sub> )	proximal rivers (predominantly alluvial fans) subject to debris flows	<i>Gms, Gm</i>	<i>St, Sp, Fl, Fm</i>
Scott type (G <sub>ii</sub> )	proximal rivers (including alluvial fans) with stream flows	<i>Gm</i>	<i>Gp, Gt, Sp, St, Sr, Fl, Fm</i>
Donjek type (G <sub>iii</sub> )	distal gravelly rivers (cyclic deposits)	<i>Gm, Gt, St</i>	<i>Gp, Sh, Sr, Sp, Fl, Fm</i>
South Saskatchewan type (S <sub>ii</sub> )	sandy braided rivers (cyclic deposits)	<i>St</i>	<i>Sp, Se, Sr, Sh, Ss, Sl, Gm, Fl, Fm</i>
Platte type (S <sub>ii</sub> )	sandy braided rivers (virtually non cyclic)	<i>St, Sp</i>	<i>Sh, Sr, Ss, Gm, Fl, Fm</i>
Bljou Creek type (S <sub>i</sub> )	Ephemeral or perennial rivers subject to flash floods	<i>Sh, Sl</i>	<i>Sp, Sr</i>

Table III. Facies assemblages and environments of the six principal braided stream models. Vertical trends are shown in figure 24 and facies codes are shown in Table II (from Miall, 1978)

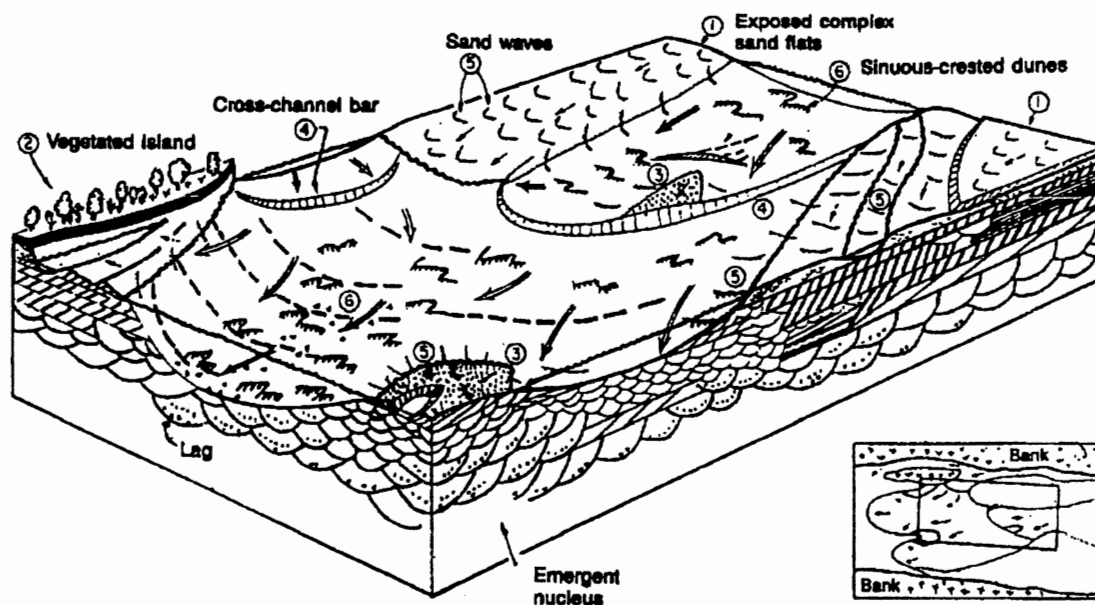


Figure 25. Block diagram summarizing the major morphological elements and their associated bedforms and stratifications. Stippled areas are emergent. Single shafted arrows indicate direction of bedform movement and double-shafted arrows indicate flow directions (from Cant, 1978)

### Bars

Several bar types are present within the braided environment. The principal types are longitudinal, linguoid or transverse, and compound bars (point and side). Figure 26 shows the morphology and growth pattern of most of these various types.

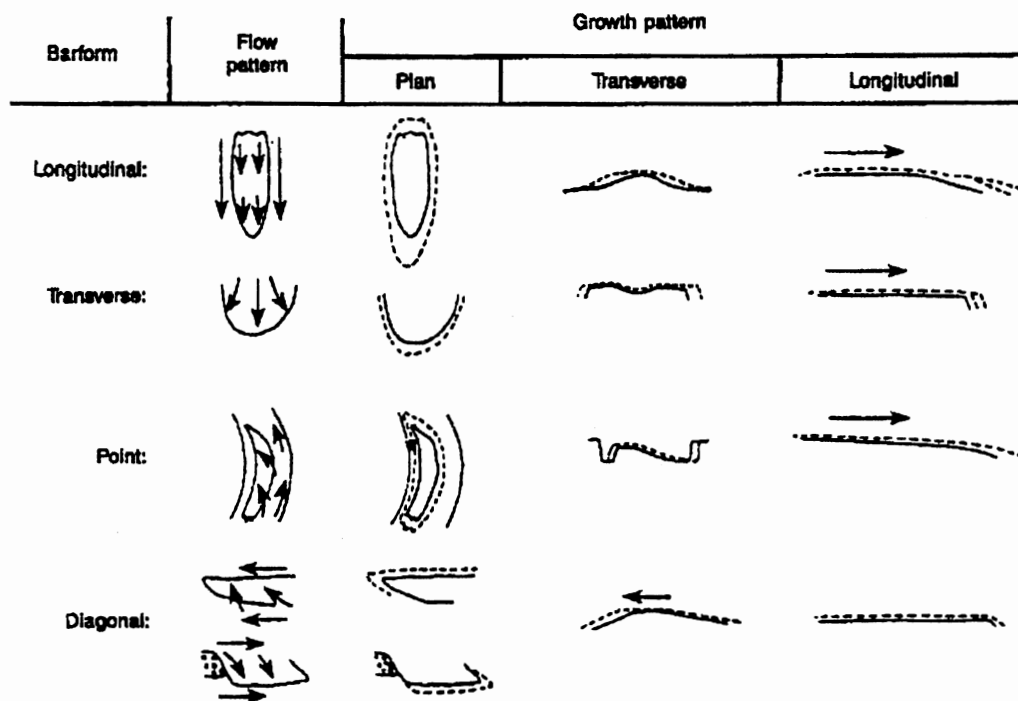


Figure 26. Morphology, pattern of growth, and water flow over and near bars commonly found in braided channels. Dashed lines indicate accretion (from Busch and Link, 1985)

Longitudinal Bars. These bars are elongated parallel to flow and are diamond or cigar shaped in plan view (Miall, 1977). They are bounded on both sides by active channels and usually have partly eroded margins. Longitudinal bars form as competency of the braided channel decreases during waning flow and deposition occurs. The coarsest load of a channel is carried along the deepest portion of the channel where competency is greatest. Waning flow will result in deposition of the coarsest bed load as a submerged central bar. Finer material is trapped within the central bar as more bed load is deposited downstream resulting in continued vertical and longitudinal growth.

Cross-channel or diagonal bars are a special type of longitudinal bar that commonly form at channel bends or junctions, but can be found anywhere

within a channel (Figure 25). These bars are characterized by asymmetric flow across the bar, rather than parallel to the bar axis (Miall, 1977). Other than the asymmetry of these bars, there seems to be little difference between them and longitudinal bars. Miall (1977) suggests the use of the general and more widely used term, longitudinal bar, for all such structures.

The internal structure of longitudinal bars is massive or crude horizontal bedding, possibly indicating transportation in planar sheets under very high flow energy (Miall, 1977). Many of the massive, medium to coarse sandstone and pebble conglomerate units seen in the core probably represent longitudinal bars (Appendix A).

Linguoid (Transverse) Bars. Linguoid bars are rhombic or lobate features with upper surfaces which dip gently upstream and downstream facing sinuous, avalanche-slope terminations (Miall, 1977). Transverse bars are similar to linguoid bars, except that they tend to have straighter crests. They may represent coalesced bars or solitary bars which extend completely across a channel (Miall, 1977). The two bar types probably could only be distinguished in the geologic record by very detailed paleocurrent work, therefore these two bar types have been grouped together. The maximum height at the crest of the avalanche-slope ranges from a few feet to several inches (Miall, 1977).

The internal character of these bedforms consist of planar-tabular cross-bedding, representing avalanche-slope progradation. Coalesced forms produce migrating sand waves under increased flow rates. When linguoid bars are exposed during low flow conditions, they are commonly covered by dunes or ripples. The planar cross-beds seen in the core from well J503Y (Appendix A) probably represent superimposed linguoidal bar deposits.



Compound Bars. Compound bars of braided rivers tend to form by the coalescence of smaller bedforms, such as dunes and linguoid bars (Miall, 1977). These bedforms build by both lateral and vertical accretion. Internal structures are complex and may include planar-tabular cross-bedding of dune or scour origin, and fine grained drape and fill deposits formed in swales (Miall, 1977). Recognition of compound bar deposits from the geologic record may be impossible unless the adjacent tract to which the bar is attached is preserved as well.

### Sand Waves

This bedform is a relatively straight crested, wedge-shaped or tabular sedimentary unit with a well defined slope face (Figure 27). It forms under moderate flow velocities and its size is related to depth of flow (Busch, Link, 1985). As mentioned earlier, this bedform can evolve from coalescing linguoid bars during increasing flow rates. During low flow, emergent or exposed sand waves are known as sand flats.

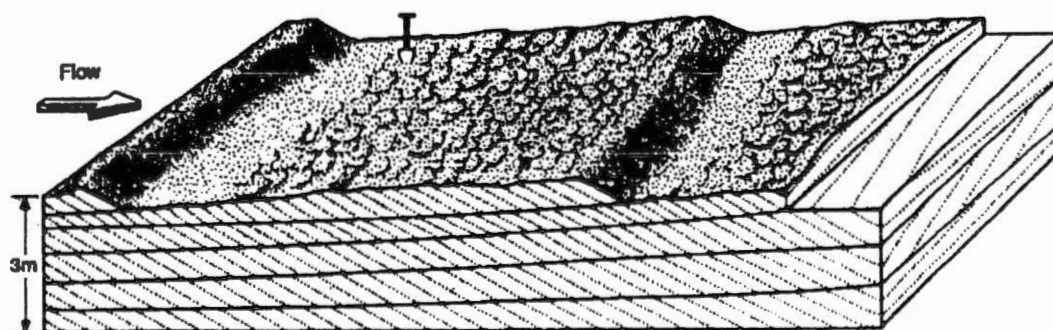


Figure 27. Tabular cross-bedding formed by migrating sand waves (from Busch and Link, 1985)

The internal structure is characterized by planar cross-bedding with ripples commonly found on the stoss sides. Ripple cross-lamination may be lateral to, or superimposed on, the cross-bedding (Cant, 1978). Distinguishing sand waves from linguoid bars in core would be difficult if not impossible due to their strong similarities.

### Dunes

These bedforms are produced under increasing flow rates where sand waves grade gradually into dunes. Dunes are characterized by irregular crest patterns with scours occurring in the trough areas down stream from avalanche faces (Figure 28). Dune size varies directly with wave velocity and water depth, and inversely with grain size (Cant, 1978). During high velocity and shallow water depth, dunes become planed off and show a rounded profile. With increasing flow rates, the planed dunes become lower and grade into the horizontal sheet sands (Busch, Link, 1985). The irregularity of this bedform produces trough cross-bedding as the internal structure (Busch, Link, 1985). Dune deposition was the most common bedform observed in the Hoback cores and was represented by facies codes  $S_t$ ,  $S_{t_1}$  and  $S_S$  (Table II).

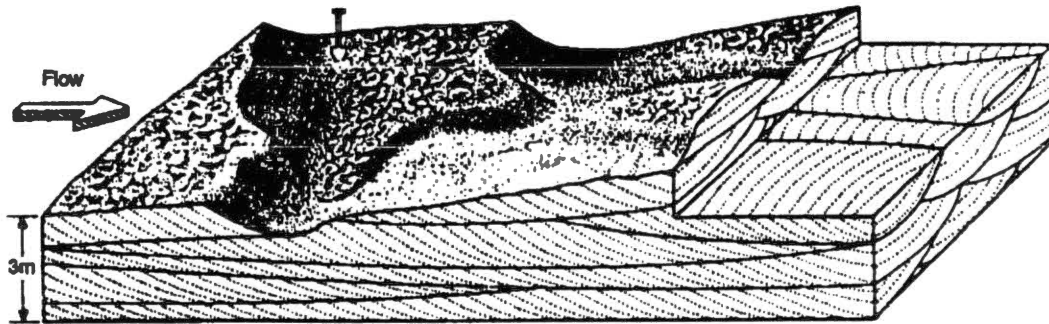


Figure 28. Trough cross-bedding formed by migrating dunes (from Busch and Link, 1985)

### Classification of the Hoback Braided River Deposits

Based on core descriptions, the Hoback formation best represents the  $S_{II}$  or south Saskatchewan model (Figure 24). Core descriptions indicate a dominance of trough cross-bedding ( $S_t$ ) with minor facies of  $S_s$ ,  $S_l$ ,  $S_r$ ,  $S_h$ ,  $F_l$  and  $F_m$  (Appendix A). Vertical changes in the Hoback sands indicate a change from this type  $S_{II}$  deposit to that of an ephemeral equivalent of type  $S_{II}$ .

The lower Hoback sands (TH-1, TH-2 and TH-3) represent a perennial braided stream deposit with cyclic deposition resulting from seasonal changes of flow rates. These changes in flow rate produced fining upward bed forms, interrupted by channel scours. The dominant bedforms would include sinuous-crested dunes, sand flats and vegetated islands (Figure 25). These cyclic deposits resulted in relatively consistent laterally extensive intervals of deposition. Prominent interval markers probably represent drought or low water conditions during which little to no deposition occurred. These conditions were rare in the lower Hoback as evidenced by the lack of regional markers.

In the upper part of the Hoback Formation (parts of TH-4 and all of TH-5) a dominance of  $S_i$ ,  $S_r$ ,  $S_h$  is seen in the sand facies, with the finer sand, silt and mud facies becoming more dominant ( $F_m$ ,  $F_l$ ). As mentioned in Chapter V, a noticeable change in the net sand map for TH-5 was observed. Due to the variability of data points, TH-5 was contoured on a larger contour interval. The percent sand values for the Hoback sands show a trend from 63 percent in TH-3 to 39 percent in TH-5 (Appendix B). This trend from sand to silt and mud dominance is gradual and may represent a change from a humid to an arid climate resulting in transition from a perennial to ephemeral braided river. This would explain the large amount of finer material as well as the unpredictable nature of the sand deposits in interval TH-5. The fine-grained material represents decreasing flow deposits followed by deposition of mud in shallow, ponded water areas within the alluvial plain. During periodic flooding the fluvial system would be reactivated. Sheet sands would braid their way across the alluvial plain scouring the fine grained deposits in channel areas and depositing over them in bar areas. As flow rates decrease, low energy bed forms (horizontal bedding and ripple cross-stratification) would dominate channel and ponded water areas until the system once again was reactivated. Without core data from interval TH-5, and more complete data from interval TH-4, this interpretation is only speculation based on well log signatures and subsurface cross-sections and maps.

### Source Area

The composition of the Hoback sands indicates a igneous and metamorphic source. Most of the grains are composed of angular quartz, feldspar and metamorphic rock fragments. Minor amounts of mica were observed throughout

the formation. Thin sections reveal kaolinite as the dominant clay of the Hoback Formation, although very minor amounts of glauconite were also observed. The glauconite most likely represents re-worked late Cretaceous sediment which was exposed at La Barge during Hoback deposition.

The composition and angularity of the grains indicate a relatively close granitic and metamorphic source (Figure 23). The only active source of this nature in the vicinity during the Paleocene was the Wind River Mountains to the northeast. The southwest flank of the Wind River Mountains shows evidence of Paleocene alluvial fan deposits, which more than likely supplied sediment to the La Barge area (Berg, 1962). Trends of the Hoback sand discussed in Chapter V indicate that sediment was entering the study area from the northeast. Possible exceptions to this include TH-5, which showed more of a northwest source. Trends and composition of most of the Hoback sands support a source from the Wind River Mountains to the northeast. Northwestern trends of interval TH-5 possibly indicate a change in source area related to movement of the Darby thrust in the area during Latest Paleocene. Core from interval TH-5 was not available, therefore composition is unknown.

Minor amounts of sedimentary sourced material were also found within the Hoback sands. This indicates a possible dual source for the Hoback Formation. Composition was mainly chert with some sandstone and dolomite grains. This material is interpreted as being sourced from the west. Some of this sedimentary material may have come directly from the overthrust belt just west of La Barge, but subsurface maps did not indicate an obvious source from this direction for intervals TH-1 through TH-4. It is the writer's belief that most of this material originated from interaction of the sedimentary sourced Hoback fluvial sands in the southwestern part of the Hoback Basin (Figure 29).

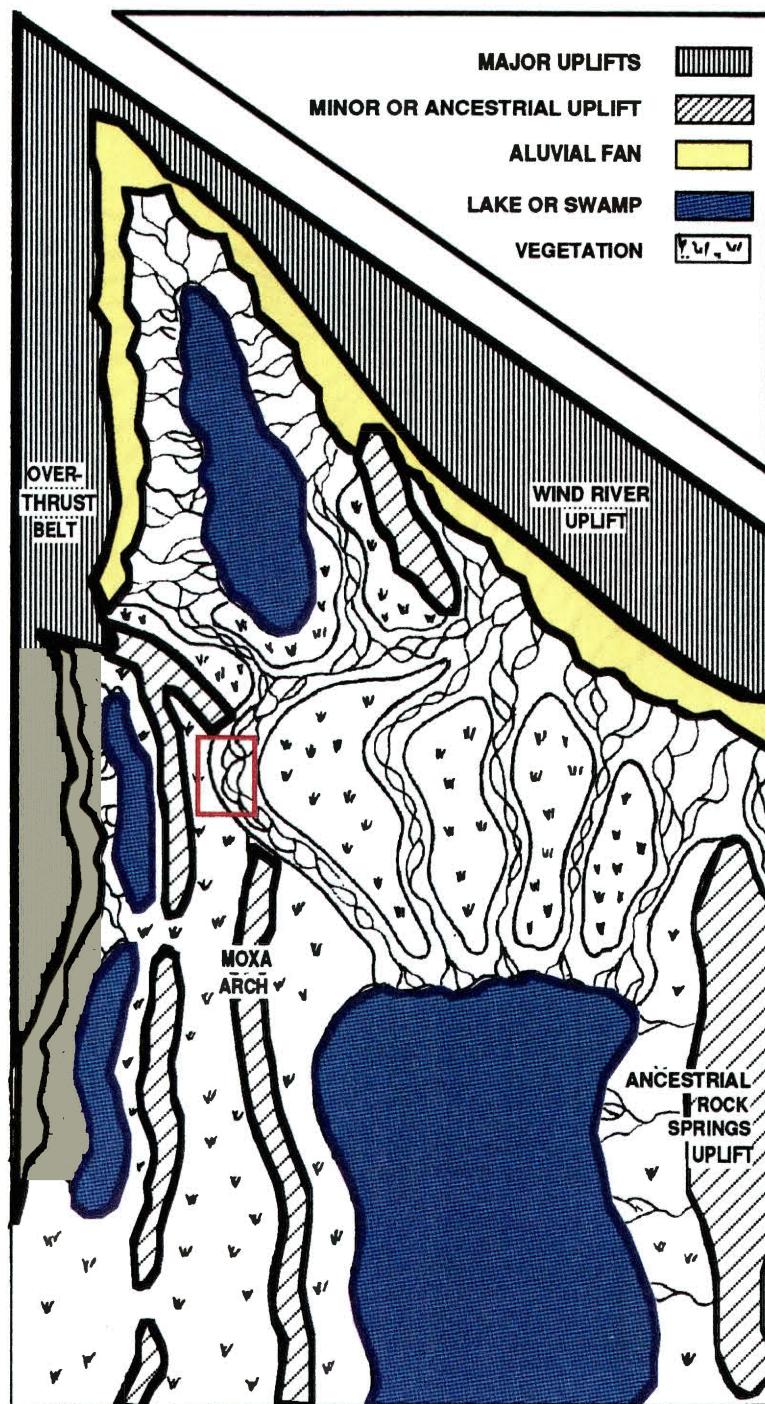


Figure 29. Late Middle Paleocene paleogeography cartoon with study area outlined in red. The uplifts west of the study area represent thrust material related to early, minor Paleocene movement, of the Darby thrust.

A generalized paleogeographic map of the Paleocene is shown in Figure 29. This map is a cartoon used to show the possible source area and general trends of the Hoback Formation and it is not intended to be taken as accurate delineation of the Hoback fluvial system.

### Paleocene Paleoenvironment

A series of generalized paleoenvironment maps of the study area were made to show structural and depositional changes in the La Barge area throughout the Paleocene. The position and trends of the fluvial systems shown are based on subsurface maps constructed within the study area, while surrounding areas are based on speculation.

The Early to Middle Paleocene of La Barge was, for the most part, characterized by a period of non-deposition during which folding and faulting of the La Barge platform occurred. During this time minor movement of the Darby thrust in the La Barge area produced a series of debris flows represented by the Middle Paleocene basal tongue of the Lookout Mountain Conglomerate Member (Figure 30).

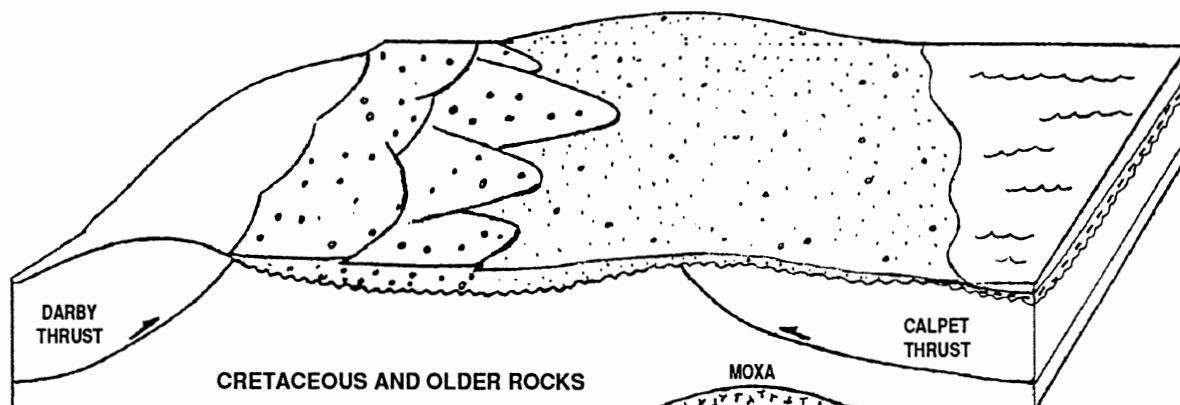


Figure 30. Early to Middle Paleocene paleoenvironment

Evidence from the eastern flank of the of the La Barge anticline suggests a shallow lake or peat swamp existed here during the Middle Paleocene. This deposit represents the beginning of Hoback deposition and overlaps the earlier debris flows on the eastern flank of the structure (Figure 31).

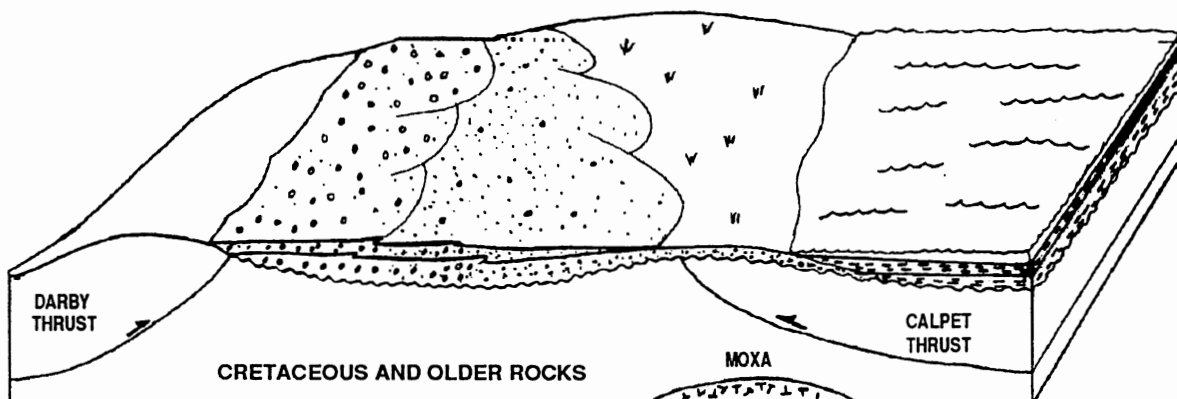


Figure 31. Middle Paleocene paleoenvironment



During the late Middle Paleocene, Hoback sands from the northeast onlaped the flank of the La Barge platform depositing interval TH-1 (Figure 32). The Middle Paleocene lake had either retreated to the southeast by this time or it had dried up as a result of sediment infill from younger Hoback sands. TH-2 deposition shows that by latest Middle Paleocene, Hoback sands had made their way across the La Barge platform (Figure 33).

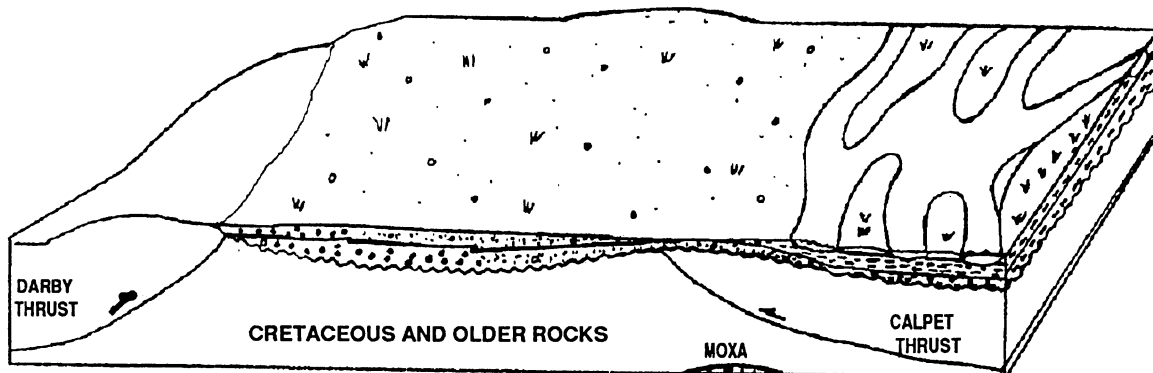


Figure 32. Late Middle Paleocene paleoenvironment (TH-1 deposition)

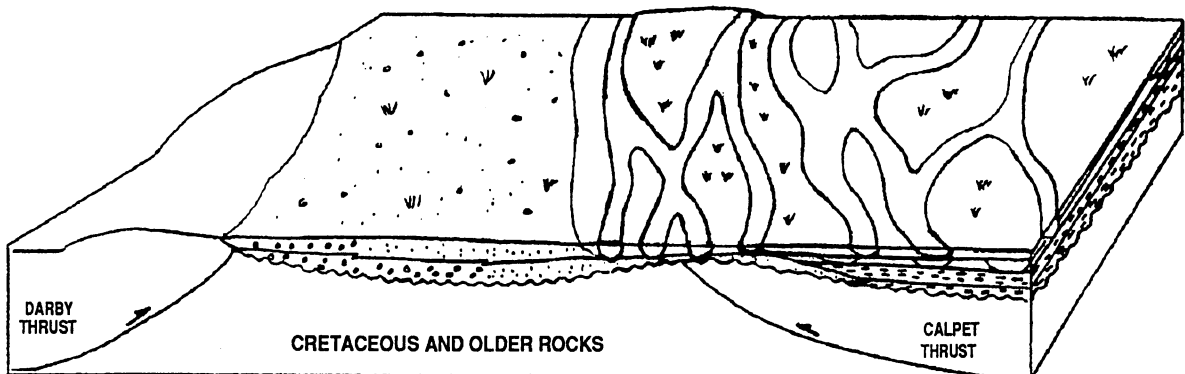


Figure 33. Late Middle Paleocene paleoenvironment (TH-2 deposition)

Throughout the early Late Paleocene, Hoback sand braided their way across the La Barge platform depositing intervals TH-3 and TH-4 (Figures 34 and 35). By TH-5 deposition, noticeable changes in deposition occurred. TH-5 sands appear to enter the study area from the northwest. Early movements of the Late Paleocene reactivation of the Darby thrust were probably the source of most of this material. Composition of these sands are unknown because core was unavailable, but they are suspected to contain higher amounts of westerly-sourced sedimentary material similar to that of the overlying Chappo Member of the Wasatch (Figure 36).

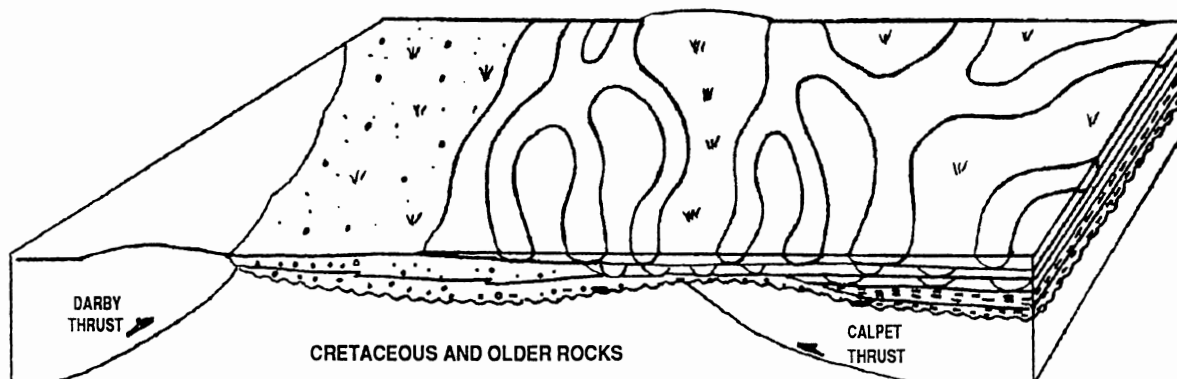


Figure 34. Early Late Paleocene paleoenvironment (TH-3 deposition)

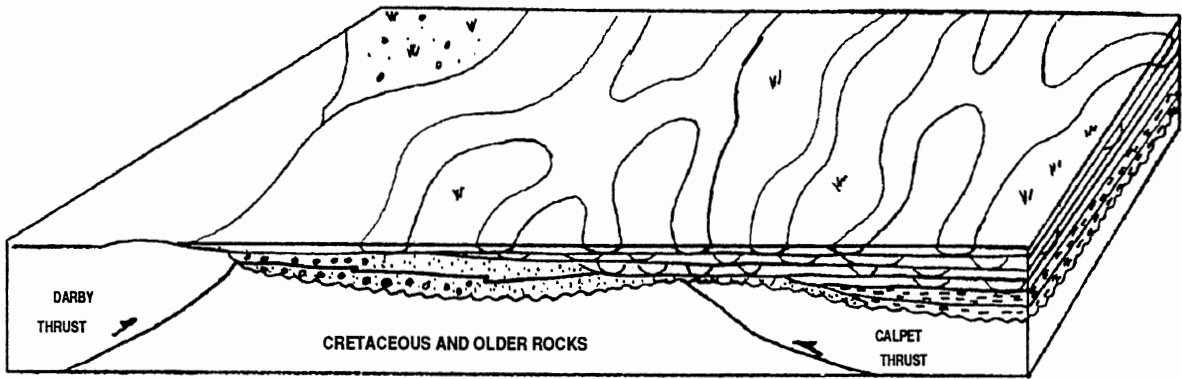


Figure 35. Early Late Paleocene paleoenvironment (TH-4 deposition)

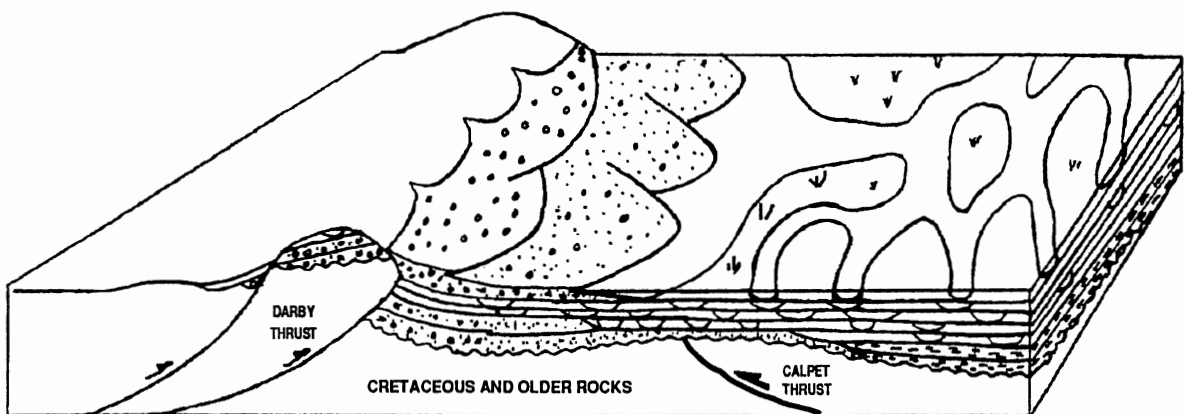


Figure 36. Late Paleocene paleoenvironment (TH-5 deposition)

Finally, continued Late Paleocene movement of the Darby thrust resulted in deposition of the alluvial fan deposits of the Lookout Mountain Conglomerate and the westerly sourced alluvium of the Chappo Member.

## CHAPTER VII

### PETROLEUM GEOLOGY

#### Introduction

The occurrence of oil in southwestern Wyoming was first noted over a century and a half ago. Many of the early trappers and fur traders knew the location of various oil springs in the region and visited them in their annual trapping tours (Schultz, 1907). It was not until the summer of 1907 that oil springs four miles east of La Barge ridge (section 34, T.27N., R.113w) were reported along Spring Creek (Figure 10). At this location, oil seeped through crevices in Tertiary rocks and an artificial pit six feet deep near the center of a drain had sufficient seepage to supply local residents with oil for some time (Schultz, 1907).

During the summer of 1924 the first well was drilled, resulting in the establishment of the La Barge field (well D703). The discovery was located on a surficial anticline where multiple oil bearing Tertiary sands between six hundred and twelve hundred feet deep were encountered. The trapping mechanism was found to be both structural and stratigraphic. This discovery launched a four year cable-tool boom at Tulsa, Wyoming, later renamed La Barge (McDonald, 1973). According to Krueger (1955), this was the first field in the Rocky Mountains to produce commercial quantities of oil and gas from reservoirs of Tertiary (Paleocene) age. In July of 1928, the north end of the La Barge structure was successfully tested and most of the field's present limits

were established. General characteristics of the Hoback reservoir at La Barge are given in Table IV.

FORMATION-----	HOBACK-TERTIARY
LITHOLOGY-----	SANDSTONE
AVERAGE POROSITY-----	26%
PERMEABILITY-----	230-450 md
AVERAGE PAY THICKNESS-----	15 FEET
INITIAL PRESSURE-----	385 psi
DRIVE MECHANISM-----	GAS SOLUTION
Rw-----	0.76-0.98 AT 70 degrees F
API GRAVITY-----	17-42 degrees API
POUR POINT-----	5 degrees F
SULPHUR CONTENT-----	0.04-0.12%
CONTINUITY OF RESERVOIR-----	DISCONTINUOUS CHANNELS
PRIMARY TRAP TYPES-----	ANTICLINAL AND STRAT.

Table IV. Hoback reservoir characteristics in the La Barge Field

Initial production revealed four distinct producing sands, which were tentatively referred to as the yellow, green, red and blue sands, with the blue sand being the basal unit. More detailed work called for a renaming of the producing sands to Almy 1, 2, 3, 4, and lower 4 with the lower Almy 4 being the basal sand (Figure 3). The lower 4 sand pinches out along the eastern flank of the La Barge anticline and therefore is not present in the western half of the field. Due to the discontinued use of the term Almy Formation in this area, the producing sands are referred to from base to top as: TH-1, TH-2, TH-3, TH-4, and TH-5, with the abbreviations referring to Tertiary Hoback Formation.

## Possible Source And Migration Path

Source

Elrod (1987), conducted a geochemical analysis of seven oil samples from various wells in Wyoming (Table V). Three of these were from the Hoback reservoir at La Barge. The purpose was to compare compositions of these samples to determine if they are genetically related. This analysis indicated that the Hoback oils (B-001, B-002 and B-003) exhibited slightly higher proportions of resins and aromatics, and lower quantities of paraffin-naphthenes than the other Wyoming oils. In addition, it was noted that the Hoback oils contained less light end material than the other samples, as evidenced by higher C<sub>9</sub>+ recoveries (Figure 37). These observations are consistent with observed heavier (27° - 30°) API gravities of the Hoback oils (Table V). In addition, oil chromatography of the Hoback samples conducted by Elrod revealed an absence of light compounds.

<b>Sample Number</b>	<b>Well Name</b>	<b>Sample Identification</b>	<b>Reservoir Formation</b>	<b>API Gravity</b>
B-001	La Barge #1	Central Tank Battery	Hoback	27.8°
B-002	La Barge #2	Steamflood Battery	Hoback	27.3°
B-003	La Barge #3	27-27N-113W	Hoback	30.4°
B-004	La Barge #4	3-26N-113W	Mesaverde	45.8°
B-005	Chevron 31-33C Cabin Creek	33-37N-114W	Mission Canyon	41.9°
B-006	Sun Lucky Ditch Federal B-4		Dakota Sand	37.5°
B-007	Dome #1-13 Hiller Federal	32-T13N-R114W	Frontier	38.8°

Table V. Identification and API gravity of oil samples (modified from Elrod,1987)

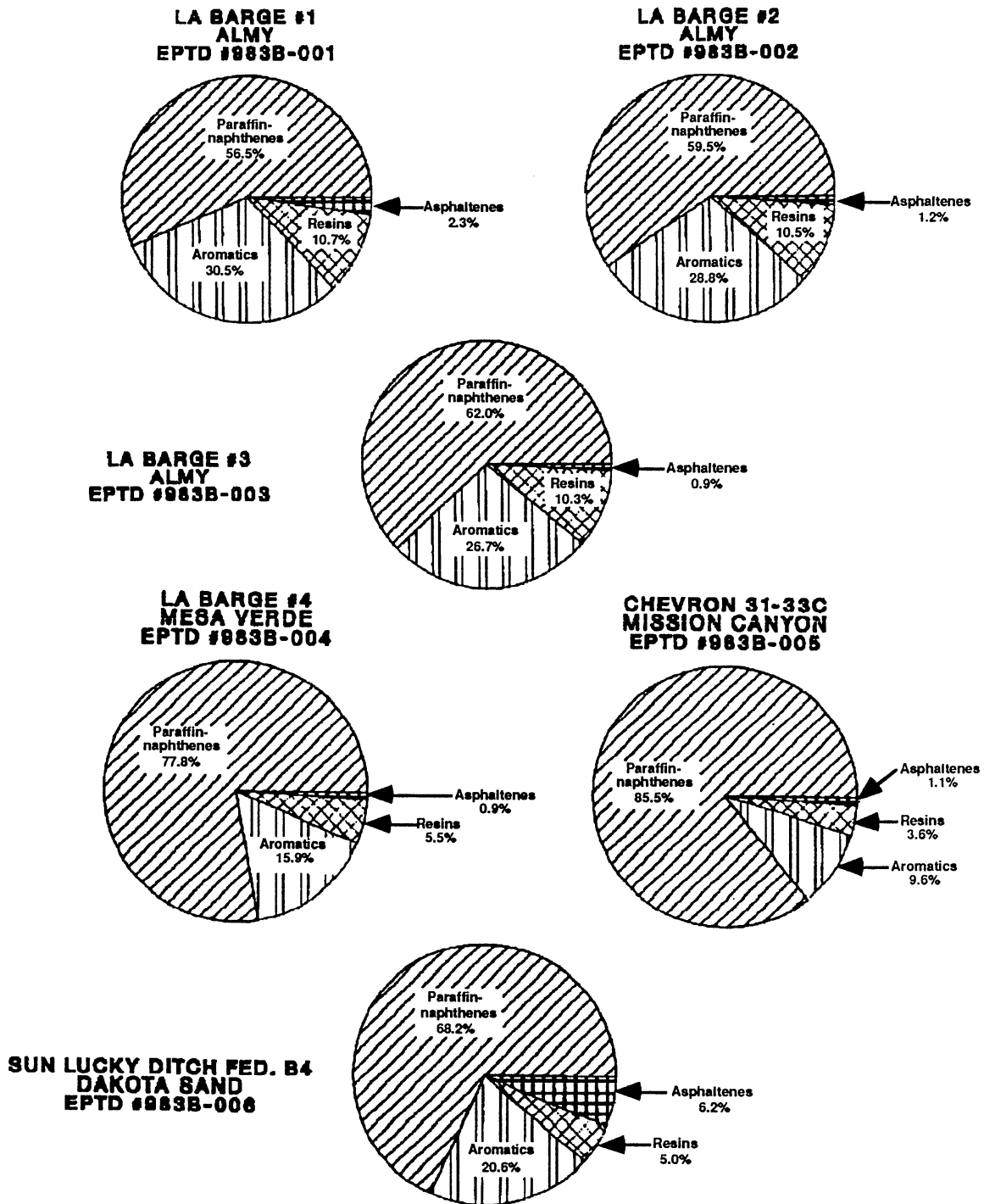


Figure 37. (1 of 2)

**DOME #1-13, HILLER FED.  
FRONTIER  
EPTD #983B-007**

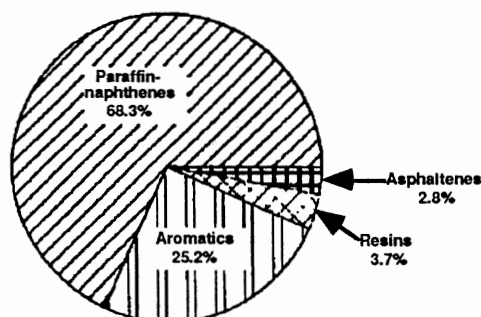


Figure 37. (2 of 2) Group analysis of the seven samples listed in Table V (Elrod, 1987)

The Hoback, Mesaverde and Mission Canyon samples revealed high pristane/ phytane ratios and elevated waxy paraffin distributions. These factors indicate sediment typically associated with peat swamps, where waxy cuticles of higher land plants provide abundant organic matter (Elrod, 1987). The data also suggested the same or similar source for these oils. The Dakota and Frontier oils display much lower pristane/phytane ratios and slightly less waxiness, suggesting a more marine setting with less terrestrial influence (Elrod, 1987).

Hopane and sterane biomarker distributions for the Hoback and Mesaverde samples are essentially identical, confirming that the oils are sourced from the same terrestrial organic matter (Elrod, 1987). Biomarker distributions from the Mission Canyon oil were slightly different, while the Dakota and Frontier samples were extremely different, indicating different organic matter sources for these samples (Elrod, 1987). These biomarker distributions indicate a much higher quantity of marine-sourced organic matter.



The Upper Cretaceous Hilliard and Mesaverde formations meet the conditions described for the source material of the Hoback and Mesaverde oils. Both formations contains marginal marine to non-marine facies with abundant terrestrial plant material. The Upper Hilliard and the entire Mesaverde Formation contain abundant coal and carbonaceous shale units.

### Migration Path

Faulting of the Mesaverde and Upper Hilliard by the Calpet and Hilliard thrust faults provided maturation and subsequent migration for the Hoback and Mesaverde oil. These faults and their auxiliary faults and fractures provided migration paths to the Hoback and Mesaverde formations as well as the surface (Figure 38). The oil springs described by Schultz (1914) lie just east of the trace of the Hilliard fault, where oil has made its way to the surface through migration paths in the younger Tertiary strata (Figure 10).

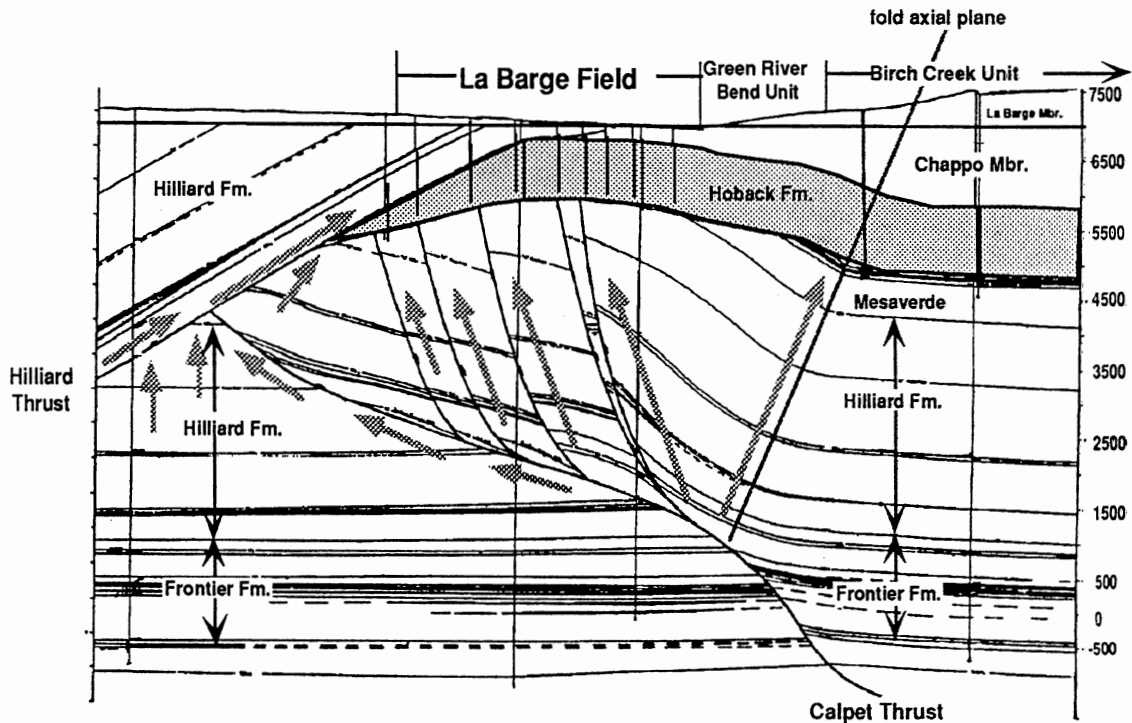


Figure 38. Hydrocarbon migration paths of Hoback oil. Large shaded arrows represent migration conduits along major faults and fold-associated fractures

### Trapping Mechanisms

The Hoback reservoir contains both structural and stratigraphic traps.

Structural traps include compressional anticline and thrust fault accumulations.

Stratigraphic traps include up dip facies change and up dip pinchout traps.

#### Structural Traps

The La Barge platform (anticline) is a compressional feature formed by the eastward compression of the overthrust belt. Hoback sands with good lateral continuity on the crest of the structure can be contained by compressional anticline traps. This is probably the second most common trap type of the

Hoback sands, but complete structural closure is probably rare due to the highly variable nature of these sands.

The second structural trap type is thrust fault traps formed by the Hilliard and its auxiliary faults. This occurs in the western part of the study area where thrust repeat sections of the Hoback formation are oil productive. This trapping type is uncommon, but does exist at La Barge.

### Stratigraphic Traps

Although these traps are primarily stratigraphic, they have been influenced by tectonic forces and should probably be referred to as combination traps. The most common trap type within the Hoback Formation is updip facies change.

Updip facies changes are the result of the highly dynamic depositional nature of the Hoback formation. Rapidly changing facies produce lateral and vertical permeability barriers which resulted in complex hydrocarbon traps. This is the most common trapping type at La Barge and will be mentioned later.

Updip pinchouts comprise the final major trapping mechanism found in the Hoback reservoir. This is the trapping mechanism found in the TH-1 interval and the lower TH-2 sand on the eastern flank of the La Barge platform.

### Cumulative Production Map

Since the beginning of production in 1924, the Hoback reservoir has produced 22,051,811 BO and 425,604 MCF of gas (National Production Service/Industry Production as of 6/1/91). Cumulative production within the La Barge field is shown in Plate XVIII. Most of the production within the La Barge field is commingled, therefore production data for each interval were not available. Wells were color coded according to their completion date in order to

clarify their cumulative production value. Areas with production values greater than 250,000 barrels were shaded to aid in interpretation of the map. Initial production of oil and water is also posted. The distribution of major production exhibits an interesting linear trend. The largest concentration of wells with cumulative production values of 250,000 barrels or more is located along a north-south trend on the west flank of the structure (Plate XVIII). This area very closely mimics the subsurface trend of the Hilliard thrust, which supports the assumption that this fault and its related fracturing was the major migration path of Hoback oil.

#### Possible Reservoir Communication Problems

Several reports have been written on enhanced oil recovery (EOR) techniques conducted on the Hoback reservoir and their relative success. Some of the authors include: Moreland (1968), Ulrich, (1976), O'Hare and Ulrich, (1976), Baker, (1977), Koehler, (1977), Hefta and Larson, (1978), and Wendte (1989). Most of these authors agree that there is a reservoir communication problem within individual sands; they attribute this to faulting of the Hoback Formation. The writer proposes that the reservoir segmentation is a function of the depositional nature of these sands and not an overwhelming imbricate structure as proposed by some. Well logs and seismic data do not support any of the faults documented by Hefta and Larson (1978). Additional evidence opposing fault segmentation of the reservoir comes from an API gravity trend study of the north half of the field. Lindsey, (1945) reported a distinctive gravitational separation of oil within each of the individual sand bodies. This gravitational separation of oil within individual sands suggests that faulting did not penetrate the producing sands. If fault zones were present

within the Hoback sands, the oil from the various sands would have migrated along some of these zones and intermingled, resulting in an overall vertical gravitational separation of the formation (Lindsey, 1945). This separation has not occurred, and in fact the lowest gravity oils are found in the highest producing sand (Lindsey, 1945).

Well log data does support highly variable sedimentation as noted in the previous Chapter. The nature of a braided river and its low bank stability results in a highly mobile channel system prone to lateral shifting and downcutting. This results in sheet sands composed of many irregular-shaped subfacies deposits. Lateral and vertical permeability and porosity barriers associated with some of these subfacies prevent homogeneity of individual sands, which results in a highly complex segmentation of the reservoir. Clay drapes on cross-bedding of the various bar subfacies act as micro permeability barriers (Figure 23), which could either impede, stop, or divert horizontal fluid movement. These phenomena result in the combined effect of limiting reservoir continuity in what appears to be homogenous laterally continuous sheet sands. In order to unravel the complex nature of this reservoir, additional facies analysis of the existing unslabbed cores should be conducted. This would assist in determining typical electric log trends as well as lateral and vertical porosity and permeability associated with individual subfacies. Using these data, net sand maps of individual sand bodies could be subdivided according to their electrical log signature, thereby revealing areas of possible reservoir compartmentalization. This type of analysis would lead to the most accurate delineation of the Hoback reservoir.

## CHAPTER VIII

### SUMMARY AND CONCLUSIONS

Detailed analysis of the Paleocene Hoback Formation in La Barge field provided a number of conclusions.

The depositional environment of the Hoback Formation was found to be that of a sand dominated braided river. Although palynology conducted on the Hoback Formation proved to be inconclusive, the age was determined to be Middle to Late Paleocene. This age range was established from previous palynology and mammalian fossil studies. In studying the Paleocene producing sands at La Barge a consistent stratigraphic nomenclature of the Early Tertiary here was proposed based on age, province and depositional nature.

The tectonic influences on the reservoir seemed to be very important in providing a structure for accumulation, as well as providing maturation and a subsequent migration path for hydrocarbons into the Hoback Formation. Although this region is structurally complex, the Hoback intervals themselves were found to be fairly consistent across the field and were not segmented by faulting.

Subsurface stratigraphy revealed these continuous intervals were composed of a variety of subfacies that produce a very complex geometry. Many interconnecting channels and their related side and

inter-channel deposits were revealed. This highly dynamic alluvial system was found to be the cause of reservoir segmentation within the field. Channel and bank instability of the braided river resulted in sheet sand deposition composed of a variety of discontinuous subfacies, some of which acted as permeability barriers.

Based on net sand maps, a generalized paleoenvironment interpretation was constructed. These data suggested a northeasterly source for the majority of the Hoback sands. Sediment composition, size and shape revealed a relatively close igneous and metamorphic source. The only structural feature capable of producing this type of material at this time was the near by Wind River Uplift.

Finally, cumulative production data revealed a concentration of high production along the west flank of the structure. This area closely corresponds to the subsurface trace of the Hilliard thrust, suggesting that migration and charging of the Hoback Formation may have occurred along this fault surface.

## REFERENCES CITED

- Asquith, D. O. (1966). Geology of Late Cretaceous Mesaverde and Paleocene Fort Union Oil Production, Birch Creek Unit, Sublette County, Wyoming: American Assoc. of Petroleum Geologists Bull., 50(10), p. 2176-2184.
- Armstrong, F. C., and Oriel, S.S. (1965). Tectonic development of Idaho-Wyoming thrust belt: American Assoc. of Petroleum Geologists Bull., 49(11), p. 1847-1866.
- Bally, A. W., and Snelson, S. S. (1980). Realms of subsidence. In A. D. Miall (Ed.), Canadian Society of Petroleum Geology Memoir, 6, p. 1-94.
- Baker, E. A. (1977). La Barge unit steamflood pilot Almy reservoir La Barge field Lincoln and Sublette Counties, Wyoming: Texaco, in-house report, 63 p.
- Bartram J. G., and Hupp, J. E. (1929). Subsurface structure of some unsymmetrical anticlines in the Rocky Mountains: American Association of Petroleum Geologists Bull., 13(10), p.1275-1289.
- Beck, R. A., Vondra, C. F., Filkins, J. E., and Olander, J. D. (1988). Syntectonic sedimentation and Laramide basement thrusting, Corilleran foreland; Timing of deformation: Geological Society of America Memoir, 171, p. 465-487.
- Berg, R. R. (1961). Laramide tectonics of the Wind River Mountains: Wyoming Geological Assoc., 16th Annual Field Conference, p. 70-79.
- Berg, R. R. (1962). Mountain flank thrusting in Rocky Mountain foreland, Wyoming and Colorado: American Assoc. of Petroleum Geologist Bull., 46(11), p. 2019-2032.
- Bertagnolli, A. J., Jr. (1941). Geology of the southern part of La Barge region, Lincoln County, Wyoming: American Assoc. Petroleum Geologists Bull., 25(9), p. 1729-1744.
- Blackstone, D. L., Jr. (1979). Geometry of the Prospect-Darby and La Barge faults at their junction with the La Barge Platform, Lincoln and Sublette Counties, Wyoming: Geological Survey of Wyoming. Report of Investigations, No 18, 34 p.
- Busch, D. A., and Link, D. A. (1985). Exploration methods for sandstone Reservoirs. Tulsa, Oklahoma: OGCI Pub.



- Cant, D. J. (1978). Development of a facies model for sandy braided river sedimentation: Comparison of the south Saskatchewan River and the Battery Point Formation. In A. D. Miall (Ed.), Fluvial Sedimentology: Canadian Society of Petroleum Geologists Memior 5 (p. 627-639). Calgary, Alberta, Canada: McAra Printing Ltd.
- Christensen, H. E., and Marshall, J. (1950). La Barge field, T. 26-27 N., R. 113 W., Lincoln and Sublette Counties, Wyoming: Wyoming Geological Assoc., 5th Annual Field Conference, p. 105-108.
- Cope, E. D. (1873). On the extinct vertebrata of the Eocene of Wyoming, with notes on the geology: U. S. Geology and Geography Survey Terr. (Hayden), 6th Annual Report, p. 543-649.
- Cobban, W. A., and Reeside, J. B., Jr. (1952). Correlation of the Cretaceous formations of the Western Interior of the United States: Geological Society of America Bull., 63(10), p. 1011-1043.
- Craddock, J. P., Kopania, A. A., and Wiltschko, D. V. (1988). Interaction between the northern Idaho-Wyoming thrust belt and bounding basement blocks, central western Wyoming: Geological Society of America Memoir, 171, p. 333-351.
- Curry, W. H., III (1973). Late Cretaceous and Early Tertiary rocks southwestern Wyoming: Wyoming Geological Assoc., 25th Annual Field Conference, p. 79-86.
- Davis, H. R., Byers, C. W., and Pratt, L. M. (1989). Depositional mechanisms and organic matter in Mowry Shale (Cretaceous), Wyoming: American Assoc. of Petroleum Geologists Bull., 73(9), p. 1103-1116.
- Devine, P. E. (1991). Transgressive origin of channeled estuarine deposits in the Point Lookout sandstone, northwestern New Mexico: A model for Upper Cretaceous, cyclic regressive parasequences of the U. S. western interior: American Assoc. of Petroleum Geologists Bull., 75(6), p. 1039-1063.
- Donovan, J. H. (1950). Intertonguing of Green River and Wasatch Formations in part of Sublette and Lincoln Counties, Wyoming: M. S. Thesis, University of Utah, 46 p.
- Dorr, J. A., Jr. (1952). Early Cenozoic stratigraphy and vertebrate paleontology of the Hoback Basin, Wyoming: Geological Society of America Bull., 63(1), p. 59-94.
- Dorr, J. A., Jr., Spearing, D. R. and Steidtmann, J. R. (1977). The tectonic and synorogenic depositional history of the Hoback Basin and adjacent areas: Wyoming Geological Assoc., 29th Annual Field Conference, p. 549-562.

- Dorr, J. A. Jr., and Gingerich, P. D. (1980). Early Ceneozoic mammalian paleontology, geologic structure, and tectonic history in the overthrust belt near La Barge, western Wyoming: Contributions to Geology, University of Wyoming, 18(2), p. 101-115.
- Dunnwald, J. B. (1969). Big Piney La Barge Tertiary oil and gas field: Wyoming Geological Society, 21st Annual Field Conference, p. 139-143.
- Eardley, A. J. Horberg, Leland, Nelson, V. E., and Church, V. (1944). Hoback-Gros Venture-Teton [Wyo.], Field Conference: 2 maps and sections [Michigan University].
- Eardley, A. J. (1960). Phases of orogeny in the fold belt of western Wyoming and southern Idaho: Wyoming Geological Assoc., 15th Annual Field Conference, p. 37-40.
- Elrod, L. W. (1987). Geochemical analysis: Oil samples from various Wyoming wells: Texaco, in-house report, 45 p.
- Fahy, M. (1987). Pre-thrusting basin morphology: Influence on geochemical "fairways" and subsequent thrust deformations in the Wyoming-Idaho thrust belt: Wyoming Geological Assoc., 38th Annual Field Conference, p. 267-274.
- Fidlar, M. M. (1950). Clay Basin gas field, Daggett County, Utah: Wyoming Geological Assoc., 5th Annual Field Conference, p. 86-87.
- Frerichs, W. E., and Steidtmann, J. R. (1971). Sea level variation during deposition of the Hilliard Formation (Upper Cretaceous), western Wyoming: Wyoming Geological Assoc., 23rd Annual Field Conference, p. 157-168.
- Galloway, W. E., and Hobday, D. K. (1983). Terrigenous clastic depositional systems. New York: Springer-Verlag.
- Gibson, R. I. (1987). Basement tectonic controls on structural style of the Laramide thrust belt interpreted from gravity and magnetic data: Wyoming Geological Assoc., 38th Field Conference, p. 27-35.
- Guennel, G. K., Spearing, D. R., and Dorr, J. A., Jr. (1973). Palynology of the Hoback Basin: Wyoming Geological Assoc., 25th Annual Field Conference, p. 173-185.
- Hamlin, H. S. (1991). Stratigraphy and depositional systems of the Frontier Formation and their controls on reservoir development, Moxa Arch, southwest Wyoming: Gas Research Institute, Topical Report, 45 p.

- Hefta, K. L., and Larson B. O. (1978). Fault interpretation and estimation of original oil in place for the southern half of the La Barge unit Sublette And Lincoln Counties, Wyoming: Texaco, in-house report, 18 p.
- Horberg, L. (1949) Structural trends in central western Wyoming: Geological Society of Amer. Bull., 99(2), p. 183-216.
- Jordan, T. E. (1981). Thrust loads and foreland basin evolution, Cretaceous, western United States: The American. Assoc. of Petroleum Geologists, 65(12), p 2506-2520.
- Klemme, H. D. (1980). Petroeum basins-classifications and characteristics: Journal of Petroleum Geology, 3 (2), p. 187-207.
- Knight S. H. (1950). Physical aspects of the Green River Basin and adjacent mountain ranges: Wyoming Geological Assoc., 5th Annual Field Conference, p. 75-80.
- Knight, W. C. (1902). The petroleum fields of Wyoming: Engineering Mining Journal, 73, p. 720-723.
- Koehler, R. C. (1977). La Barge unit chemical pilot laboratory investigation Almy II reservoir La Barge field Lincoln and Sublette Counties, Wyoming: Texaco, in-house report, 73 p.
- Kraig, D. H., Wiltchko, D. V., and Sprang, J. H. (1987). Interaction of basement uplift and thin-skinned thrusting, Moxa Arch and the western overthrust belt, Wyoming: A hypothesis: Geological Society of America Bull., 99, p. 654-662.
- Kraig, D. H., Wiltchko, D. V., and Spang, J. H. (1988). The interaction of the Moxa Arch (La Barge Platform) with the Cordilleran thrust belt, south of Snider Basin, southwestern Wyoming: Geological Society of America Memoir 171, p. 395-410.
- Kraig, D. H., and Wiltchko, D. V. (1988). Effects on the calcite fabric (Madison formation) of the Darby-Hogsback thrust sheet and La Barge Platform, Snider Basin area, Wyoming: Wyoming Geological Assoc., 38th Annual Field Conference, p. 101-108.
- Krueger, M. L. (1955). Preliminary geological report, Big Piney gas field, Sublette County, Wyoming: Wyoming Geological Assoc., 10th Annual Field Conference, p. 142-144.
- Krueger, M. L. (1960). Occurrence of natural gas in the western part of Green River Basin: Wyoming Geological Assoc., 15th Annual Field Conference, p. 194-209.

- Krumbein W. C., and Sloss L. L. (1963). Stratigraphy and Sedimentation. San Francisco: W. H. Freeman and Company.
- Lindsey, K. B. (1945). Oil gravity distribution of the Tertiary of La Barge: The Texas Company, in-house report, 12 p.
- Lowell, J. D. (1977). Underthrusting origin for thrust-fold belts with application to the Idaho-Wyoming belt: Wyoming Geological Assoc., 29th Annual Field Conference, p. 449-455.
- McDonald, R. E. (1973). Big Piney-La Barge producing complex, Sublette and Lincoln Counties, Wyoming: Wyoming Geological Assoc., 25th Annual Field Conference, p. 57-77.
- Miall, A. D. (1977). A review of the braided river depositional environment: Earth Science Reviews, 13(1), p. 1-62.
- Miall, A. D. (1978). Lithofacies types and vertical profile models in braided river deposits: A summary. In A. D. Miall (Ed.), Fluvial Sedimentology: Canadian Society of Petroleum Geologists Memior 5 (p. 597-604). Calgary, Alberta, Canada: McAra Printing Ltd.
- Miall, A. D. (1985). Multiple-channel bedload rivers. In SEPM short course no. 19, Recognition of fluvial depositional systems and their resource potential (p. 83-100). Tulsa, Oklahoma: SEPM Pub.
- Michael, R. H. (1960). Hogsback and Tip Top units, Sublette and Lincoln Counties, Wyoming: Wyoming Geological Assoc., 15th Annual Field Conference, p. 209-216.
- Moreland, H. B. (1968). Performance of the La Barge unit (Tertiary) stage I waterflood: Texaco, in-house report, 66 p.
- Mountjoy, E. W. (1966). Time of thrusting in Idaho-Wyoming thrust belt-discussion: Amer. Assoc. of Petroleum Geologists Bull., 50(12), p. 2612-2613.
- Murray, F. E. (1960). An interpretation of the Hillard thrust fault, Lincoln and Sublette, Counties, Wyoming: Wyoming Geological Assoc., 15th Annual Field Conference, p. 181-186.
- O'Hare, A. C., and Ulrich D. D. (1976). Basic reservoir study lower Almy IV reservoir La Barge field Lincoln and Sublette Counties, Wyoming: Texaco in-house report, 55 p.
- Oriel, S. S., Gazin, C. L., Tracey, and J. I., Jr. (1962). Eocene age of Almy Formation, Wyoming, in its type area: American Assoc. of Petroleum Geologists Bull., 46(10), p. 1936-1937.

- Oriel, S. S. (1962). Main body of Wasatch formation near La Barge, Wyoming: American Assoc. of Petroleum Geologists Bull., 46(12), p. 2161-2173.
- Oriel, S. S., and Armstrong, F. C. (1966). Times of thrusting in Idaho-Wyoming thrust belt: Reply: American Assoc. of Petroleum Geologists Bull., 50(12), p. 2614-2621.
- Oriel, S. S. (1969). Geology of the Fort Hill Quadrangle, Lincoln County, Wyoming: U. S. Geological Survey, Professional Paper 594 M, 40 p., map and cross sections in pocket.
- Robbins, L. S. (1940). North end of La Barge field Sublette County, Wyoming: The Texas Company, in-house report, 4 p.
- Royse, F., Jr., Warner, M. A., and Reese, D. L. (1975). Thrust belt structural geology and related stratigraphic problems, Wyoming-Idaho-northern Utah: Deep drilling frontiers of the central Rocky Mountains, Rocky Mountain Assoc. of Geologists, Symposium Volume, p. 41-54.
- Rubey, W. W., Oriel, S. S., and Tracey, J. I. (1961). Age of the Evanston Formation, western Wyoming: Wyoming Geological Assoc., 16th Annual Field Conference, p. 68-69.
- Rust B. R. (1978). Depositional models for braided alluvium. In A. D. Miall (Ed.), Fluvial Sedimentology: Canadian Society of Petroleum Geologists Memorial 5 (p. 605-625). Calgary, Alberta, Canada: McAra Printing Ltd.
- Schultz, A. R. (1907). The La Barge field, central Uinta County, Wyoming: U. S. Geological Survey Bull. 340, p. 364-373.
- Schultz, A. R. (1914). Geology and geography of a portion of Lincoln County, Wyoming: U. S. Geological Survey Bull. 543, 141 p.
- Shipp, B. G., and Dunnewald, J. B. (1962). The Big Piney-La Barge Frontier gas field, Sublette and Lincoln Counties, Wyoming: Wyoming Geological Assoc., 17th Annual Field Conference, p. 273-279.
- Spearing, D. R. (1969). Stratigraphy, sedimentation and tectonic history of the Paleocene-Eocene Hoback Formation of western Wyoming: Unpublished P. H. D. Thesis, University of Michigan, Michigan, 179 p.
- Spelman, A. R. (1976). Possible factors affecting waterflood programs in Almy sandstone reservoirs at La Barge field, Sublette and Lincoln Counties, Wyoming: Texaco, Denver Division Biostratigraphic Lab Report No. 76-76, 30 p.
- Thomaidis, N. D. (1973). Church Buttes Arch Wyoming and Utah: Wyoming Geological Assoc., 25th Annual Field Conference, p. 35-39.

- Toots, H., (1961). Beach indicators in the Mesaverde Formation: Wyoming Geological Assoc., 16th Annual Field Conference, p. 157-168.
- Ulrich, D. D. (1976). La Barge unit chemical pilot waterflood performance evaluation Almy II reservoir La Barge field Lincoln and Sublette Counties, Wyoming: Texaco, in-house report, 50 p.
- Veatch, A. C. (1907). Geography and geology of a portion of southwestern Wyoming, with special reference to oil and coal: U.S. Geol. Survey Prof. Paper 56, 178 p.
- Ver Ploeg, A. J. (1979). The overthrust belt: An overview of an important new oil and gas province: The Geological Survey of Wyoming. Public Information Circular No. 11, 15 p.
- Ver Ploeg, A. J., and De Bruin, R. H. (1982). The search for oil and gas in the Idaho-Wyoming-Utah salient of the overthrust belt: The Geological Survey of Wyoming. Public Information Circular No. 21, 21 p., maps in pocket.
- Wach, P. H. (1977). The Moxa Arch, an overthrust model?: Wyoming Geological Assoc., 29th Annual Field Conference, p. 651-664.
- Webel, S. (1987). Significance of backthrusting in the Rocky Mountain thrust belt: Wyoming Geological Assoc., 38th Annual Field Conference, p.37-53.
- Wendte, S. S. (1989). EOR feasibility study, Almy reservoir, La Barge unit, Lincoln and Sublette Counties, Wyoming: Texaco, in-house report, 33 p.
- Wiltschko, D. V., and Dorr, J. A., Jr. (1983). Timing of deformation in overthrust belt and foreland of Idaho, Wyoming, and Utah: American Assoc. of Petroleum Geologists Bull., 67(8), p 1304-1322.
- Wiltschko, D. V., and Eastman, D. B. (1983). Roll of basement warps and faults in localizing thrust fault ramps: Geological Society of America Memoir 158, p. 177-190.
- Wiltschko, D. V., and Eastman, D. B. (1988). A photoelastic study of the effects of preexisting reverse faults in basement on the subsequent deformation of the cover: Geological Society of Amer. Memoir 171, p. 111-117.
- Woodward, N. B. (1988). Primary and secondary basement controls on thrust sheet geometries: Geological Society of America Memoir 171, p. 353-366.

## APPENDICES

APPENDIX A

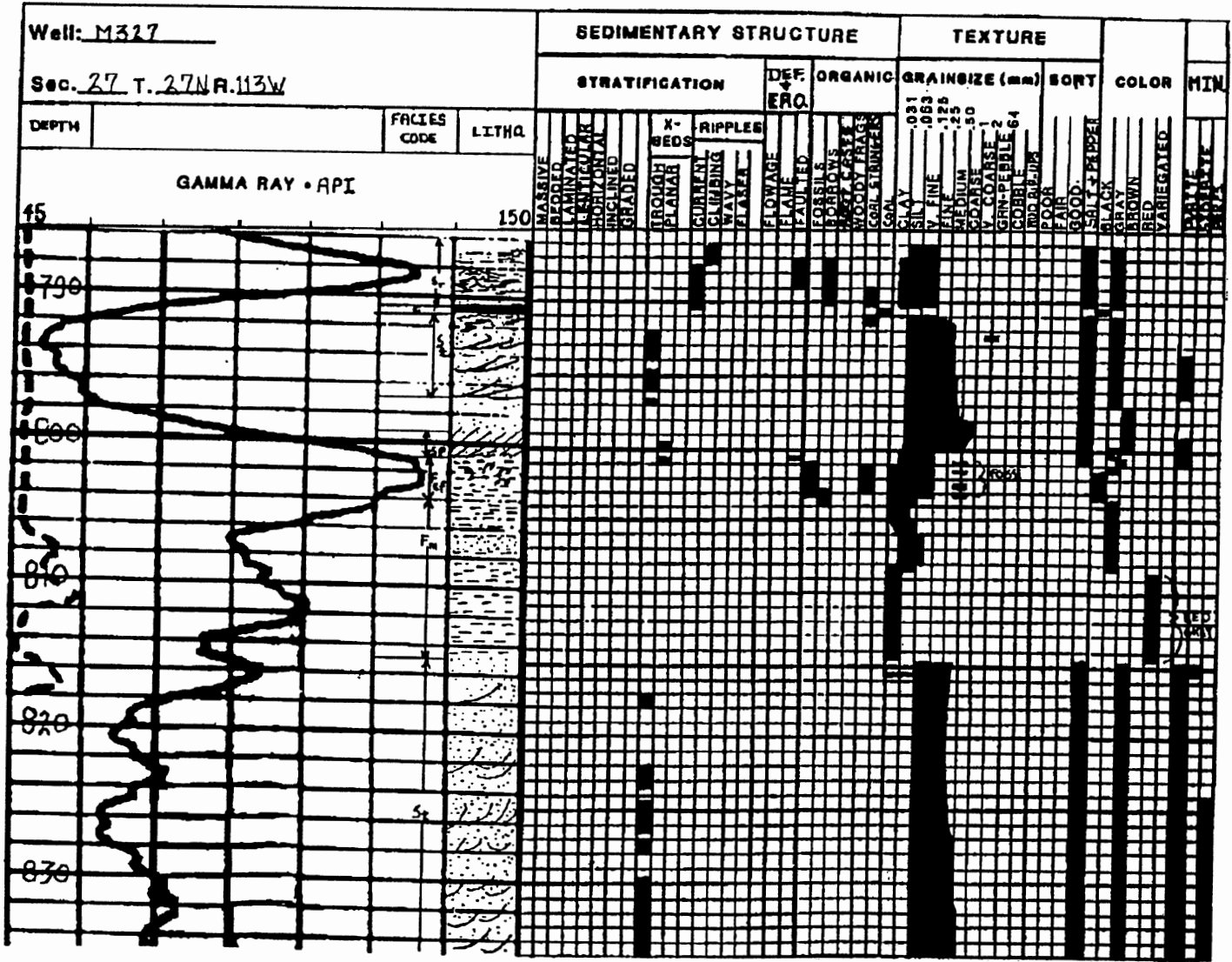
CORE DISCRPTIONS

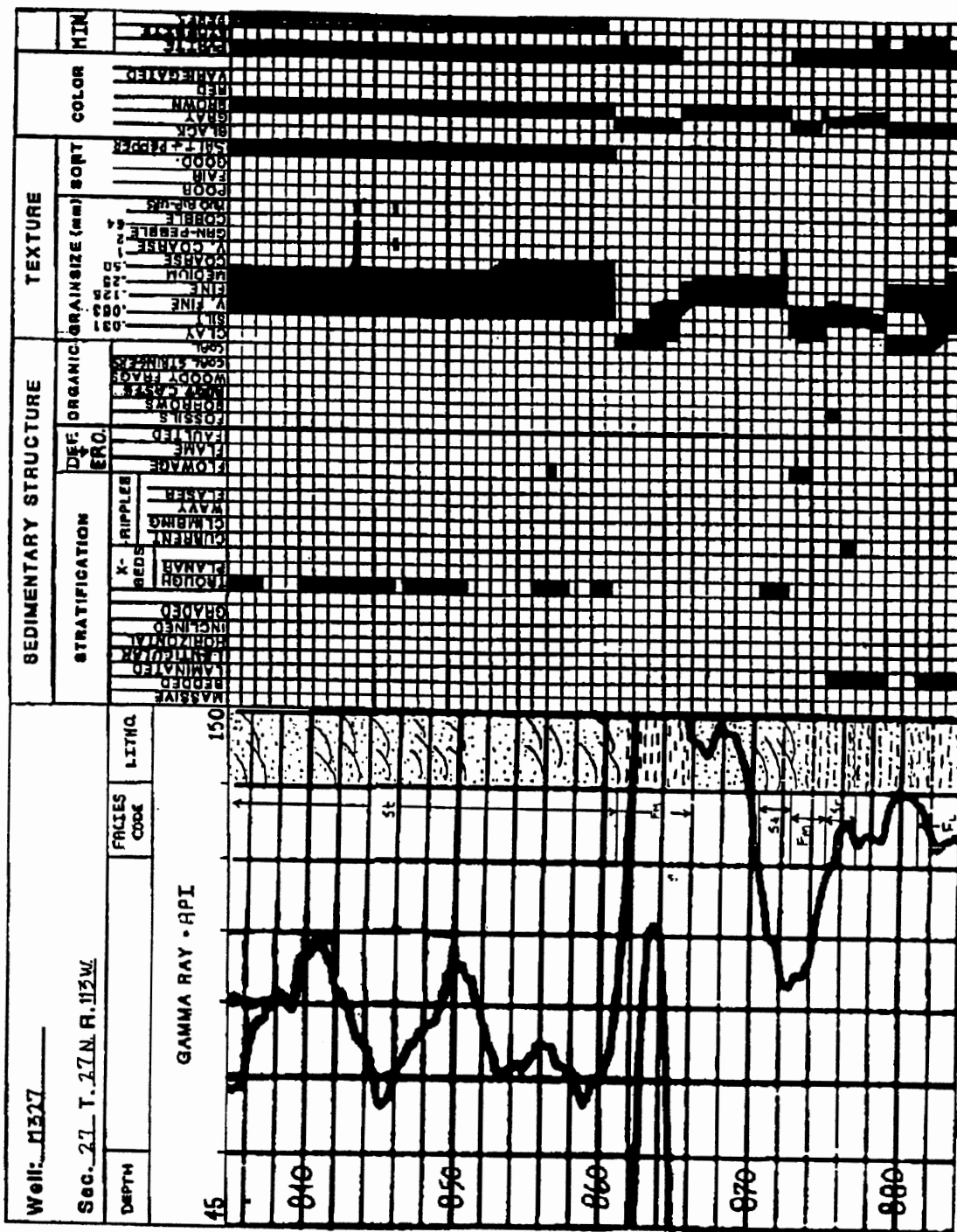


### CORE LITHOLOGY SYMBOLS

GRAVEL	SAND	SILT	MUD
COAL BED	COAL STRINGER	FOSSIL	UNCONFORMITY
TROUGH X-BEDS	PLANAR X-BEDS	HORIZONTAL BEDS	RIPPLE X-BEDS
SCOUR TROUGH X-BEDS	FACIES CODES ARE GIVEN IN TABLE II.		

WELL M327







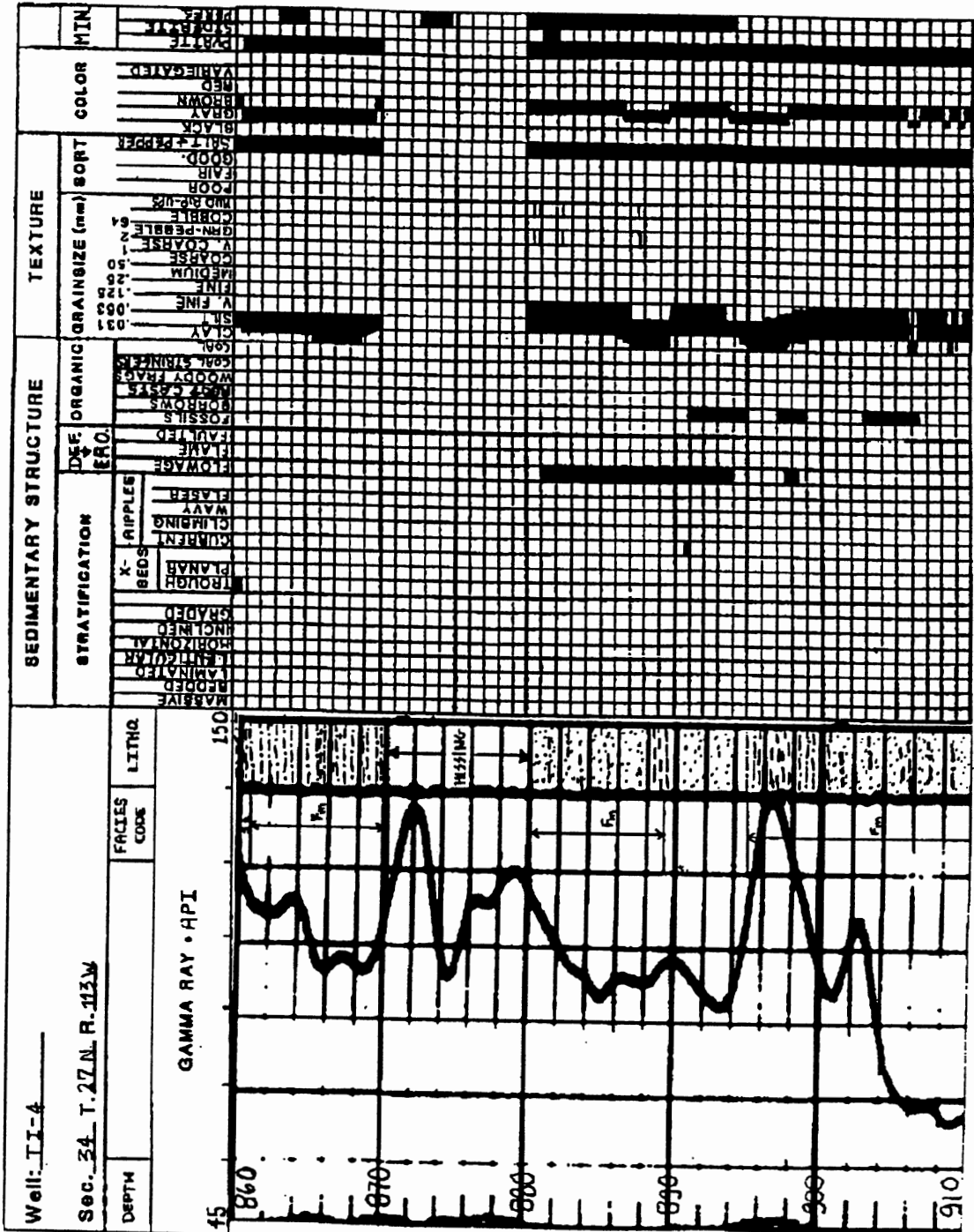


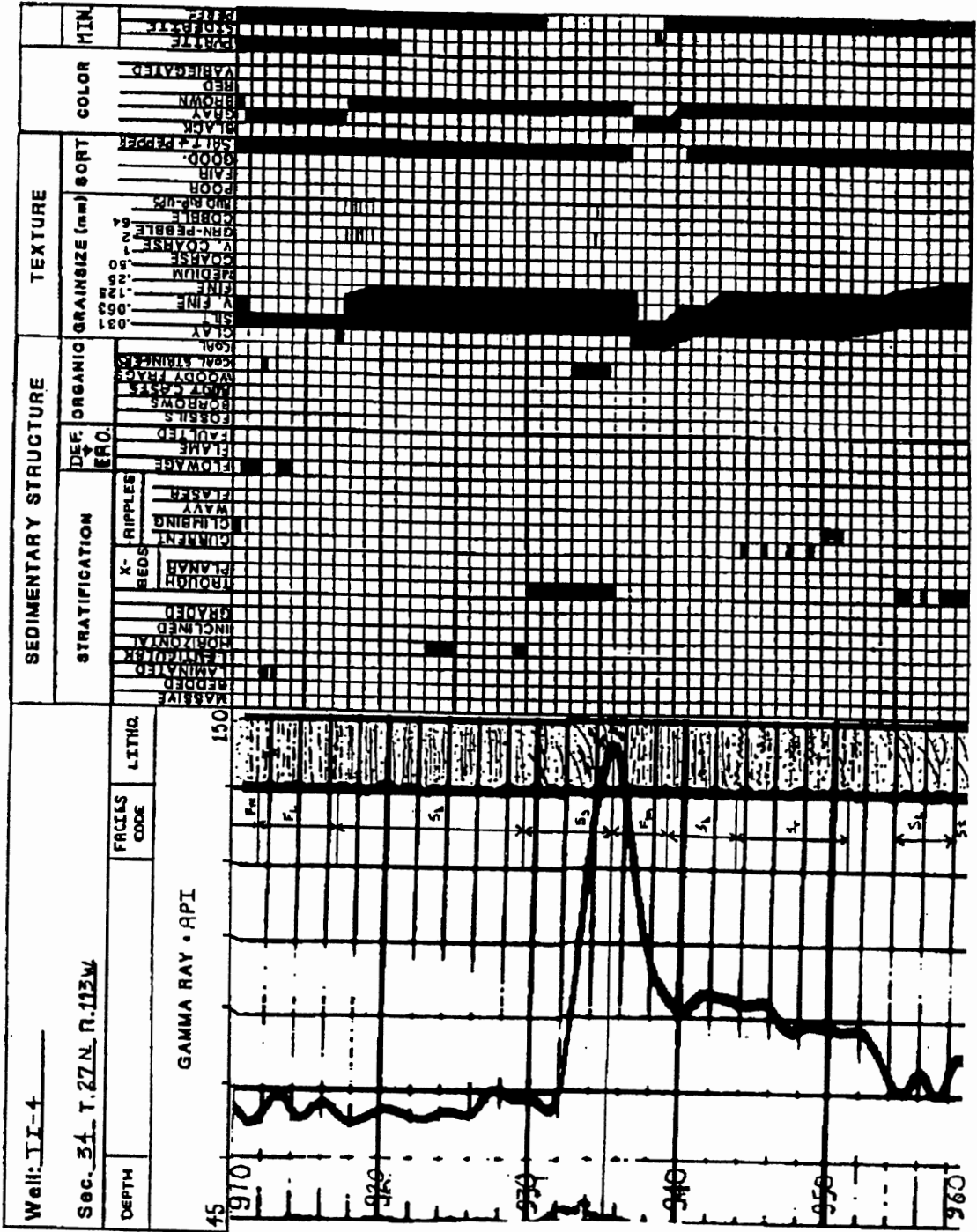


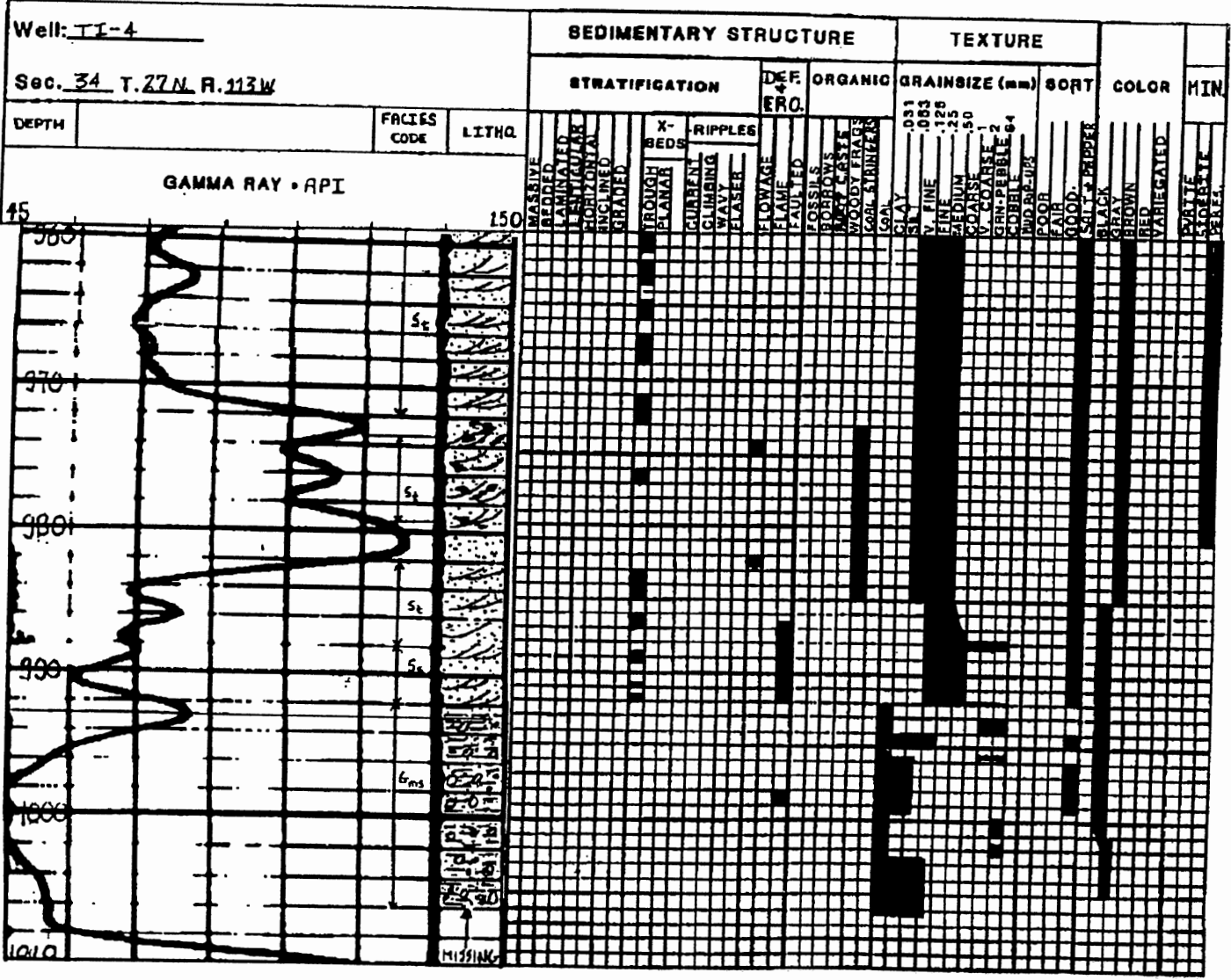
WELL TI-4

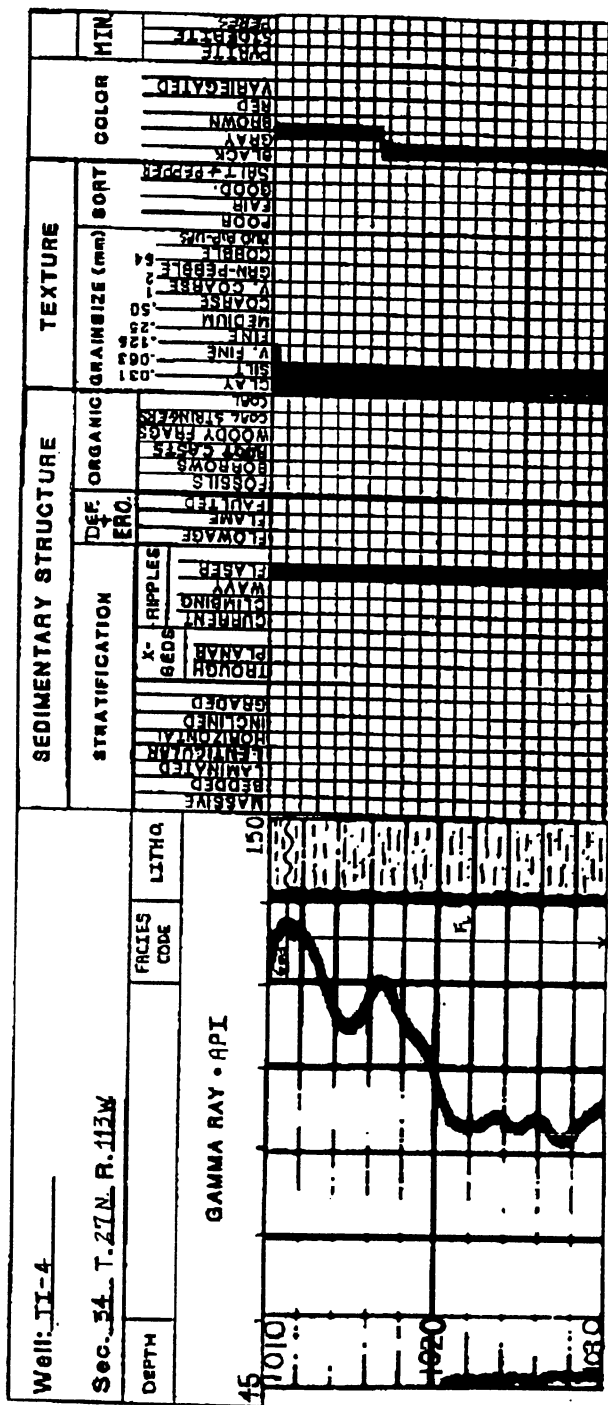




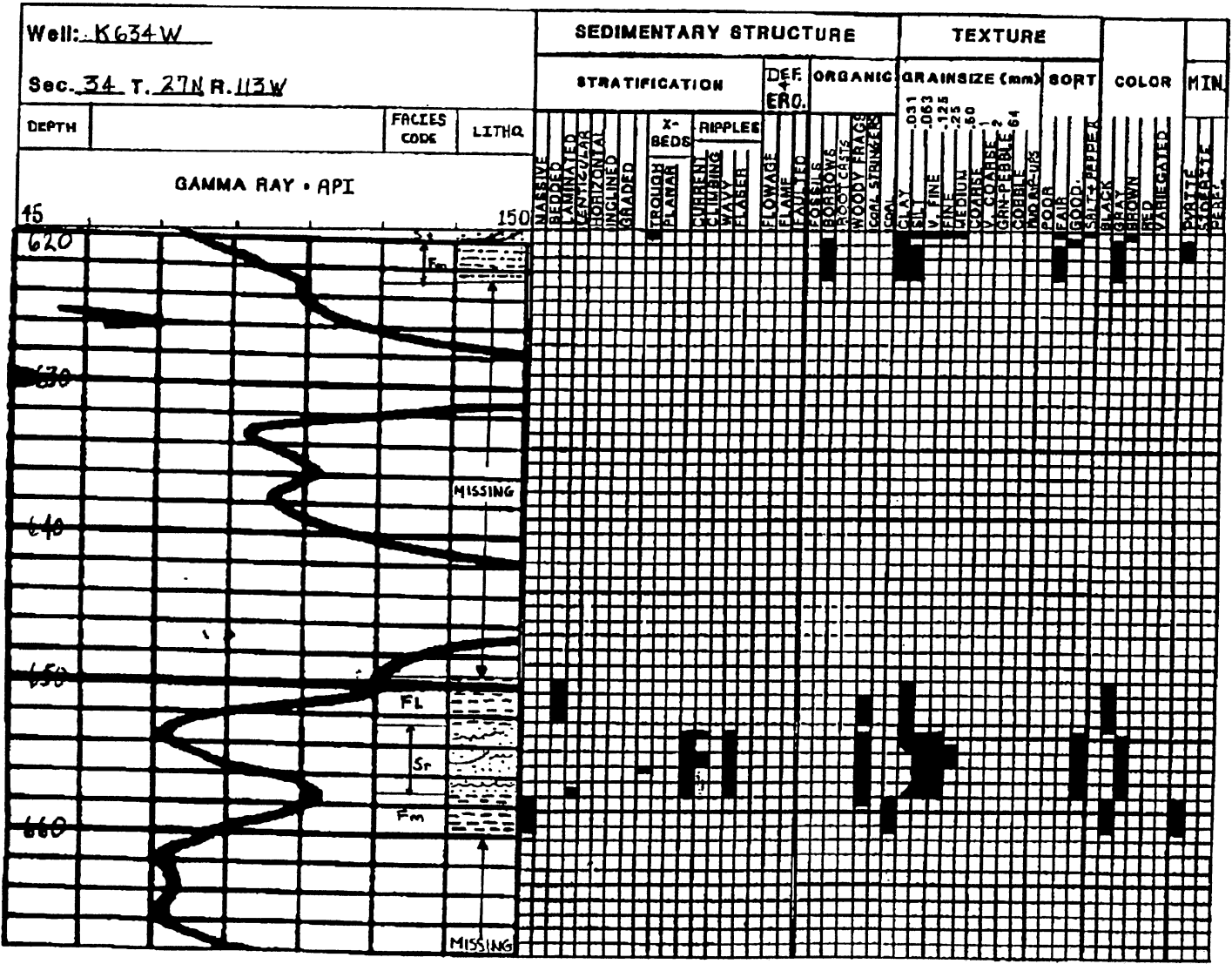








WELL K634W



GAMMA RAY • API

MISSING

FL

Sr

Fm

MISSING



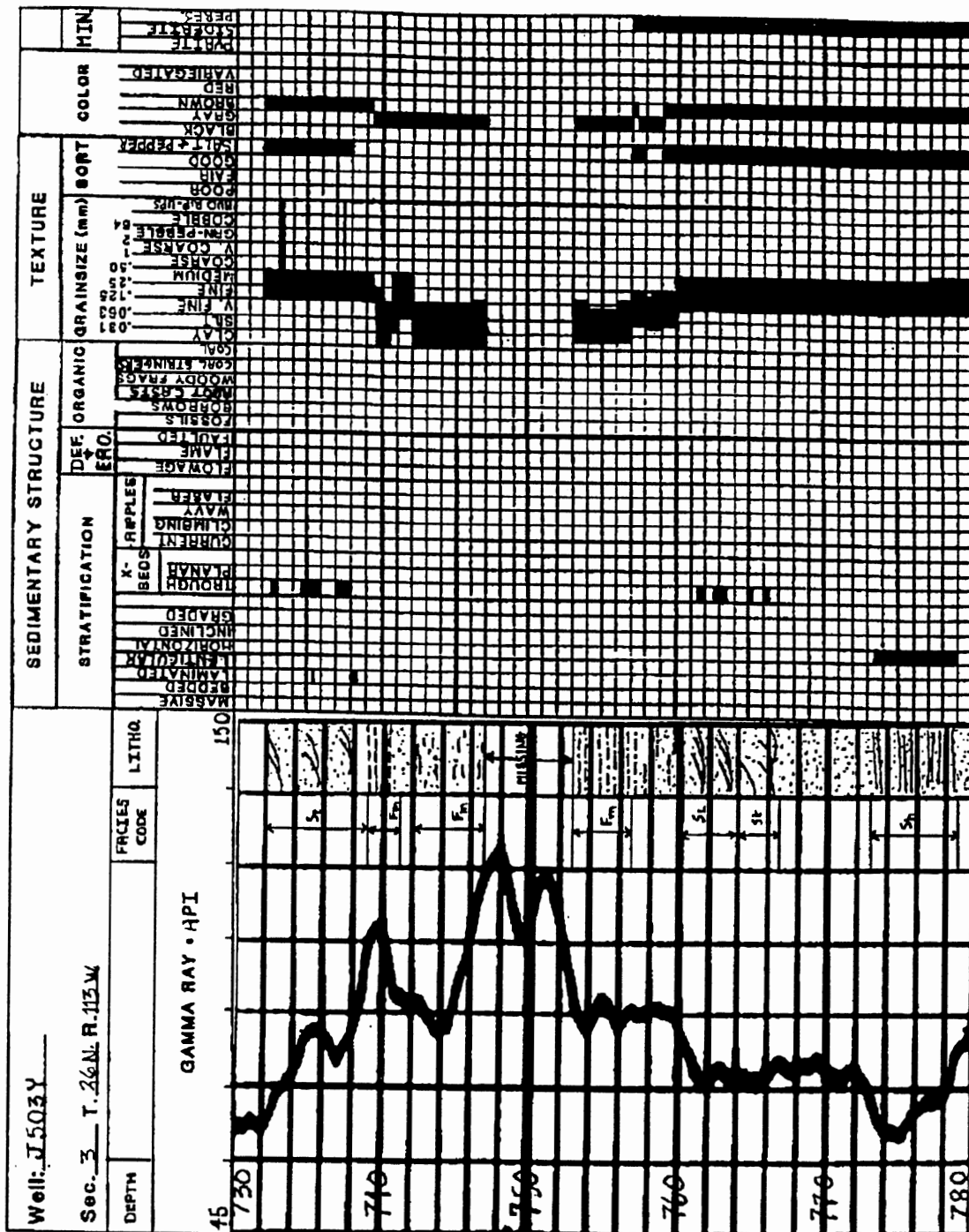




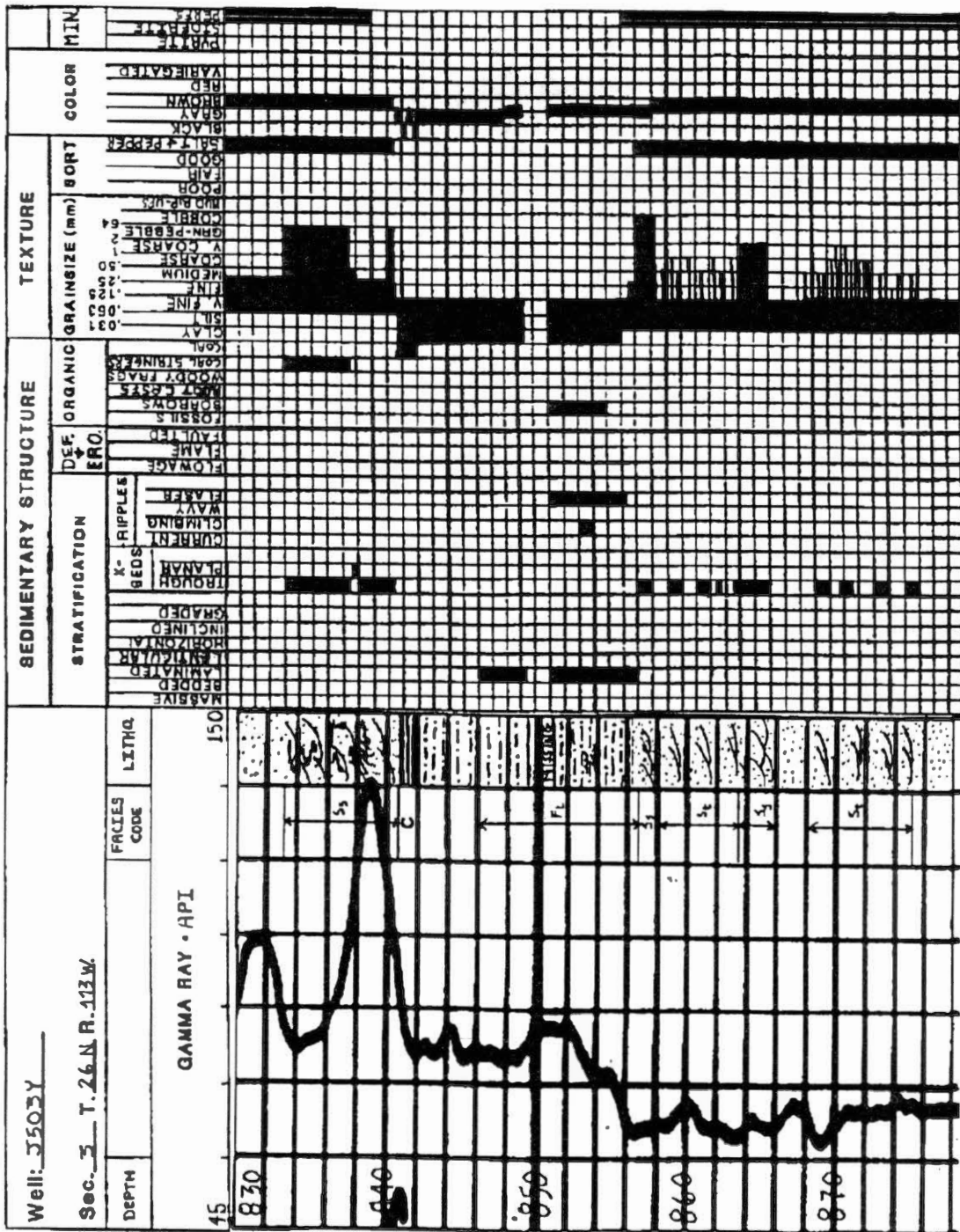




WELL J503Y















APPENDIX B

WELL LOG DATA





Corrected Name	RF EL	DW	TOP OF TH-1 SAND	BASE OF TH-1 SAND	CORRECTED TOP ELEV.	ISOPACH THICKNESS	TH-1 NET SAND	# OF TH-1 SANDS	SHAPE OF TH-1 SANDS	PERCENT TH-1 SAND
K434	6827	KB								
K434X	6825	KB								
K534	6810	EL								
K534X	6816	KB								
K634W	6806	KB								
K634X	6799	KB								
K734X	6779	KB								
K834	6772	DF	NDE	NDE	NDE	NDE	NDE			
L234	6796	KB								
L634X	6784	KB								
M234X	6813	KB								
M334	6811	KB								
M334X	6806	KB								
M434Y	6799	KB								
M434Z	6785	KB								
M534X	6789	KB								
M634W	6780	KB								
M634X	6779	KB								
M734X	6779	KB								
M734Y	6779	KB								
M734Z	6779	KB								
P1	6791	KB								
P3	6796	KB								
P5	6813	KB								
T11	6847	KB								
T12	6839	KB								
T13	6861	KB								
T14	6838	KB								
TP11	6844	KB								
TP5	6843	KB								
2-D	6870	KB								
unit5D	6833	KB								
12	6867	KB								
13	6850	KB								
15	6824	KB	1216	1315	5608	99	94	1	1	94.95
17	6800	KB	1076	1155	5724	79	69	1	1	87.34
T-14-34	6826	KB	1760	1853	5066	93	83	1	1	89.25
21	6826	KB	1885	1981	4943	96	90	1	1	93.75
T-60-34	6810	KB	1578	1710	5232	132	97	2	1,1	73.48
T-61-34	6792	KB	1476	1608	5316	132	119	1	1	90.15
T-62-34	6764	KB	1567	1686	5197	119	102	1	1	85.71
90-34	6807	KB	1658	1771	5149	113	110	1	1	97.35
T-26-35	6795	KB	1933	1994	4862	61	55	1	1	90.16
T-27-35	6861	KB	1985	2061	4876	76	57	1	1	75.00
T-28-35	6782	KB	1934	1985	4848	51	50	1	1	98.04
T-39-35	6770	KB	1920	1984	4850	64	36	2	1	56.25
52-35	6782	KB	1810	1925	4972	115	100	1	1	86.96
AVERAGES						89.97	72.35	1.30		92.13

Corrected Name	RF EL	DW	TOP OF TH-2 SAND	BASE OF TH-2 SAND	CORRECTED TOP ELEV.	ISOPACH THICKNESS	TH-2 NET SAND	# OF TH-2 SANDS	SHAPE OF TH-2 SANDS	PERCENT TH-2 SAND
23	6771	KB	1584	1725	5187	141	108	5	1,3,1	76.60
24	6765	KB	1950	2077	4815	127	86	6	1,1,1	67.72
T-30-2	6773	KB	1933	2055	4840	122	72	6	1,2,1	59.02
T-31-2	6750	KB	1897	2010	4853	113	52	5	2	46.02
T-33-2	6755	KB	1996	2135	4759	139	74	7	1,1	53.24
A2	6937	GL	1104	NDE	5833	NDE	>10(NDE)	1	4	
3AX	6880	KB	930	1040	5950	110	135	2	3,1	122.73
A12	6865	KB	940	1123	5925	183	123	1	1	67.21
A13	6870	KB	1110	1254	5760	144	121	1	1	84.03
A14	6855	KB	1127	1283	5728	156	136	3	1,2,1	87.18
A15	6881	KB	1150	NDE	5731	NDE	>38(NDE)	3	1,1	
A16	6855	KB	1054	1190	5801	136	78	4	1,1,1	57.35
A17	6839	KB	1081	1250	5758	169	60	4	1,1	35.50
A18	6839	KB	1078	1220	5761	142	59	6	1,1,1	41.55
A19	6824	KB	1089	1236	5735	147	107	5	1,1,2	72.79
A20	6837	KB	1100	1250	5737	150	55	4	2,1	36.67
A21	6826	KB	1117	1249	5709	132	65	5	1,1	49.24
A22	6925	KB	1151	1271	5774	120	82	4	1,2,2	68.33
A23	6901	KB	1197	1262	5704	65	45	2	1	69.23
A24	6891	KB	1187	1265	5704	78	47	3	2,1	60.26
A25	6876	KB	1185	1314	5691	129	114	1	1	88.37
A26	6847	KB	1133	1263	5714	130	76	5	1,2,2	58.46
A503X	6784	KB	625	NDE	6159	NDE	>87(NDE)	2	4,1	
A603X	6811	KB	993	NDE	5818	NDE	>123(NDE)	3	1,1,1	
B1	6879	KB	1014	1183	5865	169	138	4	1,1,5	81.66
B103	6816	KB	987	NDE	5829	NDE	>40(NDE)	1	1	
B203X	6803	KB	924	NDE	5879	NDE	NDE			
B303X	6797	KB	NDE	NDE	NDE	NDE	NDE			
B303Y	6796	KB	823	890	5973	67	59	2	1,1	88.06
B303Z	6794	KB	811	NDE	5983	NDE	>43(NDE)	2	1	
B403X	6801	KB	NDE	NDE	NDE	NDE	NDE			
B403Y	6803	KB	723	858	6080	135	36	1	2	26.67
B403Z	6821	KB	700	798	6121	98	32	1	1	32.65
B503W	6806	KB	810	907	5996	97	51	3	1,2	52.58
B503Y	6826	KB	817	NDE	6009	NDE	>33(NDE)	2	1	
B503Z	6835	KB	887	1001	5948	114	33	1	1	28.95
B603W	6847	KB	980	1145	5867	165	103	5	1,1,1	62.42
B603X	6860	KB	1048	NDE	5812	NDE	>107(NDE)	2	1,2	
B603Y	6834	KB	1031	NDE	5803	NDE	>41(NDE)	2	1	
B703X	6819	KB	1050	NDE	5789	NDE	NDE			
C403X	6857	KB	881	1030	5976	140	71	1	1	47.65
C603X	6868	KB	1042	1171	5846	129	95	2	2,1	73.64
D103X	6824	KB	985	NDE	5839	NDE	NDE			
D203X	6831	KB	913	973	5918	60	43	1	1	71.67
D303X	6859	KB	822	NDE	6037	NDE	NDE			
D303Y	6883	KB	807	858	6076	51	32	1	1	62.75
D403X	6922	KB	780	NDE	6142	NDE	>37(NDE)	1	1	
D403Y	6956	KB	825	867	6131	42	34	1	1	80.95
D503W	6927	KB	912	NDE	6015	NDE	>122(NDE)	2	1,1	
D503X	6966	KB	900	972	6066	72	46	1	1	63.89
D503Y	6956	KB	917	978	6039	61	46	1	1	75.41
D603X	6926	KB	993	NDE	5933	NDE	>35(NDE)	1	1	
D603Y	6900	KB	1049	1200	5851	151	126	3	1,1	83.44
E403	7038	KB	876	923	6162	51	37	1	1	72.55
E503	6964	KB	950	1072	6014	122	63	3	2,4,3	51.64
E503X	6976	KB	933	1060	6043	127	64	1	1	50.39
E603X	6912	KB	952	1100	5960	148	99	5	2,1,2,1	66.89
F203X	6941	KB	986	NDE	5955	NDE	>32(NDE)	1	1	
F203Y	6924	KB	1037	1093	5887	56	44	1	1	78.57
F303X	7043	KB	937	NDE	6106	NDE	>42(NDE)	1	1	
F403X	7049	KB	870	924	6179	54	43	1	1	79.63
F403Y	7039	KB	860	918	6179	58	30	1	1	51.72
F503W	6992	KB	930	1052	6062	122	73	5	2,3	59.84
F503X	6964	KB	892	NDE	6072	NDE	>54(NDE)	2	1,4	
F503Y	6951	KB	925	1044	6026	119	94	4	2,1	78.99
F603W	6900	KB	1040	1198	5860	158	144	3	1,2,1	91.14
F603X	6906	KB	1044	1200	5862	156	134	2	1,2	85.90
G503X	6942	KB	910	1020	6032	110	88	3	1,1,1	80.00
G503Y	6934	KB	900	1020	6034	120	86	4	2,1,1	71.67
G603X	6899	KB	997	1177	5902	180	156	4	1,2,1,1	86.67
H503X	6910	KB	928	1066	5982	138	123	4	1,1,2	89.13
J503Y	6906	KB	840	1007	6066	167	101	7	2,2,1	60.48
unit5	7024	KB	868	916	6156	48	33	1	1	68.75
1	6786	KB	1686	1817	5100	131	63	3	1,5	48.09
1	6813	RT	1330	1462	5483	132	90	1	1	68.18
19-T-3	6814	KB	1741	1870	5073	129	76	2	1	58.91
T-22-3	6784	KB	1793	1924	4991	131	71	5	1,1	54.20
T-23-3	6771	KB	1585	1725	5186	140	100	4	1,3	71.43
T-34-3	6753	KB	1554	1668	5199	114	64	3	2	56.14
4-A	6861	KB	1280	1370	5581	90	65	2	1,1	72.22
1-C-4	6898	KB	NDE	NDE	NDE	NDE	NDE			
2-C-4	6918	KB	NDE	NDE	NDE	NDE	NDE			
3-C-4	6941	KB	NDE	NDE	NDE	NDE	NDE			
4-C-4	6911	KB	NDE	NDE	NDE	NDE	NDE			
1	6861	GL	1502	1644	5359	142	80	3	1,1	56.34
21-4	6878	KB	1743	1860	5135	117	32	1	1	27.35
34	6867	KB	1734	1830	5133	96	71	3	2,1	73.96
42	6875	KB	1730	1820	5145	90	77	2	1,2	85.56
45	6924	KB	1890	1961	5034	71	37	2	1,1	52.11
35	6908	KB	1900	1995	5008	95	81	2	1,1	85.26
39	6931	KB	1938	2003	4993	65	8	1	1	12.31

Corrected Name	RF EL	DW	TOP OF TH-2 SAND	BASE OF TH-2 SAND	CORRECTED TOP ELEV.	ISOPACH THICKNESS	TH-2 NET SAND	# OF TH-2 SANDS	SHAPE OF TH-2 SANDS	PERCENT TH-2 SAND	
83											
1F-X	6916	KB	1924	2005	4992	81	39	2		48.15	
1	6819	KB	1094	1382	F	5725	288-F	9	1,1		
20	6824	KB	NDE	NDE	NDE	NDE	NDE				
T-49-10	6793	KB	1495	1711	F	5298	216-F	10	1,1,1		
T-50-10	6763	KB	1654	1783		5109	129	5	1,1	65.12	
18	6767	KB	1717	1851		5050	134	76	3	2,2	56.72
38	6962	KB	1331	1408		5631	77	62	2	2,1	80.52
39	7009	KB	1543	1645		5466	102	54	2	1	52.94
50	7166	KB	2020	2130		5146	110	74	2	1,1	67.27
C327	7290	KB	2277	2362		5013	85	46	2	1,1	54.12
C327Z	6950	KB	1139	1235		5811	96	72	3	1,1	75.00
D227	6936	KB	1156	NDE		5780	NDE	>61(NDE)	4	1,1	
D627	6949	KB	1165	1270		5784	105	85	2	1,1	80.95
E227Y	6917	KB	1223	1362		5694	139	71	3	1,1	51.08
G427	6892	KB	NDE	NDE		NDE	NDE				
G627	6919	KB	1000	1047		5919	47	38	1	1	80.85
H227	6893	KB	1033	1163		5860	130	85	3	1	65.38
J527X	6923	KB	1065	1115		5858	50	9	1	1	18.00
J527X	6907	KB	NDE	NDE		NDE	NDE				
J527X	6899	KB	850	NDE		6049	NDE	NDE			
L127X	6918	KB	1078	1242		5840	164	79	1	1	48.17
L227	6900	KB	1047	1149		5853	102	90	1	1	88.24
M127X	6867	KB	972	1075		5915	103	65	1	1	63.11
M127X	6878	KB	1154	1204		5724	50	41	1	1	82.00
M127Y	6879	KB	1058	1126		5821	68	61	1	1	89.71
M227X	6866	KB	1100	1183		5766	83	59	1	1	71.08
M327	6875	KB	961	1060		5914	99	81	1	1	81.82
M627Y	6878	KB	854	990		6024	136	94	2	1	69.12
98-27	7053	KB	1558	1650		5495	92	39	2	1	42.39
T-15	7063	KB	1825	1946		5238	121	65	2	1	53.72
T-16A-27	6975	KB	1653	1798		5322	145	104	5	1,1	71.72
T-16	6940	KB	1450	1584		5490	134	97	3	1	72.39
T-17	7042	KB	2043	2172		4999	129	99	2	1,1	76.74
T-18	6992	KB	1988	2132		5004	144	98	3	1,2,1	68.06
T-24	6939	KB	1853	1960		5086	107	47	5	2	43.93
T-32-27	6894	KB	1791	1900		5103	109	44	3	2,1	40.37
1	6932	KB	1070	1185		5823	115	73	3	1,1	63.48
3	6928	KB	1105	1193		5823	88	63	1	1	71.59
11	6861	KB	1347	1448		5514	101	35	2	2	34.65
14	6920	KB	964	1115		5936	131	98	3	1	74.81
22	7018	KB	1741	1873		5277	132	103	3	1,5	78.03
72-27	6917	KB	1564	1673		5353	109	66	3	1	60.55
94-27	6917	KB	1805	1915		5112	110	24	3	1,1	21.82
99-27	7012	KB	2062	2178		4950	116	87	2	1	75.00
G928	6948	KB	1102	1140		5846	38	25	3	1	65.79
G928X	6923	KB	1040	1125		5883	85	74	2	3,1	87.06
L928	6902	ES	1269	1310		5633	41	30	1	1	73.17
B-2	6990	KB	1149	1264		5841	115	42	3	1,1	36.52
9	6974	KB	1128	1225		5846	97	67	1	2	69.07
8	6954	KB	1078	1195		5876	117	86	1	3	73.50
6-28	7008	KB	1317	1380		5691	63	10	1	1	15.87
A1-C-33	7036	DF	FO	FO		FO	FO				
B1-C-33	7033	KB	FO	FO		FO	FO				
1-C-33	6907	KB	NDE	NDE		NDE	NDE				
3-C-33	6883	KB	1390	NDE		5493	NDE	>37(NDE)	1		
2-33	6850	KB	1700	1803		5150	103	45	3	2,2	43.69
4-33	6854	KB	1694	1796		5160	102	61	4	2,2	59.80
10	6923	KB	1587	1674		5336	87	41	2	2	47.13
37	6918	KB	FO	FO		FO	FO				
48	6905	KB	1362	1486		5543	124	90	3	1,1	72.58
A234X	6853	KB	986	1115		5867	129	81	2	1,1	62.79
B234X	6829	ES	730	848		6099	118	87	1	1	73.73
A734Y	6845	KB	820	NDE		6025	NDE	>7(NDE)	2		
B234X	6851	KB	1010	1138		5841	128	114	3	1,3,1	89.06
B334	6839	KB	684	NDE		6155	NDE	>51(NDE)	5	1,1,1	
B534	6819	KB	657	765		6162	108	92	2	1,2	85.19
B534X	6823	KB	664	765		6159	101	80	2	1,2	79.21
B634	6831	KB	724	827		6107	103	99	1	1	96.12
C534X	6832	KB	693	780		6139	87	64	1	1	73.56
D134	6888	DF	1156	1250		5732	94	34	2	2,3	36.17
D134X	6894	KB	1050	1100		5844	50	41	1	3	82.00
D434	6943	GL	753	851		6190	98	39	3	1	39.80
D434X	6851	KB	749	804		6102	55	40	1	3	72.73
D734	6837	GL	726	NDE		6111	NDE	>19(NDE)	2	1,5	
D834	6828	KB	853	984(E-NDE)		5973	131(E-NDE)	75(E-NDE)	4	1,1	
E534X	6851	KB	NDE	NDE		NDE	NDE	NDE			
E634	6807	KB	677	761		6130	84	51	3	3,1,2	60.71
F234	6850	KB	1130	1277		5720	147	84	5	2,2,1	57.14
F434X	6836	KB	821	864		6015	43	30	1	1	69.77
F434Y	6850	KB	956	1040		5894	84	51	1	1	60.71
F534X	6834	KB	740	800		6094	60	38	1	1	63.33
G634X	6826	KB	742	855		6084	113	81	2	1,3	71.68
G834X	6813	KB	802	915		6011	113	104	1	1	92.04
H334	6847	KB	1083	1196		5764	113	61	3	1,3	53.98
H434X	6818	KB	880	924(E-NDE)		5938	44(E-NDE)	18(E-NDE)	1	1	
H534V	6811	KB	744	830		6067	86	21	2	1	24.42
H534W	6818	KB	744	NDE		6074	NDE	NDE			
H634W	6812	KB	723	811		6089	88	54	3	1,2,1	61.36
H634X	6810	KB	734	843(E-NDE)		6076	109(E-NDE)	99(E-NDE)	2	1,1	
J434	6823	GL	923	1008		5900	85	28	1	1	32.94
J834	6800	KB	868	991		5932	123	84	4	1,1,2	68.29



Corrected Name	RF EL	DW	TOP OF TH-2 SAND	BASE OF TH-2 SAND	CORRECTED TOP ELEV.	ISOPACH THICKNESS	TH-2 NET SAND	# OF TH-2 SANDS	SHAPE OF TH-2 SANDS	PERCENT TH-2 SAND
K434	6827	KB	NDE	NDE	NDE	NDE	NDE			
K434X	6825	KB	897	NDE	5928	NDE	NDE			
K534	6810	EL	800	NDE	6010	NDE	>30(NDE)	1	1	
K534X	6816	KB	NDE	NDE	NDE	NDE	NDE			
K634W	6806	KB	751	NDE	6055	NDE	>79(NDE)	3	1,1,1	
K634X	6799	KB	790	930	6009	140	108	2	1,1	77.14
K734X	6779	KB	898	NDE	5881	NDE	>66(NDE)	1	1	
K834	6772	DF	902	1050(E-NDE)	5870	148(E-NDE)	128(E-NDE)	2	1,2	
L634X	6796	KB	721	NDE	6075	NDE	>11(NDE)	2		
L634X	6784	KB	740	857	6044	117	93	2	2,2	79.49
M234X	6813	KB	1017	NDE	5796	NDE	>28(NDE)	1	1	
M334	6811	KB	NDE	NDE	NDE	NDE	NDE			
M334X	6806	KB	932	NDE	5874	NDE	>15(NDE)	1	1	
M434Y	6799	KB	820	NDE	5979	NDE	>20(NDE)	1	NDE	
M534	6785	KB	815	NDE	5970	NDE	>42(NDE)	1	1	
M534X	6789	KB	768	NDE	6021	NDE	>40(NDE)	1	3	
M634W	6780	KB	730	875	6050	145	90	4	2,2,1	62.07
M634X	6779	KB	753	856	6026	102	59	2	1,1	57.84
M734X	6779	KB	870	1007	5909	137	38	1	1	27.74
M734Y	6779	KB	940	NDE	5839	NDE	>5(NDE)			
M734Z	6779	KB	927	NDE	5852	NDE	>88(NDE)	4	4,2	
P1	6791	KB	NDE	NDE	NDE	NDE	NDE			
P3	6796	KB	NDE	NDE	NDE	NDE	NDE			
P5	6813	KB	NDE	NDE	NDE	NDE	NDE			
T11	6847	KB	1035	1100	5812	65	48	1	1	73.85
T12	6839	KB	938	1011	5901	73	67	1	1	91.78
T13	6861	KB	1034	1084	5827	50	41	1	1	82.00
T14	6838	KB	933	1010	5905	77	45	1	3	58.44
TP11	6844	KB	978	1062	5866	84	50	1	1	59.52
TP5	6843	KB	1004	1113	5839	109	46	1	1	42.20
2-D	6870	KB	1000	1101	5870	101	23	1	1	22.77
unit5D	6833	KB	668	750	6165	82	72	1	1	87.80
12	6867	KB	1200	1320	5667	120	38	3	1	31.67
13	6850	KB	1197	1250	5653	53	41	1	1	77.36
15	6824	KB	1099	1216	5725	117	68	1	1	58.12
17	6800	KB	970	1076	5830	106	68	1	1	64.15
T-14-34	6826	KB	1627	1760	5199	133	61	5	2,1	45.86
21	6828	KB	1760	1885	5068	125	68	5	1,5	54.40
T-60-34	6810	KB	1463	1578	5347	115	45	1	1	39.13
T-61-34	6792	KB	1351	1476	5441	125	75	3	1,1,2	60.00
T-62-34	6764	KB	1475	1567	5289	92	66	1	1	71.74
90-34	6807	KB	1524	1658	5283	134	77	4	1,2	57.46
T-26-35	6795	KB	1802	1933	4993	131	57	3	1	43.51
T-27-35	6861	KB	1879	1985	4982	106	51	5	1	48.11
T-28-35	6782	KB	1817	1934	4965	117	57	4	1	48.72
T-39-35	6770	KB	1807	1920	4963	113	52	3	2,1	46.02
52-35	6782	KB	1698	1810	5084	112	54	2	1,1	48.21
AVERAGES						107.92	67.64	2.44		62.95

Corrected Name	RFEL	DW	TOP OF TH-3 SAND	CORRECTED TOP ELEV.	ISOPACH THICKNESS	TH-3 NET SAND	#OF TH-3 SANDS	SHAPE OF TH-3 SANDS	PERCENT TH-3 SAND
23	6771	KB	1458	5313	126	46	3	2	36.51
24	6755	KB	1900	4865	50	18	2	3	36.00
T-30-2	6773	KB	1795	4978	138	83	4	1.3	60.14
T-31-2	6750	KB	1758	4992	139	63	5	1	45.32
T-33-2	6755	KB	1955	4800	41-F	10-F	1	1	
A2	6937	GL	1004	5933	100	40	2	1.2	40.00
3AX	6880	KB	812	6068	118	48	3	3.1	40.68
A12	6865	KB	885	5980	55	87	2	1.1	158.18
A13	6870	KB	970	5900	140	120	2	4.2	85.71
A14	6855	KB	993	5862	134	93	1	1	69.40
A15	6881	KB	1000	5881	150	105	4	1	70.00
A16	6855	KB	940	5915	114	47	3	1.1	41.23
A17	6839	KB	972	5867	109	69	5	1.1	63.30
A18	6839	KB	960	5879	118	52	3	1.1	44.07
A19	6824	KB	987	5837	102	51	3	1	50.00
A20	6837	KB	1000	5837	100	59	4	1.1	59.00
A21	6826	KB	997	5829	120	53	3	1.1	44.17
A22	6925	KB	1050	5875	101	50	4	1.2	49.50
A23	6901	KB	1053	5848	144	89	2	1.2	61.81
A24	6891	KB	1024	5867	163	108	2	1.2	66.26
A25	6876	KB	1020	5856	165	136	2	1.2	82.42
A26	6847	KB	997	5850	136	66	5	2.3	48.53
A503X	6784	KB	501	6283	124	68	5	2.1	54.84
A603X	6811	KB	880	5931	113	63	3	1.1	55.75
B1	6879	KB	890	5989	124	69	3	3.1	55.65
B103	6816	KB	870	5946	117	73	2	1	62.39
B203X	6803	KB	801	6002	123	59	2	1	47.97
B303X	6797	KB	751	6046	NDE	>24(NDE)	2	1.4	
B303Y	6796	KB	690	6106	133	69	3	1	51.88
B303Z	6794	KB	701	6093	110	64	2	1	58.18
B403X	6801	KB	633	6168	NDE	>36(NDE)	1	1	
B403Y	6803	KB	619	6184	104	68	2	1	65.38
B403Z	6821	KB	604	6217	96	53	2	1	55.21
B503W	6806	KB	669	6137	141	75	3	1.1	53.19
B503Y	6826	KB	695	6131	122	71	3	1.1	58.20
B503Z	6835	KB	767	6068	120	50	3	1.1	41.67
B603W	6847	KB	863	5984	117	55	3	1.1	47.01
B603X	6860	KB	935	5925	113	75	2	1	66.37
B603Y	6834	KB	920	5914	111	75	2	1	67.57
B703X	6819	KB	943	5876	107	55	2	1	51.40
C403X	6857	KB	752	6105	129	70	2	2.1	54.26
C603X	6888	KB	944	5944	98	67	2	1	68.37
D103X	6824	KB	882	5942	103	67	2	1.1	65.05
D203X	6831	KB	809	6022	104	68	2	1	65.38
D303X	6859	KB	715	6144	107	69	1	2	64.49
D303Y	6883	KB	690	6193	117	74	1	1	63.25
D403X	6922	KB	675	6247	105	59	1	1	56.19
D403Y	6956	KB	714	6242	111	52	5	1.1	46.85
D503W	6927	KB	795	6132	117	68	2	1.3	58.12
D503X	6966	KB	790	6176	110	28	2	1	25.45
D503Y	6956	KB	813	6143	104	76	2	1.1	73.08
D603X	6926	KB	884	6042	109	70	2	1.1	64.22
D603Y	6900	KB	940	5960	109	69	1	1	63.30
E403	7038	KB	737	6301	139	60	6	1.1	43.17
E503	6964	KB	837	6127	113	74	2	1.1	65.49
E503X	6976	KB	822	6154	111	37	3	1.5	33.33
E603X	6912	KB	820	6092	132	43	4	1.3	32.58
F203X	6941	KB	885	6056	101	38	2	1	37.62
F203Y	6924	KB	932	5992	105	63	2	1.1	60.00
F303X	7043	KB	801	6242	136	31	5	1	22.79
F403X	7049	KB	737	6312	133	53	3	2.2	39.85
F403Y	7039	KB	760	6279	100	66	3	2.2	66.00
F503W	6992	KB	819	6173	111	59	3	1.1	53.15
F503X	6964	KB	777	6187	115	77	4	1.2	66.96
F503Y	6951	KB	808	6143	117	80	2	1.1	68.38
F603W	6900	KB	927	5973	113	72	3	1.5	63.72
F603X	6906	KB	936	5970	108	67	3	1.1	62.04
G503X	6942	KB	792	6150	118	78	3	1.1	66.10
G503Y	6934	KB	786	6148	114	82	3	1.1	71.93
G603X	6899	KB	888	6011	109	78	2	1.5	71.56
H503X	6910	KB	802	6108	126	83	2	1.1	65.87
J503Y	6906	KB	740	6166	100	24	4	1.1	24.00
unit5	7024	KB	766	6258	102	57	2	1.1	55.88
1	6786	KB	1535	5251	151	112	3	1.1	74.17
1	6813	RT	1184	5629	146	39	2	1	26.71
19-T-3	6814	KB	1600	5214	141	87	3	1.3	61.70
T-22-3	6784	KB	1654	5130	139	60	2	1.2	43.17
T-23-3	6771	KB	1457	5314	128	48	3	2.5	37.50
T-34-3	6753	KB	1430	5323	124	40	2	2	32.26
4-A	6861	KB	1118	5743	162	108	2	1.2	66.67
1-C-4	6898	KB	1103	5795	NDE	>90(NDE)	2	1.1	
2-C-4	6918	KB	1124	5794	NDE	NDE	NDE		
3-C-4	6941	KB	1160	5781	NDE	NDE	NDE		
4-C-4	6911	KB	1247	5664	NDE	>25(NDE)	1	1	
1	6861	GL	1355	5506	147	105	3	1.2	71.43
21-4	6878	KB	1614	5264	129	66	2	1.5	51.16
34	6867	KB	1610	5257	124	58	4	2	46.77
42	6875	KB	1600	5275	130	47	5	2.1	36.15
45	6924	KB	1755	5169	135	41	3	2	30.37
35	6908	KB	1766	5142	134	79	5	4.5	58.96
39	6931	KB	1827	5104	111	56	4	2.1	50.45

Corrected Name	RF EL	DW	TOP OF TH-3 SAND	CORRECTED TOP ELEV.	ISOPACH THICKNESS	TH-3 NET SAND	#OF TH-3 SANDS	SHAPE OF TH-3 SANDS	PERCENT TH-3 SAND
83	6916	KB	1777	5139	147	98	4	2,1,2	66.67
1F-X	6819	KB	1012	5807	82	51	3	1,1	62.20
1	6824	KB	1011	5813	NDE	NDE			
20	6793	KB	1405	5388	90	49	2	1,1	54.44
T-49-10	6763	KB	1529	5234	125	16	3		12.80
T-50-10	6767	KB	1585	5182	132	56	6	1,1	42.42
18	6962	KB	1243	5719	88	15	2	1	17.05
38	7009	KB	1414	5595	129	40	5	1	31.01
39	7166	KB	1870	5296	150	74	3	1	49.33
50	7290	KB	2115	5175	162	59	5	1,1	36.42
C327	6950	KB	1051	5899	88	22	1	1	25.00
C327Z	6936	KB	1071	5865	85	26	2	1	30.59
D227	6949	KB	1067	5882	98	42	5	3,1	42.86
D627	6917	KB	1128	5789	95	36	3	2,1	37.89
E227Y	6992	KB	NDE	NDE	NDE	NDE			
G427	6919	KB	895	6034	115	38	3	1	33.04
G627	6893	KB	988	5905	45	9	2		20.00
H227	6923	KB	904	6019	161	119	3	1,2	73.91
J527X	6907	KB	823	6084	NDE	>32(NDE)	2	1	
J527Z	6899	KB	745	6154	105	16	3	3	15.24
L127X	6918	KB	966	5952	112	89	2	1,5	79.46
L227	6900	KB	965	5935	82	40	4	1	48.78
M127	6887	KB	874	6013	98	36	2	2	36.73
M127X	6878	KB	1036	5842	118	100	2	1,5	84.75
M127Y	6879	KB	944	5935	114	86	2	1,1	75.44
M227X	6866	KB	947	5919	153	72	3	1,1	47.06
M327	6875	KB	863	6012	98	46	6	1	46.94
M627Y	6878	KB	771	6107	83	22	5		26.51
98-27	7053	KB	1456	5597	102	25	5	1	24.51
T-15	7063	KB	1700	5363	125	22	5		17.60
T-16A-27	6975	KB	1550	5425	103	32	6	1	31.07
T-16	6940	KB	1350	5590	100	33	5		33.00
T-17	7042	KB	1901	5141	142	63	6	1,1	44.37
T-18	6992	KB	1870	5122	118	19	4	5	16.10
T-24	6939	KB	1733	5206	120	34	5	1	28.33
T-32-27	6894	KB	1673	5221	118	33	6	2	27.97
1	6932	KB	966	5966	104	34	3	1	32.69
3	6928	KB	991	5937	114	96	4	1	84.21
11	6861	KB	1245	5616	102	11	2	2	10.78
14	6920	KB	867	6053	117	52	7	5	44.44
22	7018	KB	1625	5393	116	41	6	1	35.34
72-27	6917	KB	1463	5454	101	41	7	2,1	40.59
94-27	6917	KB	1685	5232	120	17	2	1	14.17
99-27	7012	KB	1904	5108	158	76	4	1,2	48.10
G928	6948	KB	NL	NL	NL	NL			
G928X	6923	KB	935	5988	105	98	1	1	93.33
L928	6902	ES	1159	5743	110	96	2	1	87.27
B-2	6990	KB	902	6088	247	126	3	1,1	51.01
9	6974	KB	985	5989	143	55	3	1,2	38.46
8	6954	KB	944	6010	134	35	5	1	26.12
6-28	7008	KB	1142	5866	175	106	2	1,1	60.57
A1-C-33	7036	DF	FO	FO	FO	FO			
B1-C-33	7033	KB	FO	FO	FO	FO			
1-C-33	6907	KB	1344	5563	NDE	>41(NDE)	1	2	
3-C-33	6883	KB	1303	5580	87	48	2	1	55.17
2-33	6850	KB	1593	5257	107	73	3	2,5	68.22
4-33	6854	KB	1578	5276	116	46	2	2,5	39.66
10	6923	KB	FO	FO	FO	27-F	1	1	
37	6918	KB	FO	FO	FO	FO			
48	6905	KB	1274	5631	88	53	3	2,1	60.23
A234X	6853	KB	858	5995	128	84	2	1,3	65.63
A334	6829	ES	633	6196	97	70	3	1	72.16
A734Y	6845	KB	703	6142	117	26	4	1	22.22
B234	6851	KB	892	5959	118	48	3	2,5	40.68
B334	6839	KB	588	6251	96	58	5	3,1	60.42
B534	6819	KB	568	6251	89	28	4	3	31.46
B534X	6823	KB	553	6270	111	79	3	2,1,2	71.17
B634	6831	KB	621	6210	103	41	7	2	39.81
C534X	6832	KB	576	6256	117	64	5	3,1,1	54.70
D134	6888	DF	1033	5855	123	37	6	2,1	30.08
D134X	6894	KB	944	5950	106	58	1	1	54.72
D434	6943	GL	660	6283	93	16	3	3	17.20
D434X	6851	KB	654	6197	95	18	1	4	18.95
D734	6837	GL	612	6225	114	61	3	1,1,3	53.51
D834	6826	KB	766	6060	87	18	2	1	20.69
E534X	6851	KB	697	6154	NDE	>12(NDE)	1	1	
E634	6807	KB	570	6237	107	20	3		18.69
F234	6850	KB	995	5855	135	68	3	1	50.37
F434X	6836	KB	680	6156	141	63	3	1,1	44.68
F434Y	6850	KB	824	6026	132	57	2	2	43.18
F534X	6834	KB	637	6197	103	28	2	2	27.18
G634X	6826	KB	616	6210	126	26	7	3	20.63
G834X	6813	KB	694	6119	108	28	8		25.93
H334	6847	KB	950	5897	133	63	3	1,1	47.37
H434X	6818	KB	756	6062	124	64	4	1	51.61
H534V	6811	KB	635	6176	109	45	4	1,2	41.28
H534W	6818	KB	621	6197	123	52	3	2	42.28
H634W	6812	KB	586	6226	137	44	6	1,1	32.12
H634X	6810	KB	608	6202	126	11	3		8.73
J434	6823	GL	786	6037	137	56	6	2,2	40.88
J834	6800	KB	761	6039	107	4	1		3.74

Corrected Name	RF EL	DW	TOP OF TH-3 SAND	CORRECTED TOP ELEV.	ISOPACH THICKNESS	TH-3 NET SAND	#OF TH-3 SANDS	SHAPE OF TH-3 SANDS	PERCENT TH-3 SAND
K434	6827	KB	780	6047	NDE	>10(NDE)	1		
K434X	6825	KB	773	6052	124	57	7	1,1	45.97
K534	6810	EL	671	6139	129	64	4	1,1,5	49.61
K534X	6816	KB	830	5988	NDE	>49(NDE)	1	2	
K634W	6806	KB	625	6181	126	51	4	1,2	40.48
K634X	6799	KB	702	6097	88	48	4	1	54.55
K734X	6779	KB	798	5981	100	29	4		29.00
K834	6772	DF	765	6007	137	30	4		21.90
K834X	6796	KB	600	6196	121	24	7		19.83
L634X	6784	KB	621	6163	119	82	2	4,1	68.91
M234X	6813	KB	873	5940	144	78	3	4,1	54.17
M334	6811	KB	858	5953	NDE	>34(NDE)	4	1	
M334X	6806	KB	780	6026	152	50	1	1	32.89
M434Y	6799	KB	706	6093	114	50	1	1	43.86
M434X	6785	KB	685	6100	130	78	3	2,5	60.00
M534X	6789	KB	638	6151	130	61	2	4	46.92
M634W	6780	KB	600	6180	130	59	3	1	45.38
M634X	6779	KB	622	6157	131	71	4	4	54.20
M734X	6779	KB	721	6058	149	71	3	1	47.65
M734Y	6779	KB	795	5984	145	61	2	1	42.07
M734Z	6779	KB	765	6014	162	57	3	1	35.19
P1	6791	KB	719	6072	NDE	>3(NDE)	1		
P3	6796	KB	751	6045	NDE	NDE			
P5	6813	KB	720	6093	NDE	>41(NDE)	2	1	
T11	6847	KB	931	5916	104	74	4	1,2,5,5	71.15
T12	6839	KB	845	5994	93	71	4	3,5,1,2	76.34
T13	6861	KB	950	5911	84	70	1	1	83.33
T14	6838	KB	830	6008	103	64	4	1,2,5,5	62.14
TP11	6844	KB	877	5967	101	59	4	1,3,5	58.42
TP5	6843	KB	923	5920	81	22	4	3	27.16
2-D	6870	KB	905	5965	95	69	2	1	72.63
unit5D	6833	KB	587	6246	81	16	2	5	19.75
12	6867	KB	1073	5794	127	87	3	1,3	68.50
13	6850	KB	1082	5768	115	69	2	1	60.00
15	6824	KB	993	5831	106	28	4		26.42
17	6800	KB	827	5973	143	25	3	1	17.48
T-14-34	6826	KB	1511	5315	116	36	3	1	31.03
21	6828	KB	1642	5186	118	53	4	1,2,1	44.92
T-60-34	6810	KB	1335	5475	128	51	4	2,1	39.84
T-61-34	6792	KB	1224	5568	127	80	2	1	62.99
T-62-34	6764	KB	1357	5407	118	88	3	4	74.58
90-34	6807	KB	1383	5424	141	99	2	4,5	70.21
T-26-35	6795	KB	1685	5110	117	65	3	1,1	55.56
T-27-35	6861	KB	1757	5104	122	48	2	1,1	39.34
T-28-35	6782	KB	1682	5100	135	79	3	1,2,1	58.52
T-39-35	6770	KB	1677	5093	130	85	4	1,1	65.38
52-35	6782	KB	1565	5217	133	88	2	2,2	66.17
AVERAGES					118.17	57.93	3.09		48.92

Corrected Name	RF EL	DW	TOP OF TH-4 SAND	CORRECTED TOP ELEV.	ISOPACH THICKNESS	TH-4 NET SAND	# OF TH-4 SANDS	SHAPE OF TH-4 SANDS	PERCENT TH-4 SAND
23	6771	KB	1331	5440	127	40	4	2.1	31.50
24	6765	KB	1728	5037	172	69	7	1.1	40.12
T-30-2	6773	KB	1657	5116	138	25	6	1	18.12
T-31-2	6750	KB	1625	5125	133	31	6	2	23.31
T-33-2	6755	KB	1782	4973	173	48	6	1	27.75
A2	6937	GL	882	6055	122	68	5	2.5,1.2	55.74
3AX	6880	KB	692	6188	120	23	3	1	19.17
A12	6865	KB	714	6151	171	75	6	2.1,1	43.86
A13	6870	KB	849	6021	121	36	2	3	29.75
A14	6855	KB	874	5981	119	34	2	1.1	28.57
A15	6881	KB	875	6006	125	54	7	2.1	43.20
A16	6855	KB	820	6035	120	47	6	2.1	39.17
A17	6839	KB	847	5992	125	54	6	2.1	43.20
A18	6839	KB	847	5992	113	48	5	2.1	42.48
A19	6824	KB	855	5969	132	35	3	2	26.52
A20	6837	KB	875	5962	125	50	6	2.2	40.00
A21	6826	KB	874	5952	123	60	7	1.1	48.78
A22	6925	KB	930	5995	120	35	5	2	29.17
A23	6901	KB	905	5996	148	36	5	4	24.32
A24	6891	KB	810	6081	214	34	3	2	15.89
A25	6876	KB	854	6022	166	56	6	1	33.73
A26	6847	KB	879	5968	118	34	6	2	28.81
A503X	6784	KB	355	6429	146	89	5	1.1	60.96
A603X	6811	KB	746	6065	134	62	7	2.1	46.27
B1	6879	KB	739	6140	151	28	6	2	18.54
B103	6816	KB	739	6077	131	64	6	2.1	48.85
B203X	6803	KB	661	6142	140	69	8	1.3	49.29
B303X	6797	KB	607	6190	144	101	6	1.1,4.4	70.14
B303Y	6796	KB	546	6250	144	25	1	1	17.36
B303Z	6794	KB	577	6217	124	24	2	2	19.35
B403X	6801	KB	504	6297	129	29	2	1	22.48
B403Y	6803	KB	454	6349	165	58	3	4.3	35.15
B403Z	6821	KB	452	6369	152	27	1	2	17.76
B503W	6806	KB	535	6271	134	47	4	1.2	35.07
B503Y	6826	KB	553	6273	142	20	2	1	14.08
B503Z	6835	KB	595	6240	172	29	4	2	16.86
B603W	6847	KB	730	6117	133	51	5	1.5	38.35
B603X	6860	KB	774	6086	161	16	3	2	9.94
B603Y	6834	KB	764	6070	156	45	6	2.1	28.85
B703X	6819	KB	787	6032	156	45	3	1	28.85
C403X	6857	KB	606	6251	146	71	6	1.1,1	48.63
C603X	6888	KB	789	6099	155	81	5	1.2,1.1	52.26
D103X	6824	KB	705	6119	177	41	4	2.3	23.16
D203X	6831	KB	672	6159	137	21	2	1	15.33
D303X	6859	KB	578	6281	137	46	3	1	33.58
D303Y	6883	KB	532	6351	158	63	5	2.1,1	39.87
D403X	6922	KB	528	6394	147	31	4	2.1	21.09
D403Y	6956	KB	557	6399	157	37	7	1.1,1	23.57
D503W	6927	KB	638	6289	157	74	8	1.4,2	47.13
D503X	6966	KB	634	6332	156	27	4	1	17.31
D503Y	6956	KB	688	6268	125	57	5	1.1,3	45.60
D603X	6926	KB	726	6200	158	23	4	1	14.56
D603Y	6900	KB	789	6111	151	77	7	2.1,1	50.99
E403	7038	KB	579	6459	158	73	8	2.1,5.1	46.20
E503	6964	KB	670	6294	167	58	5	1.4	34.73
E503X	6976	KB	690	6296	132	47	5	1	35.61
E603X	6912	KB	662	6250	158	72	6	1.1	45.57
F203X	6941	KB	757	6184	128	77	7	1.1,5	60.16
F203Y	6924	KB	755	6169	177	73	7	1.1	41.24
F303X	7043	KB	664	6379	137	29	4	2	21.17
F403X	7049	KB	597	6452	140	71	7	1.2,4.1	50.71
F403Y	7039	KB	610	6429	150	76	8	1.2,1	50.67
F503W	6992	KB	690	6302	129	62	7	1.2,5	48.06
F503X	6964	KB	619	6345	158	55	8	1.1	34.81
F503Y	6951	KB	646	6305	162	87	7	1.1,2.1	53.70
F603W	6900	KB	780	6120	147	67	6	1.3,3	45.58
F603X	6906	KB	787	6119	149	28	5	1.2	18.79
G503X	6942	KB	620	6322	172	80	7	3.1,1	46.51
G503Y	6934	KB	625	6309	161	80	7	1.1,1.5	49.69
G603X	6899	KB	725	6174	163	86	6	2.1,3	52.76
H503X	6910	KB	643	6267	159	83	7	1.2,1	52.20
J503Y	6906	KB	620	6286	120	34	5	1.1	28.33
unit5	7024	KB	645	6379	121	53	6	2.1	43.80
1	6786	KB	1394	5392	141	39	4	1	27.66
1	6813	RT	1063	5750	121	24	5	2	19.83
19-T-3	6814	KB	1465	5349	135	40	6	1.2	29.63
T-22-3	6784	KB	1510	5274	144	43	5	1.2	29.86
T-23-3	6771	KB	1331	5440	126	33	4	2.1	26.19
T-34-3	6753	KB	1304	5449	126	34	4	1	26.98
4-A	6861	KB	987	5874	131	39	5	2.1	29.77
1-C-4	6898	KB	977	5921	126	25	3	2.1	19.84
2-C-4	6918	KB	991	5927	133	52	6	1.1,1	39.10
3-C-4	6941	KB	1023	5918	137	62	6	2.3,5	45.26
4-C-4	6911	KB	1114	5797	133	55	5	2.5,1	41.35
1	6861	GL	1193	5668	162	87	5	1.1,1.2	53.70
21-4	6878	KB	1460	5418	154	60	2	1.2	38.96
34	6867	KB	1441	5426	169	60	4	2.2,1	35.50
42	6875	KB	1470	5405	130	56	5	2.2,2	43.08
45	6924	KB	1629	5295	126	24	3	1.2	19.05
35	6908	KB	1588	5320	178	96	4	1.1,2	53.93
39	6931	KB	1683	5248	144	50	3	2.1	34.72

Corrected Name	RF EL	DW	TOP OF TH-4 SAND	CORRECTED TOP ELEV.	ISOPACH THICKNESS	TH-4 NET SAND	# OF TH-4 SANDS	SHAPE OF TH-4 SANDS	PERCENT TH-4 SAND
B3	6916	KB	1614	5302	163	68	4	1	41.72
1F-X	6819	KB	894	5925	118	26	4	2	22.03
1	6824	KB	885	5939	126	68	5	1,1,1	53.97
20	6793	KB	1286	5507	119	12	4		10.08
T-49-10	6763	KB	1404	5359	125	27	6	2	21.60
T-50-10	6767	KB	1461	5306	124	24	6	2	19.35
18	6962	KB	1116	5846	127	62	3	1,1,1	48.82
38	7009	KB	1276	5733	138	63	4	1,1	45.65
39	7166	KB	1731	5435	139	44	6	1,5,1	31.65
50	7290	KB	1989	5301	126	24	4	3,1	19.05
C327	6950	KB	928	6022	123	64	7	1,2	52.03
C327Z	6936	KB	946	5990	125	47	5	1,2	37.60
D227	6949	KB	914	6035	153	45	6	1,1	29.41
D627	6917	KB	1010	5907	118	15	4		12.71
E227Y	6892	KB	779	6113	NDE	>13(NDE)	1	1	
G427	6919	KB	737	6182	148	43	5	1,1	29.05
G627	6893	KB	867	6026	121	49	4	1,4	40.50
H227	6923	KB	745	6178	159	57	8	1,5,1	35.85
J527X	6907	KB	678	6229	145	68	7	1,1,1	46.90
J527Z	6899	KB	630	6269	115	76	5	1	66.09
L127X	6918	KB	767	6151	199	98	4	1,2	49.25
L227	6900	KB	NL	NL	NL	>78(NL)	3	1,2	
M327	6887	KB	NL	NL	NL	>40(NL)	2	5	
M127X	6878	KB	863	6015	173	103	2	1,1	59.54
M127Y	6879	KB	803	6076	141	97	2	2,1	68.79
M227X	6866	KB	740	6126	207	75	5	2,1	36.23
M327	6875	KB	723	6152	140	54	8	2,1	38.57
M627Y	6878	KB	633	6245	138	76	7	2,5,2,3	55.07
98-27	7053	KB	1324	5729	132	31	5	2	23.48
T-15	7063	KB	1550	5513	150	33	6	1	22.00
T-16 A-27	6975	KB	1425	5550	125	57	3	1,2,1	45.60
T-16	6940	KB	1218	5722	132	37	4	1,2	28.03
T-17	7042	KB	1769	5273	132	27	6	1,5	20.45
T-18	6992	KB	1728	5264	142	44	4	1,2	30.99
T-24	6939	KB	1593	5346	140	68	4	1,1	48.57
T-32-27	6894	KB	1570	5324	103	32	4	1	31.07
1	6932	KB	855	6077	111	46	4	1,1,2	41.44
3	6928	KB	816	6112	175	108	5	1,1	61.71
11	6861	KB	1126	5735	119	41	2	3,1	34.45
14	6920	KB	757	6163	110	29	5	1,1	26.36
22	7018	KB	1488	5530	137	54	6	1,1,1	39.42
72-27	6917	KB	1334	5583	129	65	6	1,1,3,2	50.39
94-27	6917	KB	1580	5337	105	34	2	1	32.38
99-27	7012	KB	1777	5235	127	40	5	1,1	31.50
G928	6948	KB	NL	NL	NL	NL			
G928X	6923	KB	765	6158	170	100	3	1,2	58.82
L928	6902	ES	NL	NL	NL	>21(NL)	1	1	
B-2	6990	KB	FO	FO	FO	103-F	3	2,1	
9	6974	KB	802	6172	183	71	1	2	38.80
8	6954	KB	748	6206	196	107	3	1,2	54.59
6-28	7008	KB	FO	FO	FO	83-F	2	2,1	
A1-C-33	7036	DF	FO	FO	FO	FO			
B1-C-33	7033	KB	FO	FO	FO	FO			
1-C-33	6907	KB	FO	FO	FO	FO			
3-C-33	6883	KB	FO	FO	FO	42-F	3	2,1	
2-33	6850	KB	FO	FO	FO	16-F	3	1	
4-33	6854	KB	FO	FO	FO	59-F	4	3,1	
10	6923	KB	FO	FO	FO	FO			
37	6918	KB	FO	FO	FO	FO			
48	6905	KB	FO	FO	FO	FO			
A234X	6853	KB	722	6131	136	66	4	1,2,5	48.53
A334	6829	ES	498	6331	135	36	5	1,2	26.67
A734Y	6845	KB	558	6287	145	84	5	1,3	57.93
B234	6851	KB	NL	NL	NL	>50(NL)	1	1	
B334	6839	KB	451	6388	137	75	8	1,2,2	54.74
B534	6819	KB	421	6398	147	59	6	2,1,5	40.14
B534X	6823	KB	415	6408	138	44	4	5,3	31.88
B634	6831	KB	408	6423	213	121	6	1,1,1,1	56.81
C534X	6832	KB	456	6378	120	46	10	1	38.33
D134	6888	DF	FO	FO	FO	59-F	2	1,1	
D134X	6894	KB	FO	FO	FO	FO			
D434	6943	GL	532	6411	128	95	6	3,1,2,1,5	74.22
D434X	6851	KB	506	6345	148	65	7	2,2	43.92
D734	6837	GL	474	6363	138	87	6	1,1,3,5	63.04
D834	6826	KB	630	6196	136	35	3	2,2	25.74
E534X	6851	KB	555	6296	142	42	5	1,2	29.58
E634	6907	KB	421	6386	149	78	5	1,1,1,3	52.35
F234	6850	KB	FO	FO	FO	34-F	1	1	
F434X	6836	KB	540	6296	140	55	6	1,4,2,2	39.29
F434Y	6850	KB	676	6174	148	90	5	1,1,1,3	60.81
F534X	6834	KB	490	6344	147	86	6	1,1,2,1	58.50
G634X	6826	KB	497	6329	119	64	5	1,1,1	53.78
G834X	6813	KB	575	6238	119	63	7	1,5,1	52.94
H334	6847	KB	813	6034	137	88	6	1,1	64.23
H434X	6818	KB	620	6198	136	15	2	1	11.03
H534V	6811	KB	475	6336	160	43	6	2	26.88
H534W	6818	KB	474	6344	147	28	3	2	19.05
H634W	6812	KB	470	6342	116	53	6	1,1	45.69
H634X	6810	KB	500	6310	108	24	1	2	22.22
J434	6823	GL	NL	NL	NL	>44(NL)	2	1	
J834	6800	KB	606	6194	155	73	5	1,2,1,5	47.10

Corrected Name	RFEL	DW	TOP OF TH-4 SAND	CORRECTED TOP ELEV.	ISOPACH THICKNESS	TH-4 NET SAND	# OF TH-4 SANDS	SHAPE OF TH-4 SANDS	PERCENT TH-4 SAND
K434									
K434X	6827	KB	680	6147	100	70	3	1,2,2	70.00
K434X	6825	KB	651	6174	122	40	4	1	32.79
K534	6810	EL	555	6255	116	83	3	1,1,2	71.55
K534X	6816	KB	694	6122	136	99	6	1,2,1,2	72.79
K634W	6806	KB	481	6325	144	77	5	2,1,1	53.47
K634X	6799	KB	549	6250	153	44	2	2	28.76
K734X	6779	KB	649	6130	149	51	5	2,4	34.23
K834	6772	DF	586	6186	179	116	6	2,1,1,5,5	64.80
K834	6796	KB	461	6335	139	49	5	2,5	35.25
L634X	6784	KB	461	6323	160	113	6	1,1,1,3,1	70.63
M234X	6813	KB	727	6086	146	55	8	1,2	37.67
M334	6811	KB	714	6097	144	50	6	2	34.72
M334X	6806	KB	636	6170	144	39	4	2	27.08
M434Y	6799	KB	552	6247	154	30	3	1	19.48
M434	6785	KB	550	6235	135	49	4	5,5	36.30
M534X	6789	KB	485	6304	153	23	1	4	15.03
M634W	6780	KB	444	6336	156	80	6	1,2,1	51.28
M634X	6779	KB	448	6331	174	49	1	4	28.16
M734X	6779	KB	602	6177	119	19	1	2	15.97
M734Y	6779	KB	670	6109	125	30	1	1	24.00
M734Z	6779	KB	619	6160	146	40	7	1	27.40
P1	6791	KB	566	6225	153	49	6	1,2	32.03
P3	6796	KB	608	6188	143	29	3	2	20.28
P5	6813	KB	570	6243	150	23	1	1	15.33
T11	6847	KB	796	6051	135	77	4	1,1,1	57.04
T12	6839	KB	697	6142	148	99	5	1,2,2	66.89
T13	6861	KB	800	6061	150	99	4	1,1	66.00
T14	6838	KB	683	6155	147	78	6	1,5,5	53.06
TP11	6844	KB	711	6133	166	60	3	1,2	36.14
TP5	6843	KB	758	6085	165	77	5	1	46.67
2-D	6870	KB	760	6110	145	46	4	1,2	31.72
unit5D	6833	KB	NL	NL	NL	>34(NL)	3	3	
12	6867	KB	915	5952	158	75	3	1,1,1	47.47
13	6850	KB	960	5890	122	38	4	2,1	31.15
15	6824	KB	874	5950	119	49	5	2,5	41.18
17	6800	KB	NL	NL	NL	>19(NL)	2	1	
T-14-34	6826	KB	1379	5447	132	27	3	1	20.45
21	6828	KB	1510	5318	132	43	6	1	32.58
T-60-34	6810	KB	1192	5618	143	30	2	1	20.98
T-61-34	6792	KB	1113	5679	111	24	2	1	21.62
T-62-34	6764	KB	1228	5536	129	32	6	2	24.81
90-34	6807	KB	1240	5567	143	98	6	1,1,3,3	68.53
T-26-35	6795	KB	1549	5246	136	11	2		8.09
T-27-35	6861	KB	1625	5236	132	27	5	1	20.45
T-28-35	6782	KB	1556	5226	126	22	6		17.46
T-39-35	6770	KB	1547	5223	130	16	6		12.31
52-35	6782	KB	1435	5347	130	22	2	2,4	16.92
AVERAGES					141.82	53.50	4.60		37.46

Corrected Name	RF EL	DW	TOP OF TH-5 SAND	CORRECTED TOP ELEV.	ISOPACH THICKNESS	TH-5 NET SAND	# OF TH-5 SANDS	SHAPE OF TH-5 SANDS	PERCENT TH-5 SAND
23	6771	KB	1145	5626	186	67	5	2,1,2	36.02
24	6765	KB	1476	5289	252	109	7	1,3,1,5	43.25
T-30-2	6773	KB	1480	5293	177	35	3	1	19.77
T-31-2	6750	KB	1411	5339	214	79	4	2,2	36.92
T-33-2	6755	KB	1521	5234	261	81	6	2,3	31.03
A2	6937	GL	638	6299	244	169	2	2,2	69.26
3AX	6880	KB	499	6381	193	20	3	4	10.36
A12	6865	KB	512	6353	202	9	3		4.46
A13	6870	KB	655	6215	194	0			0.00
A14	6855	KB	675	6180	199	11	2	2	5.53
A15	6881	KB	674	6207	201	82	8	1,1,5	40.80
A16	6855	KB	630	6225	190	31	5	5	16.32
A17	6839	KB	654	6185	193	31	4	1	16.06
A18	6839	KB	652	6187	195	22	5		11.28
A19	6824	KB	664	6160	191	13	5		6.81
A20	6837	KB	680	6157	195	59	8	2,1	30.26
A21	6826	KB	684	6142	190	20	4	1	10.53
A22	6925	KB	717	6208	213	106	3	1,1,2	49.77
A23	6901	KB	705	6196	200	124	4	1,1,2	62.00
A24	6891	KB	676	6215	134	158	2	1,3	117.91
A25	6876	KB	690	6186	164	71	6	1,4,2	43.29
A26	6847	KB	682	6165	197	5	3		2.54
A503X	6784	KB	147	6637	208	71	10	1,1,3	34.13
A603X	6811	KB	550	6261	196	136	8	2,1	69.39
B1	6879	KB	578	6301	161	5	1		3.11
B103	6816	KB	507	6309	232	131	4	1,1	56.47
B203X	6803	KB	428	6375	233	84	4	2,2,2	36.05
B303X	6797	KB	403	6394	204	47	7	4	23.04
B303Y	6796	KB	350	6446	196	121	1	3	61.73
B303Z	6794	KB	360	6434	217	0			0.00
B403X	6801	KB	296	6505	208	47	3	1	22.60
B403Y	6803	KB	250	6553	204	85	2	3,2	41.67
B403Z	6821	KB	228	6593	224	10	1	1	4.46
B503W	6806	KB	306	6500	229	38	7	1,1	16.59
B503Y	6826	KB	301	6525	252	43	2	1	17.06
B503Z	6835	KB	327	6508	268	16	2	1	5.97
B603W	6847	KB	566	6281	164	63	11	1,1	38.41
B603X	6860	KB	578	6282	196	27	1	2	13.78
B603Y	6834	KB	548	6286	216	30	3	1	13.89
B703X	6819	KB	588	6231	199	30	2	2	15.08
C403X	6857	KB	389	6468	217	142	7	1,3,1,2	65.44
C603X	6888	KB	583	6305	206	118	6	1,3,1	57.28
D103X	6824	KB	497	6327	208	17	1	2	8.17
D203X	6831	KB	410	6421	262	131	7	1,1,5	50.00
D303X	6859	KB	359	6500	219	137	4	3,1,2	62.56
D303Y	6883	KB	316	6567	216	163	3	1,1	75.46
D403X	6922	KB	314	6608	214	68	5	1,1,2	31.78
D403Y	6956	KB	348	6608	209	173	2	1	82.78
D503W	6927	KB	420	6507	218	146	7	1,1	66.97
D503X	6966	KB	414	6552	220	149	8	1,1,2	67.73
D503Y	6956	KB	441	6515	247	176	7	1,1,1	71.26
D603X	6926	KB	511	6415	215	145	5	1,1,2	67.44
D603Y	6900	KB	581	6319	208	94	3	1	45.19
E403	7038	KB	393	6645	186	107	4	1,2,2	57.53
E503	6964	KB	465	6499	205	134	8	1,3,1,1	65.37
E503X	6976	KB	483	6493	207	107	5	1,1,1	51.69
E603X	6912	KB	470	6442	192	79	7	1,3,1,5	41.15
F203X	6941	KB	556	6385	201	131	5	2,1,1	65.17
F203Y	6924	KB	554	6370	201	120	4	1,2	59.70
F303X	7043	KB	456	6587	208	160	4	2,1,1	76.92
F403X	7049	KB	377	6672	220	147	9	1,2,3,4	66.82
F403Y	7039	KB	395	6644	215	113	7	1,2,1,2,1	52.56
F503W	6992	KB	438	6554	252	150	8	1,3,1,5	59.52
F503X	6964	KB	404	6560	215	22	3	1	10.23
F503Y	6951	KB	435	6516	211	143	6	1,2,3,2,4	67.77
F603W	6900	KB	564	6336	216	118	9	1,4,2	54.63
F603X	6906	KB	576	6330	211	126	5	2	59.72
G503X	6942	KB	421	6521	199	119	11	1,2,1,1	59.80
G503Y	6934	KB	424	6510	201	134	10	1,3,2,4,4	66.67
G603X	6899	KB	519	6380	206	114	11	1,3,1,1	55.34
H503X	6910	KB	459	6451	184	111	11	1,1	60.33
J503Y	6906	KB	418	6488	202	89	9	1,1,1	44.06
unit5	7024	KB	384	6640	261	157	12	1,1	60.15
1	6786	KB	1199	5587	195	71	2	1,4	36.41
1	6813	RT	875	5938	188	70	2	2	37.23
19-T-3	6814	KB	1254	5560	211	109	2	1,1	51.66
T-22-3	6784	KB	1292	5492	218	110	3	2,5	50.46
T-23-3	6771	KB	1144	5627	187	71	5	2,2,1	37.97
T-34-3	6753	KB	1125	5628	179	20	2	1	11.17
4-A	6861	KB	786	6075	201	45	6	2,2	22.39
1-C-4	6898	KB	798	6100	179	24	5		13.41
2-C-4	6918	KB	813	6105	178	43	7	1,1	24.16
3-C-4	6941	KB	846	6095	177	33	4	1,1	18.64
4-C-4	6911	KB	935	5976	179	64	4	2,1	35.75
1	6861	GL	1001	5860	192	84	7	1,2,1	43.75
21-4	6878	KB	FO	FO	FO	10-F	1	1	
34	6867	KB	1231	5636	210	139	3	2,2,3	66.19
42	6875	KB	1273	5602	197	134	4	1,1,3	68.02
45	6924	KB	1456	5468	173	99	3	1,2,1	57.23
35	6908	KB	1401	5507	187	83	5	1,3,1	44.39
39	6931	KB	1510	5421	173	85	2	1,2	49.13



Corrected Name	RFEL	DW	TOP OF TH-5 SAND	CORRECTED TOP ELEV.	ISOPACH THICKNESS	TH-5 NET SAND	# OF TH-5 SANDS	SHAPE OF TH-5 SANDS	PERCENT TH-5 SAND
83	6916	KB	1410	5506	204	81	6	1,1,5,1	39.71
1F-X	6819	KB	688	6131	206	36	4	1,1	17.48
1	6824	KB	688	6136	197	49	4	1,1	24.87
20	6793	KB	1141	5652	145	46	3	1	31.72
T-49-10	6763	KB	1220	5543	184	52	6	1	28.26
T-50-10	6767	KB	1254	5513	207	41	4	1	19.81
18	6962	KB	952	6010	164	34	4	2,2	20.73
38	7009	KB	1109	5900	167	59	6	2,2,2,2	35.33
39	7166	KB	1560	5606	171	40	6	2,2,1	23.39
50	7290	KB	1803	5487	186	79	7	1,2,3,2	42.47
C327	6950	KB	727	6223	201	93	6	2,1,1	46.27
C327Z	6936	KB	747	6189	199	93	5	2,1,1	46.73
D227	6949	KB	730	6219	184	111	4	1	60.33
D627	6917	KB	810	6107	200	64	5	1,2,1	32.00
E227Y	6892	KB	600	6292	179	103	5	1,1	57.54
G427	6919	KB	558	6361	179	100	4	1,1	55.87
G627	6893	KB	684	6209	183	71	3	1	38.80
H227	6923	KB	520	6403	225	91	10	1,2,1,1	40.44
J527X	6907	KB	474	6433	204	149	10	1,2,1,1,2	73.04
J527Z	6899	KB	445	6454	185	34	2	2	18.38
L127X	6918	KB	570	6348	197	85	2	2,2	43.15
L227	6900	KB	NL	NL	NL	NL			
M127	6887	KB	NL	NL	NL	NL			
M127X	6878	KB	672	6206	191	69	3	1,2	36.13
M127Y	6879	KB	590	6289	213	58	2	2,2	27.23
M227X	6866	KB	534	6332	206	49	4	1,1	23.79
M327	6875	KB	504	6371	219	56	8	2,1	25.57
M627Y	6878	KB	434	6444	199	129	8	2,2,2	64.82
98-27	7053	KB	1152	5901	172	43	3	2	25.00
T-15	7063	KB	1363	5700	187	88	5	1,2	47.06
T-16A-27	6975	KB	1240	5735	185	67	6	2,2,1	36.22
T-16	6940	KB	1030	5910	188	56	3	1,2	29.79
T-17	7042	KB	1590	5452	179	48	7	2	26.82
T-18	6992	KB	1545	5447	183	43	4	1,1	23.50
T-24	6939	KB	1404	5535	189	71	6	2,1	37.57
T-32-27	6894	KB	1343	5551	227	86	3	1,2	37.89
1	6932	KB	688	6244	167	88	4	1,1,1	52.69
3	6928	KB	627	6301	189	104	3	2,1	55.03
11	6861	KB	934	5927	192	25	3	2	13.02
14	6920	KB	NL	NL	NL	NL			
22	7018	KB	1303	5715	185	47	4	2,1	25.41
72-27	6917	KB	1161	5756	173	76	8	2,2	43.93
94-27	6917	KB	1351	5566	229	76	4	1,2	33.19
99-27	7012	KB	1602	5410	175	51	7	1,2	29.14
G928	6948	KB	NL	NL	NL	NL			
G928X	6923	KB	569	6354	196	86	3	1,1,1	43.88
L928	6902	ES	NL	NL	NL	NL			
B-2	6990	KB	FO	FO	FO	FO			
9	6974	KB	626	6348	176	104	4	1,1,1,1	59.09
8	6954	KB	563	6391	185	49	6	3,1,1	26.49
6-28	7008	KB	FO	FO	FO	FO			
A1-C-33	7036	DF	FO	FO	FO	FO			
B1-C-33	7033	KB	FO	FO	FO	FO			
1-C-33	6907	KB	FO	FO	FO	FO			
3-C-33	6883	KB	FO	FO	FO	FO			
2-33	6850	KB	FO	FO	FO	FO			
4-33	6854	KB	FO	FO	FO	FO			
10	6923	KB	FO	FO	FO	FO			
37	6918	KB	FO	FO	FO	FO			
48	6905	KB	FO	FO	FO	FO			
A234X	6853	KB	494	6359	228	129	4	1,4,2	56.58
A334	6829	ES	248	6581	250	142	7	2,5,1,5	56.80
A734Y	6845	KB	359	6486	199	51	4	2	25.63
B234	6851	KB	NL	NL	NL	NL			
B334	6839	KB	253	6586	198	109	8	1,1	55.05
B534	6819	KB	240	6579	181	67	4	1,2	37.02
B534X	6823	KB	249	6574	166	27	3	4	16.27
B634	6831	KB	252	6579	156	116	7	1,1,3,2	74.36
C534X	6832	KB	218	6614	238	121	9	1,2,1	50.84
D134	6888	DF	FO	FO	FO	FO			
D134X	6894	KB	FO	FO	FO	FO			
D434	6943	GL	310	6633	222	72	5	2,2	32.43
D434X	6851	KB	315	6536	191	129	5	4,1,2,1	67.54
D734	6837	GL	NL	NL	NL	>79(NL)	7	1,1,4	
D834	6826	KB	401	6425	229	163	5	2,1,2	71.18
E534X	6851	KB	305	6546	250	119	6	1,2,1,2	47.60
E634	6807	KB	227	6580	194	43	6	4	22.16
F234	6850	KB	FO	FO	FO	FO			
F434X	6836	KB	348	6488	192	52	2	1	27.08
F434Y	6850	KB	455	6395	221	144	8	1,2,1,1	65.16
F534X	6834	KB	260	6574	230	92	5	4,4,2	40.00
G634X	6826	KB	302	6524	195	109	9	1,2,1,5	55.90
G834X	6813	KB	387	6426	188	98	8	2,2,1	52.13
H334	6847	KB	FO	FO	FO	46-F	4	5,2,1	
H434X	6818	KB	434	6384	186	36	1	1	19.35
H534V	6811	KB	312	6499	163	22	4	1	13.50
H534W	6818	KB	304	6514	170	9	1	2	5.29
H634W	6812	KB	260	6552	210	123	8	2,2,1,2	58.57
H634X	6810	KB	329	6481	171	32	5	2	18.71
J434	6823	GL	NL	NL	NL	NL			
J834	6800	KB	403	6397	203	82	6	2,1,2	40.39

Corrected Name	RF EL	DW	TOP OF TH-5 SAND	CORRECTED TOP ELEV.	ISOPACH THICKNESS	TH-5 NET SAND	# OF TH-5 SANDS	SHAPE OF TH-5 SANDS	PERCENT TH-5 SAND
K434	6827	KB	465	6362	215	167	5	3,2,2	77.67
K434X	6825	KB	456	6369	195	156	5	2,1,2,5	80.00
K534	6810	EL	361	6449	194	88	8	1,5,5,5,1	45.36
K534X	6816	KB	523	6293	171	120	7	2,5,1	70.18
K634W	6806	KB	310	6496	171	103	6	2,1,2,1,5	60.23
K634X	6799	KB	346	6453	203	0			0.00
K734X	6779	KB	468	6311	181	53	4	2,1	29.28
K834	6772	DF	403	6369	183	118	7	2,2,2,5	64.48
L334	6796	KB	254	6542	207	91	7	1,1,1,1	43.96
L634X	6784	KB	258	6526	203	130	9	3,1,2	64.04
M234X	6813	KB	522	6291	205	109	8	2,1,1,5	53.17
M334	6811	KB	544	6267	170	114	5	2,3	67.06
M334X	6806	KB	434	6372	202	0			0.00
M434Y	6799	KB	360	6439	192	0			0.00
M534	6785	KB	373	6412	177	5			2.82
M534X	6789	KB	310	6479	175	0			0.00
M634W	6780	KB	237	6543	207	142	5	1,1,2,2	68.60
M634X	6779	KB	273	6506	175	0			0.00
M734X	6779	KB	385	6394	217	42	3	3,2,1	19.35
M734Y	6779	KB	451	6328	219	0			0.00
M734Z	6779	KB	407	6372	212	53	11	2,1	25.00
P1	6791	KB	378	6413	188	129	4	2,2,1	68.82
P3	6796	KB	425	6371	183	96	4	2,2	52.46
P5	6813	KB	344	6469	226	0			0.00
T11	6847	KB	620	6227	176	86	2	1,2	48.86
T12	6839	KB	475	6364	222	64	3	2	28.83
T13	6861	KB	608	6253	192	95	6	1,3,2,2	49.48
T14	6838	KB	464	6374	219	89	7	1,3	40.64
TP11	6844	KB	492	6352	219	58	2	2	26.48
TP5	6843	KB	577	6266	181	79	3	2,3,1	43.65
2-D	6870	KB	FO	FO	FO	0-F			
unit5D	6833	KB	NL	NL	NL	NL			
12	6867	KB	FO	FO	FO	0-F			
13	6850	KB	768	6082	192	73	3	2,2,2	38.02
15	6824	KB	NL	NL	NL	>40(NL)	2	2	
17	6800	KB	NL	NL	NL	NL			
T-14-34	6826	KB	1180	5646	199	58	4	2,2,2	29.15
21	6828	KB	1316	5512	194	43	2	2	22.16
T-60-34	6810	KB	988	5822	204	54	3	1,2	26.47
T-61-34	6792	KB	887	5905	226	154	3	1,1,1	68.14
T-62-34	6764	KB	1052	5712	176	81	5	1,1	46.02
90-34	6807	KB	1040	5767	200	155	4	1,1,2,1	77.50
T-26-35	6795	KB	1356	5439	193	43	3	2,2	22.28
T-27-35	6861	KB	1425	5436	200	44	2	2,2	22.00
T-28-35	6782	KB	1345	5437	211	64	6	2,2	30.33
T-30-35	6770	KB	1342	5428	205	97	2	1,2	47.32
52-35	6782	KB	1247	5535	188	147	5	2,2,1	78.19
AVERAGES					199.70	79.89	4.95		39.80

Corrected Name	RF EL	DW	HOBACK SD. THICKNESS	HILLARD FAULT	CORRECTED ELEV.	THRUST FAULT	CORRECTED ELEV.	NORMAL FAULT	CORRECTED ELEV.
23	6771	KB	655						
24	6765	KB	749						
T-30-2	6773	KB	640						
T-31-2	6750	KB	664						
T-33-2	6755	KB						1967	4788
A2	6937	GL		360	6577				
3AX	6880	KB	541						
A12	6865	KB	611						
A13	6870	KB	599						
A14	6855	KB	608						
A15	6881	KB							
A16	6855	KB	560						
A17	6839	KB	596						
A18	6839	KB	568						
A19	6824	KB	572						
A20	6837	KB	570						
A21	6826	KB	565						
A22	6925	KB	554	427	6498				
A23	6901	KB	557						
A24	6891	KB	589	385	6506				
A25	6876	KB	624						
A26	6847	KB	581						
A503X	6784	KB							
A603X	6811	KB							
B1	6879	KB	605						
B103	6816	KB		204	6612				
B203X	6803	KB		108	6695				
B303X	6797	KB							
B303Y	6796	KB	540						
B303Z	6794	KB							
B403X	6801	KB							
B403Y	6803	KB	608						
B403Z	6821	KB	570						
B503W	6806	KB	601						
B503Y	6826	KB							
B503Z	6835	KB	674						
B603W	6847	KB	579						
B603X	6860	KB							
B603Y	6834	KB							
B703X	6819	KB							
C403X	6857	KB	641						
C603X	6888	KB	588						
D103X	6824	KB							
D203X	6831	KB	563						
D303X	6859	KB							
D303Y	6883	KB	542						
D403X	6822	KB							
D403Y	6956	KB	519						
D503W	6927	KB							
D503X	6966	KB	558						
D503Y	6956	KB	537						
D603X	6926	KB							
D603Y	6900	KB	619						
E403	7038	KB	534						
E503	6964	KB	607						
E503X	6976	KB	577						
E603X	6912	KB	630						
F203X	6941	KB		293	6548				
F203Y	6924	KB	539	290	6644				
F303X	7043	KB							
F403X	7049	KB	547						
F403Y	7039	KB	523						
F503W	6992	KB	614						
F503X	6964	KB							
F503Y	6951	KB	609						
F603W	6900	KB	634						
F603X	6906	KB	624						
G503X	6942	KB	599						
G503Y	6934	KB	596						
G603X	6899	KB	658						
H503X	6910	KB	607						
J503Y	6906	KB	589						
unit5	7024	KB	532						
1	6786	KB	731						
1	6813	RT	696						
19-T-3	6814	KB	707						
T-22-3	6784	KB	740						
T-23-3	6771	KB	656					1300	5471
T-34-3	6753	KB	755						
4-A	6861	KB	584						
1-C-4	6898	KB		460	6438				
2-C-4	6918	KB		473	6445				
3-C-4	6941	KB		510	6431				
4-C-4	6911	KB		600	6311				
1	6861	GL	643		578	6283			
21-4	6878	KB		1404	5474				
34	6867	KB	599	972	5895				
42	6875	KB	547	975	5900				
45	6924	KB	505	948	5976				
35	6908	KB	594	1047	5861				
39	6931	KB	493	1034	5897				

Corrected Name	RF EL	DW	HOBACK SD. THICKNESS	HILLARD FAULT	CORRECTED ELEV.	THRUST FAULT	CORRECTED ELEV.	NORMAL FAULT	CORRECTED ELEV.
83	6916	KB	595	1045	5871				
1F-X	6819	KB				1240	5579		
1	6824	KB							
20	6793	KB				1621	5172		
T-49-10	6763	KB	674						
T-50-10	6767	KB	612						
18	6962	KB	526						
38	7009	KB	595						
39	7166	KB	570						
50	7290	KB	559						
C327	6950	KB	508	453	6497				
C327Z	6936	KB		476	6460				
D227	6949	KB	540						
D627	6917	KB	654						
E227Y	6892	KB		295	6597				
G427	6919	KB	489						
G627	6893	KB	479						
H227	6923	KB	595						
J527X	6907	KB							
J527Z	6899	KB							
L127X	6918	KB	672	404	6514				
L227	6900	KB							
M127X	6878	KB	532	521	6357				
M127Y	6879	KB	536	336	6543				
M227X	6866	KB	649	270	6596				
M327	6875	KB	556						
M627Y	6878	KB	556						
98-27	7053	KB	557						
T-15	7063	KB	670						
T-16A-27	6975	KB	558						
T-16	6940	KB	554						
T-17	7042	KB	582						
T-18	6992	KB	587						
T-24	6939	KB	601						
T-32-27	6894	KB	652						
1	6932	KB	497						
3	6928	KB	566	426	6502				
11	6861	KB	565						
14	6920	KB							
22	7018	KB	610						
72-27	6917	KB	609						
94-27	6917	KB	616						
99-27	7012	KB	671						
G928	6948	KB							
G928X	6923	KB	556	377	6546				
L928	6902	ES							
B-2	6990	KB		753	6237				
9	6974	KB	599	520	6454				
8	6954	KB	632						
6-28	7008	KB		1020	5988				
A1-C-33	7036	DF							
B1-C-33	7033	KB							
1-C-33	6907	KB		1226	5681				
3-C-33	6883	KB		1199	5684				
2-33	6850	KB		1534	5316				
4-33	6854	KB		1486	5368				
10	6923	KB		1523	5400				
37	6918	KB							
48	6905	KB		1260	5645				
A234X	6853	KB	621						
A334	6829	ES	600						
A734Y	6845	KB							
B234	6851	KB							
B334	6839	KB		170	6669				
B534	6819	KB	525						
B534X	6823	KB	516						
B634	6831	KB	575						
C534X	6832	KB	562						
D134	6868	DF		970	5918				
D134X	6894	KB		930	5964				
D434	6943	GL	541						
D434X	6851	KB	489						
D734	6837	GL							
D834	6826	KB							
E534X	6851	KB							
E634	6807	KB	534						
F234	6850	KB		940	5910				
F434X	6836	KB	516	142	6694				
F434Y	6850	KB	585	435	6415				
F534X	6834	KB	540						
G634X	6826	KB	553						
G834X	6813	KB	528						
H334	6847	KB		708	6139				
H434X	6818	KB							
H534V	6811	KB	518						
H534W	6818	KB							
H634W	6812	KB	551						
H634X	6810	KB							
J434	6823	GL							
J834	6800	KB	588						

Corrected Name	RF EL	DW	HOBACK SD. THICKNESS	HILLARD FAULT	CORRECTED ELEV.	THRUST FAULT	CORRECTED ELEV.	NORMAL FAULT	CORRECTED ELEV.
K434	6827	KB							
K434X	6825	KB							
K534	6810	EL							
K534X	6816	KB							
K634W	6806	KB							
K634X	6799	KB	584						
K734X	6779	KB							
K834	6772	DF							
L334	6796	KB							
L634X	6784	KB	599						
M234X	6813	KB		204	6609				
M334	6811	KB							
M334X	6806	KB							
M434Y	6799	KB							
M634	6785	KB							
M534X	6789	KB							
M634W	6780	KB	638						
M634X	6779	KB	582						
M734X	6779	KB	622						
M734Y	6779	KB							
M734Z	6779	KB							
P1	6791	KB							
P3	6796	KB							
P5	6813	KB							
T11	6847	KB	480	304	6543				
T12	6839	KB	536						
T13	6861	KB	476	473	6388				
T14	6838	KB	546	217	6621				
TP11	6844	KB	570						
TP5	6843	KB	536	228	6615				
2-D	6870	KB		737	6133				
unit5D	6833	KB							
12	6867	KB		888	5979				
13	6850	KB	482						
15	6824	KB							
17	6800	KB							
T-14-34	6826	KB	673						
21	6828	KB	665						
T-60-34	6810	KB	722						
T-61-34	6792	KB	721						
T-62-34	6764	KB	634						
90-34	6807	KB	731						
T-26-35	6795	KB	638						
T-27-35	6861	KB	636						
T-28-35	6782	KB	640						
T-39-35	6770	KB	642						
52-35	6782	KB	678						
AVERAGES			591						

VITA

David E. Schmude

Master of Science

thesis: PALEOCENE DEPOSITION OF THE HOBACK FORMATION ON THE LA  
BARGE PLATFORM OF THE GREEN RIVER BASIN

Major Field: Geology

Biographical:

Personal Data: Born in Houston, Texas, September 23, 1966, the son of  
Donald H. and Alice A. Schmude.

Education: Graduated from Bishop Kelley High School, Tulsa,  
Oklahoma, in May, 1985; received Bachelor of Science Degree in  
Geology from Oklahoma State University in May, 1989; completed  
requirements for the Master of Science degree at Oklahoma State  
University in December, 1991.

Professional Experience: Teaching Assistant, Department of Geology,  
Oklahoma State University, January, 1990, to December, 1990.